A Phase II, Double Blind, Randomised, Placebo-Controlled Trial of Neuroprotection with Phenytoin in Acute Optic Neuritis

Rhian Elizabeth Raftopoulos

A thesis submitted to University College London for the degree of Doctor of Philosophy

November 2015

Abstract

Acute optic neuritis is a common and often presenting feature of multiple sclerosis, and attacks can lead to persistent visual impairment through neurodegeneration in the retina and optic nerve. The acute inflammatory lesion in the optic nerve resembles the demyelinating plaques elsewhere in the CNS.

As with other MS relapses, corticosteroids have no or little impact on the extent to which vision recovers nor do they prevent optic nerve atrophy on MRI or improve VEP latency after an attack of optic neuritis. There is currently no treatment for the acute phase of the disease to improve long-term visual outcome, and in this context neuroprotection remains a major unmet need.

Progress in the development of potential neuroprotective therapies in optic neuritis and MS relies upon the identification of key mechanisms and treatment targets.

Among possible mechanisms of neurodegeneration, there is growing evidence of a cascade of accumulation of sodium ions in demyelinated axons that arises from neuronal energy failure leading to the reverse operation of the Na^{+}/Ca^{2+} exchanger and subsequent toxic accumulation of injurious calcium ions. Inhibition of voltage-gated sodium channels is neuroprotective in preclinical models of inflammatory demyelination.

The anterior visual system has many advantages for testing neuroprotective treatments in MS. In particular, the retinal nerve fibre layer is a relatively pure compartment of unmyelinated axons whose thickness can be measured sensitively and non-invasively using optical coherence tomography making it an attractive biomarker of axonal loss.

In this thesis I investigated whether early and sustained sodium channel inhibition with phenytoin is neuroprotective in acute optic neuritis. 86 people were randomized within 2 weeks of optic neuritis symptom onset to receive phenytoin or placebo for 3 months. Retinal nerve fibre layer (RNFL) thickness and macular volume (MV) were measured at baseline, then 6 months later, using optical coherence tomography. Visual function, optic nerve MRI, and visual evoked potentials were also measured. The primary outcome was

mean RNFL thickness in the affected eye at 6 months, adjusted for fellow eye RNFL thickness at baseline.

In the intention to treat comparison, average affected eye RNFL thickness at 6 months was 7.15 μm greater in the active group (n=39) vs. placebo (n=42), a 30% protective treatment effect (p=0.021). Adjusted MV was 0.20 mm^3 greater in the active group, a 34% treatment effect (p=0.005). There was also a near significant treatment effect on optic nerve cross-sectional area (p=0.06). Per protocol comparisons showed similar treatment effects. Treatment did not affect visual outcome.

These findings support the concept of neuroprotection with phenytoin in acute optic neuritis. Inhibition of voltage-gated sodium channels could also be neuroprotective in other relapses of multiple sclerosis, and further investigation of its effect is warranted in this major area of unmet therapeutic need.

Declaration

I, Rhian Raftopoulos confirm that the work presented in this thesis is my own. Where information has been derived from other sources I confirm that this has been indicated in the thesis.

I performed the following: assisted in writing of applications for ethics approval, setting up the trial infrastructure and advertising the trial to the patient identification centres, writing of the trial standard operating procedures, screening and recruitment of all patients at the London site, development of MRI protocols with the assistance from the physicists. I was also responsible for arranging all visits at the London site, baseline, one month and three month clinical assessments, pharmocovigilence, maintaining case record forms and liaising with the trial monitor, performing the baseline retinal imaging, taking and processing of blood and urine samples for the biomarker sub study, data acquisition and entry, data analysis (with the exception of the MTR analysis) and the writing of this thesis.

The study was designed by the trial working group who included: Dr Simon Hickman, Dr Ahmed Toosy, Dr Basil Sharrack, Daniel R Altmann, Dr Rose Sheridan, Professor Martin Koltzenburg, Professor Claudia AM Gandini Wheeler-Kingshott, Professor Klaus Schmierer, Professor Gavin Giovannoni, Professor David H Miller and Dr Raju Kapoor

Dr Rose Sheridan was the project manager for the trial and assisted in the writing of applications for ethics, MHRA and R+D approval as well as obtaining R+D approval at all of the patients identicication centres.

Dr Simon Hickman and Dr Basil Sharrack were responsible for patient screening, recruitment, clinical assessments and pharmacovigilence at the Sheffield site. The Sheffield trial nurses were responsible for maintenance of case record forms taking and processing of blood and urine samples for the biomarker sub study and data acquisition at the Sheffield site.

The patients were identified and referred by colleagues in a number of patient identification sites across the country including: Mr. James Acheson and the Ophthalmology Specialist

Registrars (Moorfields Eye Hospital NHS Foundation Trust,) Dr Richard Nicholas (Western Eye Hospital, Imperial College Healthcare NHS Trust) Dr Luke Bennetto (North Bristol NHS Trust), Mr. Mike Burdon (University Hospitals Birmingham NHS Trust), Dr Jeremy Hobart (Plymouth Hospitals NHS Trust), Dr Edward Hughes, Dr Waqar Rashid, Dr Sarah Vickers and Dr Dominic Heath (Brighton and Sussex University Hospitals NHS Trust), Professor Cris Constantinescu (Nottingham University Hospitals NHS Trust), Professor Irene Gottlob (University Hospitals of Leicester NHS Trust), Dr Matt Craner and Dr Jackie Palace (Oxford University Hospitals), Professor Keith Martin and Professor Alasdair Coles (Cambridge University Hospitals NHS Trust), Professor Clive Hawkins (University Hospitals of North Midlands NHS Trust), and Mr David Bessant (London North West Healthcare NHS Trust).

Six-month visual assessments and retinal imaging were performed by Dr Shahruckh Mallik (at the London site) and retinal imaging at the Sheffield site was performed by the OCT technicians, all of whom were blinded to treatment allocation.

Blinded electrophysiological testing was performed by Prasad Malladi and analysed by Professor Martin Koltzenburg at the London site and Dr Ptolemaios G Sarrigiannis at the Sheffield site.

Professor Claudia Wheeler-kingshott, Dr Rebecca Samson and Marios Yiannakas assisted with the development of the MRI protocol.

Dr Ahmed Toosy and Marios Yiannakas assisted with lesion identification and location in the optic nerve.

Dr Katherine Miszkiel and Dr Nigel Hoggard reported on the brain MRI of the patients at the London Sheffield sites respectively both of whom were blinded to treatment allocation.

Dr Vincente performed the MTR analysis of the optic nerve imaging at the London site and was blinded to treatment allocation.

Dr Daniel Altmann performed the statistical analysis for the trial.

Kelvin Hunter created the trial database and assisted with data management.

Acknowledgments

There are a many people who I would like to thank for their invaluable help and support during this PhD project.

First and foremost I would like to thank the patients for agreeing to participate in the trial and giving up so much of their time to return for follow up visits. This work would not have been possible without them.

I would also like to thank to Dr Simon Hickman and the rest of the trial team in Sheffield who were responsible for the recruitment and care of the patients at the Sheffield trial site. Without their commitment and collaboration this project would not have been possible.

Special thanks also goes to Dr Ahmed Toosy who was extremely helpful in setting up the recruitment pathway in Moorfields that has been so instrumental to the success of the trial. I learnt a huge amount about neuro-opthalmology thanks to his tutelage. In addition to this he helped teach me about MRI analysis of the optic nerve.

I am also extremely grateful to Mr Acheson and the ophthalmology registrars at Moorfields eye hospital who were so helpful in contacting me every time a patient with optic neuritis was seen in eye casualty. Without this recruitment of sufficient numbers of patients into the trial would have been extremely difficult if not impossible.

I would also like to give special mention to Dr Rose Sheridan who was project manager and responsible for overseeing all aspects of the trial. She really was indispensible and this project would not have got off the ground without her.

In addition, I would like to thank the radiographers in the NMR unit who performed the MRI scans for the patients with particular thanks to Marios Yiannakos who also assisted with the development of the MRI protocols as well as helping identify the lesion on the optic nerve imaging.

Prasad Malladi performed the electrophysiology for the trial patients and was so accommodating in fitting them in at the last minute.

I am also indebted to the physicists in particular Professor Claudia Wheeler-kingshott and Dr Rebecca Samson for the development of the MRI protocol for the trial.

Dr Daniel Altmann developed the statistical analysis plan and performed all the statistics for the trial. I am extremely grateful for his patience, precision and attention to detail as well as his pragmatic approach to explaining statistical concepts.

I have been lucky enough work alongside some fantastic clinical fellows in the NMR unit and would like to thanks Dr David Paling for his assistance with visual testing as well as Dr Shahruckh Mallik for performing the six-month OCT scans. Thanks also to Dr Hugh Kearney, Dr Varun Sethi, Dr Nils Mulhert, Dr Wallace Brownlee and Niamh Cawley for making my time at Queen Square such an enjoyable and fulfilling experience and for being not only great colleagues but also valued friends.

I am hugely indebted to my PhD supervisor's Dr Raj Kapoor and Professor David Miller who along with others in the trial steering group conceived the idea for the project and obtained funding to allow it to proceed. They have both been tremendously supportive throughout my time in Queen Square and I have benefited enormously from their guidance, wisdom and wealth of experience. I could not have asked for better supervisors.

Finally, last but definitely not least, I would like to thank my partner Simon for his unwavering love and support and for enduring with me the highs and the lows that are part and parcel of undertaking a PhD.

Financial support for this project was provided by grants from the National MS society and MS Society of Great Britain and Northern Ireland, UCL, UCLH Biomedical Research Centre and Novartis

Table of Contents

Abbreviations

3T	Three Teslar
ACE	Angiotensin converting enzyme
ACTH	Adrenocorticotrophic hormone
ADEM	Acute disseminated encephalomyelitis
ANCA	Anti-neutrophil cytoplasmic antibody
ANCOVA	Analysis of covariance
APP	Amyloid precursor protein
AQP4	Aquaporin four
ATP	Adenosine triphosphate
AZOOR	Acute zonular occult outer retinopathy
C+S	Culture and sensitivity
Ca^{2+}	Calcium
CD4	Cluster of differentiation 4
CD8	Cluster of differentiation 8
CIS	Clinically isolated syndrome
CNS	Central nervous system

CRION	Chronic relapsing inflammatory optic neuropathy
CSF	Cerebrospinal fluid
CT	Computed tomography
CXR	Chest X-ray
DARC	Detection of Apoptosing Retinal Cells
DMDs	Disease modifying drugs
EAE	Experimental autoimmune encephaloyelitiis
ECG	Electrocardiogram
EDSS	Expanded disability status score
ERG	Electroretinography
ESR	Eryrthrocyte sedimentation rate
ETRDS	Early treatment diabetic retinopathy study
FBC	Full blood count
FFE	Fast field echo
FLAIR	Fluid attenuated inversion recovery
FM 100-Hue	Farnsworth munsell 100-Hue
FOV	Field of view

FSE	Fast spin echo
GC/IPL	Ganglion cell/inner plexiform layer
GCA	Giant cell arteritis
GCL	Ganglion cell layer
HCVA	High contrast visual acuity
HIV	Human immunodeficiency virus
HLA	Human leukocyte antigen
Ig	Immunoglobulin
IM	Intramuscular
INL	Inner nuclear layer
IPL	Inner plexiform layer
IV	Intravenous
IVIG	Intravenous immunoglobulin
K^+	Potassium
LCLA	Low contrast letter acuity
LGN	Lateral geniculate nucleus
LogMAR	Logarithm of minimum angle of resolution

LP	Lumbar puncture
mfVEPs	Multifocal VEPs
MMA	Methylmalonic acid
MME	Microcystic macular oedema
MP	Methylprednisolone
MRI	Magnetic resonance imaging
MS	Multiple Sclerosis
MSFC	Multiple sclerosis functional composite
MSON	Multiple sclerosis related optic neuritis
MT	Magnetisation transfer
MTP	Macular thinning predominant
MTR	Magnetisation transfer ratio
MV	Macular volume
Na^+	Sodium
NEX	Number of excitations
NMDA	N-methyl-D-asparate
NMO	Neuromyelitis optica

NO	Nitric oxide
OCT	Optical coherence tomography
ON	Optic neuritis
ONL	Outer nuclear layer
ONTT	Optic neuritis treatment trial
OPL	Outer plexiform layer
P value	Probabilty value
PCR	Polymerase chain reaction
PERG	Pattern electroretinography
PET	Positron emission tomography
PO	Orally
PP	Per protocol
PPMS	Primary progressive multiple sclerosis
QOL	Quality of life
RAPD	Relative afferent pupillary defect
RGC	Retinal ganglion cell
RNFL	Retinal nerve fibre layer

RPE	Retinal pigment epithelium
RRMS	Relapsing remitting multiple sclerosis
SD	Standard deviation
SL0	Scanning laser ophthalmoscopy images
SLE	Systemic lupus erythematosus
SPMS	Secondary progressive multiple sclerosis
sTE-FLAIR	Short echo time fluid attenuated inversion recovery
STIR	Short tau inversion recovery
TE	Echo time
TPO	Thyroid peroxidase
TR	Repetition time
TSE	Turbo spin echo
UK	United Kingdom
US	United States
USS	Ultrasound scan
VA	Visual acuity
VEPs	Visual evoked potentials

VFMD Visual Field Mean Deviation

List of Figures

List of Tables

Chapter 1 Anatomy and Physiology of the Anterior Visual System

1.1 Histology of the Retina

The sensory retina is part of the central nervous system and develops from the optic cup. It is approximately 0.5mm thick and lines the back of the eye. It is a unique CNS structure as it contains axons and glia in the absence of myelin.

The central retina is a circular field approximately 6 mm around the fovea and beyond that the peripheral retina extends to the ora serrata which is approximately 21 mm from the fovea(Polyak, 1941) .

The macula is a circular area approximately 1.5 mm in diameter with a centre located 17 degrees or 4.0-5.0mm temporal to and 0.53-0.8 mm inferior to the centre of the optic disc T (Kincaid and Green, 1999). It is easily identified due to the oval shaped depression at its centre called the fovea. The foveal part of the macula confers the greatest visual acuity and has the highest density of cone receptors (199,000/mm^2), which are elongated to maximize light detection (Oyster, 1999; Curcio et al., 1990).

There are no rods in the foveola but these are the predominant photoreceptor in the peripheral retina.

The neurosensory retina consists of three layers of nerve cell bodies and two layers of synapses. The ganglion cell layer lies innermost, proximal to the lens and anterior chamber of the eye and the photoreceptor layer is outermost next to the retinal pigment epithelium. Light must therefore travel the entire thickness of the inner retina before reaching the rods and cones.

1.2 The Retinal Layers.

Bruch's membrane

Is an elastic membrane extending from the optic disc posteriorly, where it is thickest, to the ora serrata anteriorly. It is located between the retinal pigment epithelium RPE and the choriocapillaris.

The Retinal Pigment Epithelium (RPE)

Provides structural and metabolic support to the photoreceptors primarily via vitamin A metabolism. The tight junctions between RPE cells help maintain the selective blood retina barrier.

The Photoreceptor Layer (The Outer Nuclear Layer)

Photoreceptors (rods and cones) contain a visual pigment that absorbs photons of light and converts them into an electrochemical signal.

The human retina contains three types of cone and rods. The three types of cone operate at different wavelengths: short (blue), middle (green) and long (red). Rods are saturated by natural light and cannot distinguish colours but are effective for scotopic vision. Humans have a rod: cone ratio of 20:1 and approximately 50% of cones are located within the central 30 degrees of visual field. (Rizzo, 1994). The density of rods is highest in the 'rod ring' approximately 4.5mm from the foveola. (Rizzo, 1994).

The Outer Plexiform Layer

This is where the photoreceptors form synaptic connections with the bipolar and horizontal cells. It is where the initial processing of the photoreceptor signal takes place.

The Inner Nuclear Layer

This layer consists of bipolar, horizontal and amacrine cells. These form complex neuroretinal connections in the inner and outer plexiform layers that modify the photoreceptor signal and transmit it to the ganglion cells.

Photoreceptors connect to bipolar cells that relay messages to ganglion cells. Amacrine and horizontal cells form lateral connections between these layers and may contribute to contrast enhancement. In the fovea cone bipolar cells may receive input from a single cone photoreceptor that allows a high degree of spatial acuity. Conversely, in the peripheral retina up to 70 rods may converge and provide information to a bipolar cell (Sharma et al, 2003).

The Inner Plexiform Layer

This is where the second stage of retinal processing occurs and acts as a relay station for vertical information. It is the neuropil layer where bipolar cells synapse with the dendrites of ganglion cells. In addition to this different varieties of horizontally and vertically directed amacrine cells interact to integrate and influence bipolar cell outputs. There are around 40 types of amacrine cell and each type has a particular neurotransmitter and connects with a particular type of bipolar cell. (Kolb et al., 1995)

The Ganglion Cell Layer

The ganglion cells transfer visual information from the retina to the brain. Adults have on average 1.2 million retinal ganglion cells and approximately 70% of these sub serve central vision (Rizzo, 1994). Although up to 20 different types of ganglion cell have been described the most common (80%) are midget (parvocellular cells) and 10% are parasol (magnocellular cells) that are named after their target locations in the lateral geniculate nucleus. (Wurtz et al, 2000). The Midget pathways consist of midget bipolar cells and midget ganglion cells. The fovea has a high concentration of midget ganglion cells. Midget cells have cone opponent receptive fields. They are high acuity cells and also carry red or green color specific signal. This allows them to confer high spatial acuity, colour vision and fine stereopsis. Midget cells

come in high branching varieties that are probably physiologically off centre as well as low branching types that are probably ON centre physiologically. The connections between midget bipolar and midget ganglion cells have previously been thought to be one to one. Although this is likely to be the case in the foveal area it may not be true in the peripheral retina where the midget ganglion cells have larger dendritic trees and can have input from 3-5 midge bipolar cells (Kolb and Marshak, 2003).

Parasol (magnocellular cells), so called because of their resemblance to an open umbrella on histological sections, have a much larger dendritic tree and make connections with several bipolar cells receiving convergent input from a much larger area of the retina. They are more numerous in the peripheral retina. They have a larger receptive field and lower spatial resolution than midget cells and transmit signals from many rods and cones. They demonstrate spatial but not spectral opponency. They confer low spatial resolution, motion detection and coarse stereopsis but do not detect colour (Livingstone and Hubel, 1988).

The smallest ganglion cells are koniocellular. They have a small cell body but diffuse dendritic tree. They include bistratified cells that make contact at both upper and lower sublaminae of the inner plexiform layer. They project to intercalated layers (koniocellular layers) in the LGN. They have S (Short-length) cone ON receptive fields and one of the major roles of the koniocellular pathway may be to serve the blue yellow axis of colour vision. The koniocellular layer of the LGN comprises a diffuse layer of mostly small cell codes intercalated between the main laminae (Dacey and Lee, 1994) (Hendry and Yoshioka, 1994)

The ganglion cell layer also contains displaced amacrine cells and astrocytes.

The Retinal Nerve Fibre Layer

Retinal ganglion cell axons travel towards the optic nerve head within the nerve fibre layer. The retinal nerve fibre layer is located between the inner limiting membrane and the ganglion cell layer. It is composed of ganglion cell axons, astrocytes, retinal vessels and Muller cells. Astrocytes and Muller cells comprise a neuroglial system that provides structural and nutritional support to the nerve fibres. Muller cells occupy nearly all the

intracellular retinal space and form the inner limiting membrane covering the nerve fibre layer on its vitreal surface. The astrocytic processes partially envelope all nerve fibres and also cover the retinal capillaries isolating the axons from retinal blood flow. The large retinal arterioles and venules lie in the superficial part of the nerve fibre layer. A previous study in primates demonstrated that glia occupies at least 18% of the cross-sectional area of every nerve fibre bundle but this varies with location across the retina and in some areas (nasal retina) was as much as 42% (Ogden, 1983). Another study in humans demonstrated that retinal nerve fibre layer (RNFL) thickness, measured histomorphometrically at the optic disc border in patients with absolute glaucoma, was 40 μms which would be consistent with a glial content of around 23-30% of the total RNFL thickness (Dichtl et al., 1999). The glial content of the retinal nerve fibre layer may increase with disease. In a histological study on eyes of 82 patients with multiple sclerosis gliosis with a related glial mesodermal reaction was seen in more than 70% of optic nerves and immunohistochemistry demonstrated perivenular astrocytic gliosis in the optic disc and intense gliomesodermal reaction in the optic nerve (Green et al., 2010). This is important to highlight given that OCT measured RNFL thickness measures do not give cytological detail and therefore may not be purely measuring axonal loss after optic neuritis but may also be affected by gliosis.

The RNFL is thinnest in the peripheral retina and thickest towards the superior and inferior margins of the optic disc where it measures approximately 200 μms (Dichtl et al., 1999). Retinal nerve fibre layer thickness is known to decrease gradually with age (Alamouti and Funk, 2003).This occurs diffusely without the development of localised defects (Jonas and Schiro, 1994)**.**

The axons are separated into bundles by the cell processes of the Muller cells. The axons of the foveal ganglion cells project directly to the temporal aspect of the optic disc via the papillomacular bundle. The remaining axons from the temporal retina form the arcuate bundle around the papillomacular bundle on either side of the horizontal raphe and enter the superior temporal and inferior temporal sections of the optic disc. Axons that originate from the nasal retina project directly to the nasal aspect of the optic disc in a radial pattern.

The horizontal raphe creates a physiological separation between the superior and inferior hemi field of the nasal visual field (temporal retina). The vertical meridian that separates the nasal and temporal retina is a vertical line that passes through the fovea.

The diameter of the nerve fibres in the temporal retina is smaller than in the nasal region or vertical disc poles presumably due to the higher density of parvocellular ganglion cells in the fovea (Jonas and Dichtl, 1996)

Within the nerve fibre layer axons from central RGCs lie superior to those from peripheral RGCs. Axons from the nasal retina decussate at the optic chiasm whereas axons from the temporal retina remain ipsilateral.

Figure 1-1: Diagram illustrating RNFL axons as they project form RGCs to the optic disc

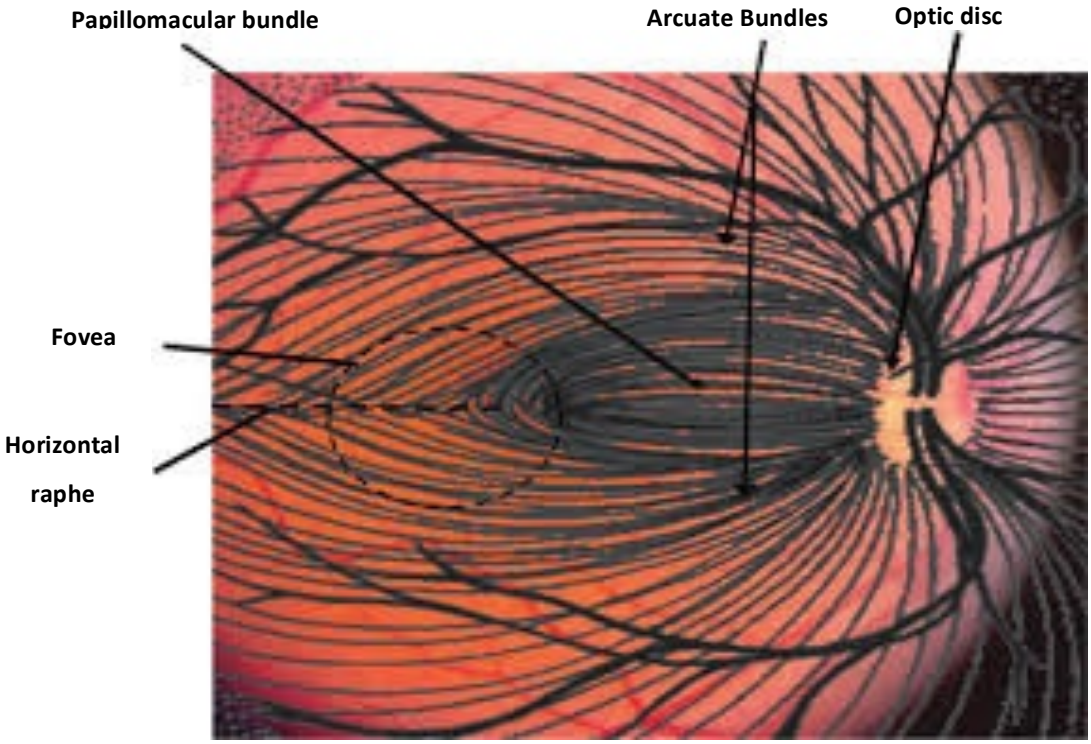

(Taken from Prasad and Galetta, 2011 (page 9, Figure 1.7))

Figure 1-2: Diagram illustrating different retinal layers (ONL- outer nuclear layer, OPL- outer plexiform layer, INL -inner nuclear layer, GCL- ganglion cell layer, RNFL – retinal nerve fibre layer)

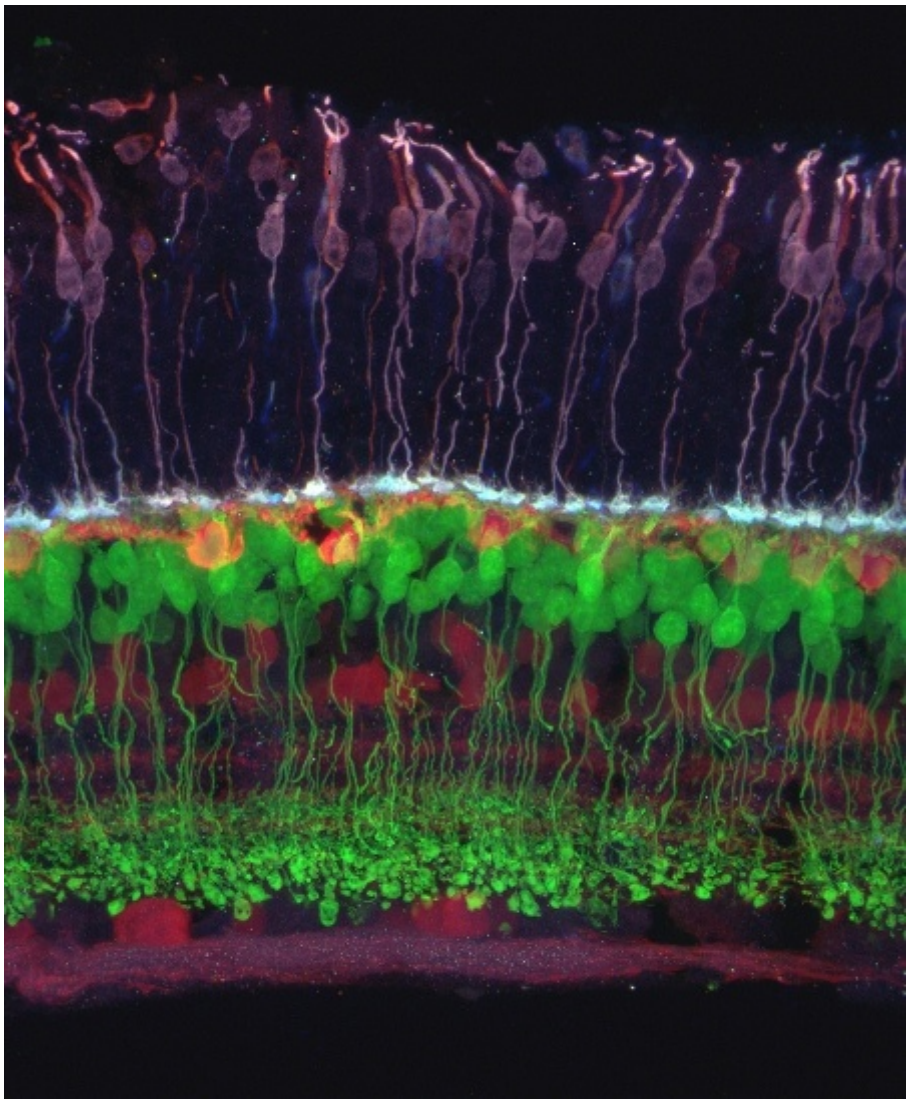

(webvision.med.utah.edu)

1.3 The Optic Nerve

The optic nerves are phylogenetically an evagination of the brain and their histological composition is analogous to that of brain tissue.

Each optic nerve consists of approximately 1.2 million retinal ganglion cell axons (Rizzo, 1994). There is a wide variation in the length of the optic nerve, even between the two eyes of the same individual, with a range of 35-55mm from globe to chiasm (Hayreh, 2011).

Each optic nerve can be segmented into four portions according to location along its course: the intraocular, intraorbital, intracanalicular and intracranial portions.

Table 1-1: Approximate length of each segment of the optic nerve

Part of Optic Nerve	Approximate Length
Intraocular (Optic nerve head)	1mm
Intraorbital	25 mm
Intracanalicular	4-10mm
Intracranial	10mm

The Intraocular Portion

The optic nerve head is approximately 4.5 mm or 15 degrees nasal to the fovea. It contains no retinal photoreceptors and is responsible for the blind spot. It is approximately 1 mm deep and 1.5mm in diameter (Hayreh, 2011). It has a central depression called the optic cup. The intraocular portion of the optic nerve head is visible on fundoscopy. Retinal axons enter the optic disc at a 90-degree angle. The nerve fibres are arranged in bundles and are unmyelinated at this point.

The topography of axons within the nerve fibre layer and optic nerve head is somewhat controversial with conflicting reports of the positioning of ganglion cell axons. Some studies have indicated that central retinal axons are positioned in the inner part of the optic nerve head and the peripheral retinal axons in the outer part of the optic nerve head whereas others have found the opposite (Garway-Heath et al., 2000). These conflicting results may be explained in part by inter-species variation. A study in human eyes indicated that the nerve fibre layer was not topographically organized with respect to eccentricity and

peripheral nerve fibres were scattered throughout the thickness of the RNFL. However, there was a rough topographic organization of nerve fibres within the optic nerve head with respect to the circumferential origin of axons. Foveal fibres were found to occupy a large proportion of the temporal aspect of the optic nerve head whereas fibres from areas temporal to the fovea were displaced to more superior and inferior regions. Arcuate fibres occupied a peripheral position in the optic nerve head. This topographic organization was maintained going in to the optic nerve (Fitzgibbon and Taylor, 1996).

Garway-Heath et al produced a map relating regions of the visual field to sectors of the optic disc using a Humphrey 24-2 visual field grid superimposed onto the RNFL photographs of patients with well-defined RNFL defects. In their map the optic disc is divided into 6 sectors. The central macular region of the visual field was associated with the temporal sectors of the disc, the superior arcuate region of the field with the inferior temporal sector of the disc and the inferior arcuate region of the visual field with the superior temporal sector of the disc as well as three regions of the visual field corresponding to the nasal half of the optic disc (See Figure 1-3 (Garway-Heath et al., 2000)).

Figure 1-3: Diagram taken from Garway-Heath et al demonstrating division of visual field (A) and optic nerve (B) into sectors as described above.

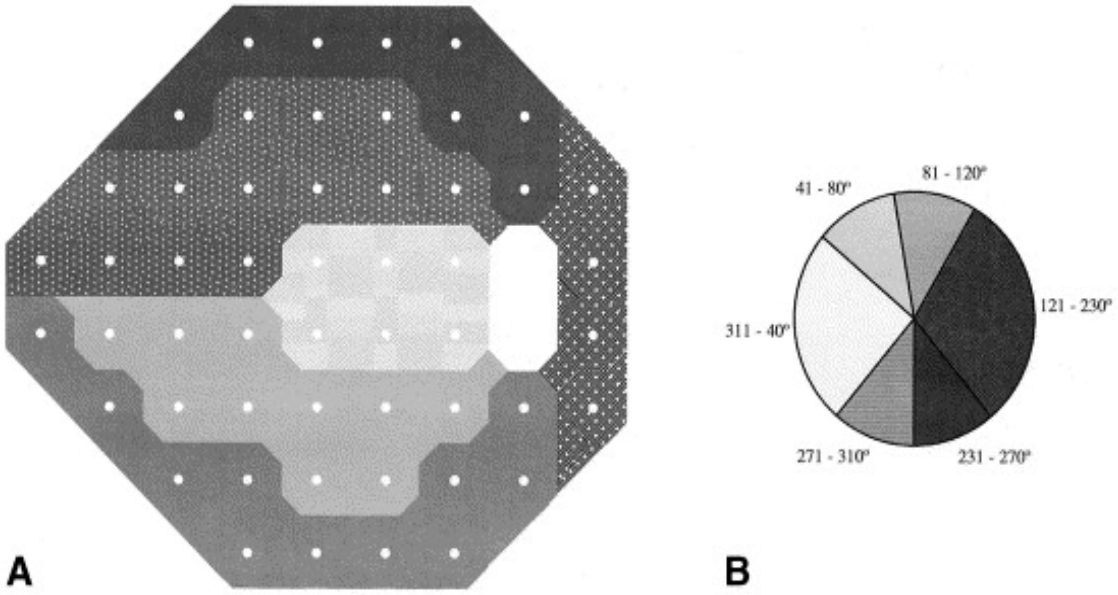

The Optic nerve head is composed of:

The Nerve Fibre Layer

Prelaminar region

Lamina Cribrosa

Retrolaminar region

The intraorbital optic nerve

The intraorbital part of the optic nerve begins where the nerve exits at the lamina cribrosa and as it does so it becomes myelinated with oligodendrocytes and increases in diameter to between 3-4 mm. The acquisition of myelin at the lamina cribrosa allows the transformation of action potentials from slow membrane to fast salutatory conduction. It is also at this point that the optic nerve becomes ensheathed in the meninges and CSF fills the tube shaped subarachnoid space between nerve and sheath. The subarachnoid space is continuous from

the middle cranial fossa, along the nerve and into the posterior sclera. The subarachnoid space of the optic nerve is widest near the globe and contains a multitude of arachnoid trabeculae arranged in a reticular fashion. Some of the larger trabeculae contain blood vessels. Elevated intracranial pressure is transmitted through the subarachnoid space to the optic nerve head resulting in papilloedema.

The intraorbital portion of the optic nerve is between 25 – 30 mm in length and is at least 5mm longer than the direct distance from the globe to the orbital apex (Glaser and Sadun, 1990). This 'slack in the system' allows movements of the eye.

Most of the optic nerve receives it blood supply from the ophthalmic artery that is a branch of the internal carotid artery just after it has exited the cavernous sinus. In the cranial cavity the ophthalmic artery lies mostly in the subdural space. The ophthalmic artery then passes through the orbital canal below the optic nerve and gives rise to the posterior cililary arteries and the central retinal artery. The central retinal artery pierces the optic nerve approximately 10-15 mm behind the globe and runs anteriorly within the optic nerve. The blood supply to the orbital segment of the optic nerve is via the pial network that is supplied either directly via branches of the ophthalmic artery or indirectly via branches of the short posterior cilliary arteries or a branch of the central retinal artery. Branches of the central retinal artery may also contribute to the optic nerve blood supply. Branches of the short posterior cililary arteries provide the major blood supply to the optic nerve head via the circle of Zinn- Haller(Hayreh, 2011).

The Intracanalicular Portion

Upon exiting the orbit the optic nerve enters the optic canal at the orbital apex. The optic canal lies within the lesser wing of the sphenoid bone and is approximately 10mm long and 3-4mm wide (Rizzo, 1994). The CSF filled subarachnoid space is markedly attenuated as it passes through the optic canal and so is usually not seen on T2 weighted MRI at this point. The orbital canal makes an angle of 45 degrees with sagittal plane. The intracanalicular portion of the optic nerve is fixed and immobile and may be particularly susceptible to damage from trauma or swelling.

The Intracranial portion

The intracranial portion of the optic nerve is approximately 10 mm long. It lies below the A1 segment of the anterior cerebral artery and lateral to the internal carotid artery. The ophthalmic artery is a branch of the internal carotid. The ophthalmic artery enters the subarachnoid space of the optic canal inferolaterally to the nerve.

The Optic Chiasm

The dumbbell shaped optic chiasm is where the two optic nerves merge. It is positioned in the subarachnoid space of the suprasellar cistern above the diaphragma sella and the pituitary gland. It lies inferior to the hypothalamus and anterior to the infundibulum.

The chiasm is usually around 10mm above the pituitary gland. In 15% of people the chiasm is displaced anterior to the pituitary gland (a prefixed chiasm) and in 5% is displaced posteriorly (a post fixed chiasm)(Doyle, 1990).

Within the chiasm, nerve fibres from the nasal retina of each eye decussate to join the temporal fibres of the contralateral eye. In this way, fibres that carry information from the same part half of the visual field are brought together.

The optic chiasm lies amongst the arteries that make up the circle of Willis and these vessels provide an anastomotic supply to the chiasm.

1.4 Optic Nerve Fibres

Each optic nerve contains between 770,000 and 1.7 million nerve fibres. The nerve fibres vary in diameter (between 0.7μm and 10μm) (Jonas and Dichtl, 1996). In the retrolaminar and orbital parts of the optic nerve they are arranged in bundles separated by septa. The presence of these septa distinguishes the optic nerve from the other CNS white matter tracts. Within the nerve fibre bundles are rows of supporting astrocytes, oligodendrocytes and microglial cells.

Hoyt et el studied the topographic organization of the nerve fibres in the anterior portion of the optic nerve in primates. By photocoagulating different regions of the retina they were able to histologically localize nerve fibre degeneration in the optic nerve. They found that lesions in the superior and inferior temporal retina (sparing the macula) caused degeneration of nerve fibres in the upper and lower temporal sectors of the intraorbital optic nerve. Lesions in the macular region led to degeneration of fibres temporally in a sector occupying at least one third of the cross-sectional area of the anterior optic nerve. Lesions in the nasal retina led to degeneration medially in the anterior optic nerve (Hayreh, 2011).

Due to the lack of pathological data on MS associated optic neuritis it is unclear whether there is a predisposition for the location of MS lesions within the optic nerve (e.g. peripheral rather than central).

.

Chapter 2 An Overview of the clinical aspects of optic neuritis

Optic Neuritis is a generic term used to describe the pathophysiological process of inflammation of the optic nerve. There are a variety of infectious, autoimmune, inflammatory and vascular conditions that can cause optic neuritis. However, the majority of cases are due to idiopathic inflammatory demyelination, which can occur in isolation or in association with multiple sclerosis.

Acute idiopathic demyelinating optic neuritis is a relatively common condition with a reported incidence of up to 5 in 100,000 per year in high-risk populations for MS (1 in 100,000 in lower risk populations). Women are more commonly affected than men with a ratio of approximately 3:1. However there may be racial differences with a ratio of 1:1.22 in a Japanese cohort (Wakakura et al., 1995). Although there is a wide variation in age of onset it most commonly affects young people, between the ages of 20-50 years. The incidence is highest in Caucasians, in countries at higher latitude and lowest in regions closer to the equator (Jin et al., 1998; Rodriguez et al., 1995). There is reported to be a seasonal variation with a higher incidence in spring/ early summer (Jin et al., 1999).

The inflammatory lesion in the optic nerve is similar to the acute plaques seen elsewhere in the CNS in MS. The pathological process is thought to be immune mediated where there is activation of systemic T lymphocytes that cross the blood brain barrier leading to a delayed type hypersensitivity reaction with inflammation, demyelination and subsequent axonal loss. The exact target antigen remains elusive. A genetic predisposition has been proposed and this is supported by an over-representation of certain HLA types (e.g., HLA–DRB*1501) amongst patients with Optic Neuritis (Hauser et al., 2000; Oksenberg et al., 2008). It is likely that as yet unknown environmental factors trigger the condition in a genetically susceptible individual. There is an association between higher incidence rates and previous exposure to Epstein Barr virus (Lucas et al., 2011). In addition to this prospective studies have shown that other common viral infections are probably risk factors for MS relapses (Sibley et al., 1985) and one study demonstrated a significant correlation between adenovirus CSF titre rises with the occurrence of a major MS relapse (Andersen et al., 1993).

The Optic Neuritis treatment trial has provided a wealth of information on the clinical presentation and course of acute demyelinating optic neuritis.

2.1 Clinical Features

Optic Neuritis is diagnosed clinically on the basis of history and clinical examination. It usually presents with sub-acute monocular visual loss, which progresses over 7-10 days before reaching a nadir. Continued deterioration in vision beyond two weeks is unusual and may indicate an alternative diagnosis. It is unilateral in >90% of adults in contrast to paediatric cases where it is bilateral in 60-70% of cases (Boomer and Siatkowski, 2003).

Retro-orbital pain, which is exacerbated by eye movements, is also typical and in the optic neuritis treatment trial 92% of patients experienced pain. The pain may proceed or be concomitant with the visual loss (Optic Neuritis Study Group, 1991). The pain varies in severity but typically does not interfere with sleep and usually resolves within a week. Pain can be absent or present as a headache particularly if the lesion is limited to the intracanalicular or intracranial portion of the nerve. Patients may also report difficulty in perceiving colours and may describe reds in particular as looking 'washed out'. Phosphenes (flashes of light) and positive visual phenomena on eye movements are also described, and were reported in 30% of patients in the ONTT.

Visual acuity in the affected eye ranges from 6/6 or better to no perception of light. In the ONTT, median visual acuity was 20/80 at study entry. Colour vision is usually abnormal and may be disproportionately affected compared to visual acuity. It would be very atypical to have acute optic neuritis with poor visual acuity but retain colour vision. In the ONTT, colour vision as assessed by Ishihara pseudo isochromatic plates was abnormal in 88% of affected eyes (Optic Neuritis Study Group, 1991). The dyschromatopsia of optic neuritis has a mixed spectral pattern with blue-yellow defects more common in the acute phase and red-green more likely at 6 months (Katz, 1995).

A visual field defect in the affected eye is frequently present. Although a central scotoma with sloping border of the isopters is classically described, in reality almost any type of visual field defect can occur. In the ONTT the most common visual field defect was 'diffuse' with

generalised reduction of the entire central 30 degrees of visual field, which occurred in 48.2% of patients (Optic Neuritis Study Group, 1991). Central defects including central scotomas, paracentral defects and centrocaecal scotomas were also seen and imply involvement of the central portion of the optic nerve. Nerve fibre bundle defects such as altitudinal and arcuate defects can also occur and imply localization to a particular group of nerve fibres (e.g. superior arcuate bundle). In general they respect the horizontal meridian because of the anatomic boundary of the horizontal raphe (Lui et al., 2010). Involvement of the chiasm can lead to bitemporal visual field defects. Sparing of central vision suggests an optic perineuritis. The visual field defects usually resolve and in the ONTT 56% had normalised by 1 year and 73% by 10 years. During the first year of follow up in the ONTT diffuse central visual field loss changed to a more localised pattern in the form of nerve fibre bundle defects and at 1 year these accounted for 35.7% of abnormalities in the affected eye. (Keltner et al., 1994; Kawasaki et al., 1996).

Low contrast acuity is reduced and can be demonstrated even in patients with acuities of 6/6 or more.

A relative afferent pupillary defect is almost always present in the affected eye, although it may be absent in mildly affected eyes, if there is bilateral involvement or if there is a pre-existing optic neuropathy in the fellow eye. Its absence may be a clue to a retinal cause for the visual loss, e.g. central serous retinopathy. An RAPD can be exaggerated by holding a 0.3 log unit density filter in front of the affected eye (Kawasaki et al., 1996).

Papillitis or disc swelling may be present in up to a third of patients and is diffuse. Marked haemorrhages are unusual as are segmental or altitudinal swelling, disc pallor or arterial attenuation and lipid maculopathy, and are more suggestive of other diagnoses (e.g. anterior ischaemic optic neuropathy). Two thirds of patients have a retrobulbar optic neuritis with normal fundoscopy in the acute phase (Optic Neuritis Study Group, 1991).

Uveitis or cells in the anterior chamber would be atypical and are more commonly present in other autoimmune diseases or infections.

Retinal periphelibitis (perivenous sheathing) has been reported in up to 12% of patients with optic neuritis and their presence is associated with a higher risk of subsequent conversion to clinically definite multiple sclerosis (Lightman et al., 1987). More detailed information of the clinical features (typical and atypical) and differential diagnosis are provided in Table 2-1, Table 2-2 and Table 2-3.

Other associated symptomatology includes Uhthoff's and Pulfrich's phenomenon (these are discussed in more detail later on see section 2.9)

Table 2-1: Clinical features of typical optic neuritis (% taken from ONTT)

Female (77%)
White (85%)
Young adult (mean age 32+/- 6.7 yrs.)
Periocular pain (92%) Exacerbated by eye movements (87%).
Progressive unilateral visual loss over days of variable severity
Spontaneous improvement within 2 weeks regardless treatment (>90% of patients)
Previous history of neurological symptoms
Uhthoff's phenomenon (exercise or heat-induced deterioration of visual symptoms, occurs in 50% of patients)
Pulfrich's phenomenon: misperception of the direction of movement due to asymmetry of conduction velocity in the optic nerves)
Photopsias
Dychromatopsia (85%) and reduced contrast vision
Swollen optic disc (35%), normal optic disc (65%).
Visual field defect (any type – most common in ONTT diffuse (48%))
Relative afferent pupillary defect
Normal macular and peripheral retina
Retinal periphlebitis/uveitis
Ancillary investigations suggestive of MS

Table 2-2: Clinical features of atypical optic neuritis (Adapted from Hickman et al 2002, panel 3)

(Hickman et al., 2002)

Age>50
Afro-Caribbean
Bilateral simultaneous onset of optic neuritis or rapidly sequential optic neuritis in an adult
Chiasmitis
Severe visual loss to no perception of light without early recovery
Lack of pain
Severe pain that restricts eye movements or disrupts sleep
Persistent pain for > 2 weeks
Severe headache
Photophobia
Ocular findings suggestive of an inflammatory process e.g. anterior uveitis, macular exudates, retinal inflammation
Severe disc swelling
Marked haemorrhage
Lack of significant improvement of visual function or worsening of visual function after 30 days
Lack of at least one line of improvement in visual acuity within 3 weeks of onset of symptoms

Table 2-3: Differential diagnosis of optic neuritis (Adapted from Hickman et al 2002, panel 2)

Corticosteroid-responsive optic neuropathies	Clinical features	Investigations
Sarcoidosis SLE Autoimmune optic neuritis Chronic relapsing inflammatory optic neuritis Optic Perineuritis Behcet's disease Neuromyelitis Optica	Progressive severe visual loss Recurrent episodes of ON Pain may be severe Often bilateral Multisystem More common in Afro Caribbeans	MRI brain and orbits with contrast Serum ACE, Biopsy of accessible tissue LP Autoimmune profile CXR, PET scan AQP4 antibodies
Other inflammatory Post-infectious Post-vaccination ADEM Neuroretinitis	Bilateral Often in children, swollen discs, lipid exudates, macular star Good prognosis	MRI brain and orbits with contrast LP Bartonella, borrelia and syphilis serology
Infectious Bacteria Syphilis Tuberculosis Lyme disease Bartonella henselae (Cat scratch disease) Whipple's disease Brucellosis	Progressive loss after exposure to infectious agent Cells in the anterior chamber Severe disc swelling History of travel	MRI brain and orbits with contrast LP Bartonella, borrelia, syphiilis serology Lyme serology CXR, Mantoux test Duodenal biopsy
Fungal Aspergillus Histoplasmosis Cryptococcus **Protozoal** Toxoplasmosis	Immunosuppressed History of exposure Immunosuppressed History of exposure	MRI brain and orbits with contrast LP, CXR C+S Tissue biopsy Histioplasma antibodies Western blot PCR
Viral Viral optic neuritis HIV related		HIV serology CT brain with contrast

Local infection		
Periorbital cellulitis Paranasal sinusitis		
Toxic and nutritional		
Vitamin B12 deficiency Tobacco-alcohol amblyopia Methanol intoxication Ethambutol toxicity Emerging evidence of cobalt toxicity Cuban and Tanzanian epidemic optic neuropathies Radiation	Bilateral, painless, progressive History of alcohol/tobacco excess History of exposure to toxin History of brain irradiation	Serum B12/folate levels MMA FBC
Inherited optic neuropathies		
Leber's hereditary optic neuropathy	Young male (80-90%) sequential, bilateral visual loss Painless Circumpapillary telangiectasia Family history	Genetic testing (Leber's mutations)
Compressive optic neuropathies		
Primary tumours e.g. meningiomas, gliomas Metastases Tuberculomas Thyroid opthalmopathy Arterial aneurysms	Painless, progressive visual loss Optic atrophy at presentation History of Malignancy Proptosis, diplopia	CT/MRI brain and orbits with contrast Consider biopsy Thyroid function tests + TPO antibodies Cerebral angiogram
Ischaemic optic neuropathies		
Anterior ischaemic optic neuropathy Giant cell arteritis (GCA) Diabetic papillopathy Susac's syndrome	Older patient Sudden onset Painless (except GCA) Altitudinal field defect Disc swelling, haemorrhages Fellow eye crowded with small cup Hearing loss, encephalitis	ESR, temporal artery biopsy echo, 24 hr tape Carotid dopplers Audiogram, OCT
Ocular or retinal disease		

Posterior scleritis Central serous retinopathy White dot syndromes acute zonular occult outer retinopathy (AZOOR) Autoimmune retinopathies (melanoma –associated retinopathy).	severe pain, relatively preserved vision, proptosis painless, central blurring metamorphopsia, young male, good recovery VF abnormality with preserved colour vision History of malignancy (melanoma)	USS orbits, ANCA OCT, fluorescein Angiogram electroretinogram
Miscellaneous		
Functional	May be associated with other neurological symptoms. Inconsistencies between symptoms & subjective visual function tests	Flash VEPS
Snake bite Bee or wasp sting		

2.2 Investigations

Generally, optic neuritis is a clinical diagnosis based on history and examination findings and an ophthalmic examination is an essential part of this. As such diagnostic tests should be aimed at excluding atypical causes of optic neuritis and prognostication of future risk of MS.

With the exception of prognostic information, the yield from diagnostic tests in typical cases of demyelinating optic neuritis is extremely low (Shams and Plant, 2009). However, in the presence of any atypical features suggestive of an alternative diagnosis investigations should be initiated promptly and should be guided by the clinical presentation (See table 3). In atypical cases, delay in diagnosis and treatment can result in a much worse visual outcome(Hickman et al., 2002b). Early follow up should be arranged to ensure visual recovery has begun, and if not, the diagnosis revisited.

2.2.1 Magnetic resonance Imaging

MRI of the brain may provide confirmation of the diagnosis of MS or identify patients at higher risk of MS In the future. The McDonald 2010 criteria (Polman et al., 2011) require evidence of dissemination in time and space to confirm a diagnosis of multiple sclerosis using the following criteria:

Dissemination in space

At least one lesion visible on a T2-weighted scan in at least two of four locations: juxtacortical, periventricular, infratentorial, and spinal cord

Dissemination in time

A new T2 lesion or gadolinium-enhancing lesion visible on a follow-up MRI scan when compared with a previous scan obtained at any time after the onset of symptoms; or

An MRI scan showing both gadolinium-enhancing and non-enhancing lesions that do not cause clinical signs (i.e. asymptomatic lesions)

These criteria have subsequently been updated further by the MAGNIMS network in Jan 2016 (Filippi et al., 2016) based on the availability of new evidence on the application of MRI to demonstrate dissemination in time and space as well as improvements in MRI technology resulting in new acquisition sequences. The main revisions to the above criteria are detailed below:

1) An increase in the number of lesions required in the periventricular area from one to three in order to demonstrate dissemination in space (as a single lesion was not deemed sufficiently specific for a demyelinating inflammatory event)

2) To include one or more lesions in the optic nerve as evidence of dissemination in space

3) Expansion of the term 'juxtacortical lesion' to cortical/juxtacortical lesions since intracortical, leukocortical and juxtacortical lesions cannot be reliably distinguished using conventional MRI scans. Where available advanced imaging techniques should be used to visualise cortical lesions

4) No distinction between symptomatic and asymptomatic lesions for dissemination in time and space as evidence suggests inclusion of the symptomatic lesion may increase the sensitivity of MRI diagnostic criteria for MS without compromising specificity.

5) Imaging of the whole spinal cord is recommended to define dissemination in space (especially in patients who do not fulfill brain MRI criteria for dissemination in space) but spinal cord imaging has a limited role for identification of dissemination in time.

Although historically difficult to image due to its small size and propensity for motion artifact, short tau inversion recovery, fast spin echo and fluid attenuated inversion recovery with fat suppression techniques have improved imaging of the optic nerve. These sequences allow identification of intrinsic lesions within the optic nerve as well as compressive (Gass and Moseley, 2000) .

Optic nerve inflammation, as suggested by high T2 weighted signal abnormality, swelling and contrast enhancement on T1 weighted images, can be demonstrated in 95% of patients with acute optic neuritis (Kupersmith et al., 2002). The longitudinal extent of the optic nerve lesion correlates with visual loss at presentation as well as overall visual outcome. Gadolinium enhancement persists for a mean of 30 days (68 days (median) with triple dose gadolinium)(Hickman et al., 2004b) after onset of symptoms. Contrast enhancement features have little impact on visual recovery and final visual outcome (Hickman et al., 2004b). T2 weighted signal abnormality persists even after visual recovery. Longer lesions involving the intracranial optic nerve and chiasm are more typical of NM0 (Khanna et al., 2012).

In granulomatous disease, e.g., sarcoidosis, an optic perineuritis may be seen (enhancement of the optic nerve sheath) in addition to basal meningeal enhancement and enhancing brain lesions.

White matter lesions on T2 weighted and gadolinium enhanced MRI are usually seen in 50-70% of demyelinating optic neuritis (Ormerod et al., 1986; Beck et al., 1993; Frederiksen et al., 1989). Characteristic demyelinating lesions are typically ≥ 3mm in diameter, ovoid in shape and often located in the periventricular white matter. Other typical locations of white matter lesions include juxtacortical, infratentorial and the spinal cord. Flair sequences allow for improved identification of periventricular lesions due to suppression of CSF.

It is important to note that T2 weighted white matter abnormalities are not specific for demyelination and can be due to other causes e.g. small vessel disease.

In the optic neuritis treatment trial the risk of developing multiple sclerosis within 10 years of the first episode of optic neuritis was 56% amongst patients with one or more white matter lesions on MRI compared to 22% of patients with no lesions (Beck et al., 2003).

The risk of conversion to clinically definite MS increases if asymptomatic spinal cord lesions in addition to brain lesions are present at baseline. In one study of patients with clinically isolated syndromes 48% of patients with brain and spinal cord lesions developed MS compared to 18% of patients with brain lesions in isolation (Brex et al., 1999; Swanton et al., 2010). However the yield of spinal cord imaging in unselected patients is low (Dalton et al., 2003) it is therefore not recommended that imaging of the spinal cord is undertaken routinely after an episode of optic neuritis. Swanton et al., 2010 found that higher numbers of baseline periventricular T2 weighted lesions and new T2 lesions on early follow up scan were predictive of clinically definite MS after isolated optic neuritis. The same group found that spinal cord, infratentorial and gadolinium enhancing lesions within 3 months of optic neuritis was predictive of disability but only spinal cord lesions were predictive in patients converting to clinically definite MS (Swanton et al., 2009).

2.2.2 Lumbar puncture

Lumbar puncture should be considered if an atypical cause, particularly infectious or inflammatory, is suspected. In typical demyelinating optic neuritis lumbar puncture as a routine investigation is not generally required. In the optic neuritis treatment trial no patient had the diagnosis or management altered as a result of CSF findings. Approximately 60-80% of patients with acute optic neuritis have non-specific CSF abnormalities (Jacobs, 1997). In the ONTT CSF abnormalities included raised WCC (36% of patients had >6 white cells per cubic mm, highest WCC 27/ml), raised total protein (9.4% of patients had total protein > 50mg/dl), raised CSF Ig G concentration, oligoclonal bands (present in 50%) of patients and raised myelin basic protein levels.

In the ONTT the presence of oligoclonal bands in the CSF was correlated with subsequent risk of developing MS but this was not independent of MRI abnormalities as these patients also tended to have abnormal baseline MRI brain scans. CSF oligoclonal bands may be a more useful predictor of future MS risk in patients with a normal MRI brain (Rolak et al., 1996).

2.2.3 Visual Evoked Potentials

Are generally of limited utility in the diagnosis of optic neuritis and do not allow differentiation between the different causes of an optic neuropathy in the acute phase except in the case of functional visual loss.

The combination of visual evoked potentials (VEP) and pattern electroretinogram can be helpful in distinguishing optic nerve from retinal disorders. In retinal disorders both the P50 (early) and (N95) late components of the PERG are abnormal whereas only the late N95 component is abnormal in optic nerve disorders (although both may be affected acutely).

In acute optic neuritis the VEP typically demonstrates a delayed P100 response with a well preserved waveform and only modestly reduced amplitude, which is a manifestation of conduction slowing and partial block in the optic nerve as a result of demyelination. After one year 80-90% of patients will have residual abnormalities on VEPs (Brusa et al., 2001).

Mulitfocal VEPs appear to be more sensitive and specific than conventional VEPs for diagnosing optic neuritis (Fraser et al., 2006) although they are technically more challenging.

2.2.4 Optical Coherence Tomography

This modality is the optical analogue of B mode ultrasound and uses the backscatter of near infrared light to produce two and three-dimensional images of retinal ultrastructure. It has been used to demonstrate axonal loss in the optic nerve by taking measurements of retinal nerve fibre layer (RNFL) thickness and is increasingly being used as an outcome measure for axonal loss in MS and optic neuritis research. 85 % of patients will have demonstrable retinal nerve fibre layer thinning after an episode of optic neuritis and lower RNFL thickness measurements have been shown to correlate with worse visual outcome (Costello et al., 2006; Trip et al., 2005). Acutely there may be RNFL swelling and this is much more common than once thought, occurring in approximately 82 % of affected nerves and remains evident in at least one quadrant in the majority of patients at 12 weeks (Costello et al., 2006). It is therefore prudent to allow at least three months after an episode of optic neuritis before attempting to quantify RNFL atrophy (Henderson et al., 2010).

Isolated thickening of the inner nuclear layer with associated microcystic macular oedema has also been reported in association with MS related optic neuritis (Gelfand et al., 2012; Gelfand et al., 2013). However this is much more common in NMO (20% of patients), (Gelfand et al., 2013) than MSON (5% of patients) and should prompt testing with aquaporin 4 antibodies. A more detailed evaluation of the role of OCT in optic neuritis is given in Section 3.6.

Figure 2-1: Optical coherence tomography scan demonstrating atrophy of the retinal nerve fibre layer six months after optic neuritis

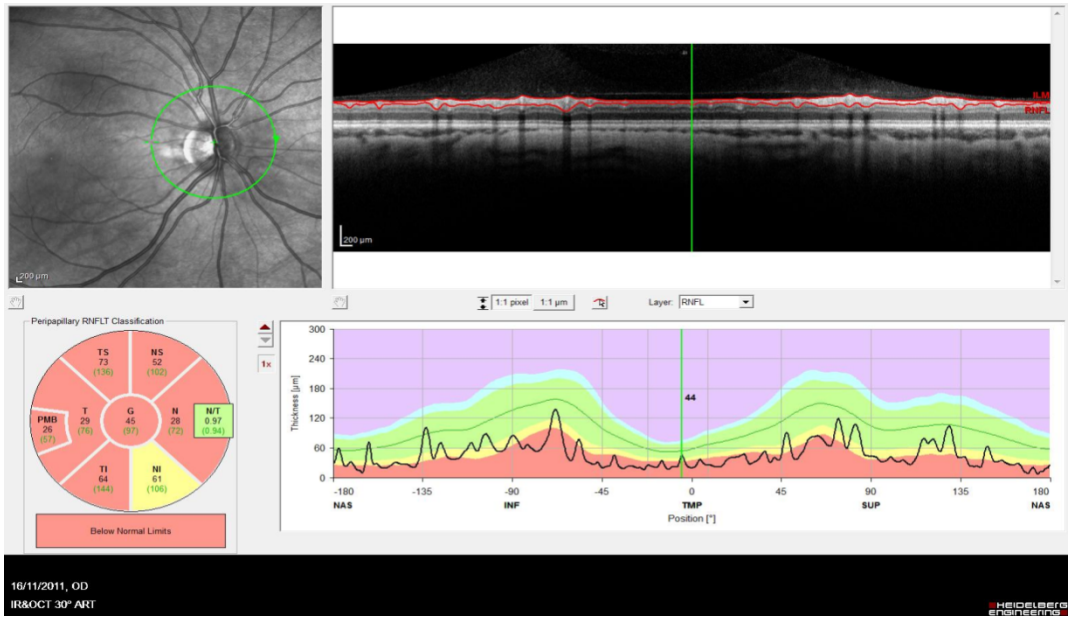

Heidelberg Spectralis retinal nerve fibre layer scan. **Top left image**: Fundus photograph-Retinal nerve fibre layer measurements are taken from the peripapillary region, as delineated by the green circle of 3.4mm diameter centered on the optic disc, and compared to a normative database. **Top right image**: OCT image of the peripapillary retina. OCT software automatically segments the retinal fibre layer delineated by the red lines. **Bottom left image:** Pie chart demonstrating mean global and sectoral RNFL thickness measurements. Top value is the measured mean RNFL thickness for each sector. Bottom value is the mean age adjusted normal value. If the RNFL thickness of the sector is above the 5th percentile of the normal distribution it is coloured green, between 1st and 5th percentile it's coloured yellow and below the 1st percentile it's coloured red. **Bottom right**: Graph demonstrating the RNFL thickness profile measured along the circular scan (black line) and its comparison to the normal range. The green band represents the normal range of RNFL thickness defined as between 5th and 95th percentile of normal distribution. Red area denotes range below 1st percentile and yellow band represents values below 5th but above the 1st percentile of normal distribution.

2.3 Treatment

2.3.1 Acute treatment

The findings of the optic neuritis treatment trial (ONTT) and its extension study have had a major influence on current clinical practice of the treatment of acute demyelinating optic neuritis. The primary aim of the ONTT was to evaluate the effect of intravenous methylprednisolone and oral corticosteroid therapy on visual outcome. The secondary aim was to assess the affect of corticosteroid treatment on future risk of conversion to clinically

definite multiple sclerosis. 457 patients were enrolled within 8 days of visual loss and were (Beck et al., 1992b)randomised to one of three arms (Beck et al., 1992b):

1) Oral prednisone 1mg/kg/day for 14 days followed by a 4 day oral taper
2) Intravenous methylprednisolone 250mg every 6 hours for 3 days followed by oral prednisone 1mg/kg/day for 11 days with 4 day taper.
3) Oral placebo for 14 days.

The trial was double blinded

Patients in the intravenous methyprednisolone arm experienced faster visual recovery particularly during the first 15 days compared to the other arms. However at 1 year follow up there was no significant difference in visual outcomes between the three treatment groups. When the presenting visual acuity was 6/12 or better corticosteroids conferred no benefit.

Patients randomised to the intravenous methylpredisolone arm were also at reduced risk of conversion to clinically definite MS at 2 years compared to the other arms (7.5% IVMP versus 14.7% placebo) and 16.7% prednisone). However, this effect was not born out after five years (Optic Neuritis Study Group, 1997). These findings were as a result of a post-hoc analysis and patients in the IV methylprednisolone group were not blinded to treatment.

In the ONTT the use of oral prednisone was associated with an increased rate of recurrent optic neuritis in either eye compared with the other two treatment arms (30% vs. 13% methylprednisolone and 16.7% placebo) within the first two years. At 10 years the risk of recurrent optic neuritis remained higher in the oral prednisone group but was no longer statistically significant (Beck et al., 2004). This result should be interpreted with caution given that this effect has not been confirmed in other studies and the trial was not designed to investigate this as an outcome measure. There is no definitive biological explanation and it may therefore be a chance finding.

Findings in other trials of corticosteroids in optic neuritis are reported in Table 2-4.

Table 2-4: Trials of corticosteroids in acute optic neuritis (Adapted from Kaufman et al, 2000 (Table 2))

Study	Treatment arms	Visual Outcome
Rawson et al 1966 (Class I)	40 units IM ACTH/ IM placebo a day for 30 days	Faster recovery of VA at 30 days in active arm; at 1 yr no significant difference between arms; small number of pts. (25 per arm)
Bowden et al 1974 (Class I)	40 units IM ACTH/IM placebo a day for 30 days	No significant difference in VA between treatment arms at 1 year small number of pts. (27 per arm)
Kapoor et al 1998 (Class I)	1g IV methylprednisnolone/ iv saline for 3 days	No significant treatment affect at 6 months, no treatment effect on lesion all patients had optic canal lesions (33 pts per arm)
Sellebjerg et al 1999 (Class I)	500mg po methylprednisolone/placebo for 5 days with 10 day oral taper	Increased speed of recovery in treated group (p=0.008), no long term benefit compared to placebo. Increase in recurrence of ON at 1 yr in methylprednisolone group (30 pts per arm)
Gould et al 1977 (Class I)	stat dose 40mg retrobulbar triamcinolone No placebo group Follow up at 6 months	Treatment group faster visual recovery but no significant difference at 6 months 31 pts treatment arm 30 controls)
Wakakura et al 1990 (Class II)	1g 1VMP for 3 days/ iv mecobalamin 500 µ for 3 days followed by oral taper for 7 days	IVMP group faster rate of visual recovery but no significant difference at 12wks/ 1 yr (33 pts per arm) (33 pts per arm)
Trauzettel-Klosinski et al 1991 (Class II)	100mg po MP per day/ followed by tapering dose for 24d or po thiamine	Faster visual recovery in MP group but no significant treatment effect at 12

		months Partially randomized
Spoor and Rockwell et al 1988 (Class III)	1-2 g IVMP, not randomised or placebo controlled	Rapid rate of recovery in 12 pts given IVMP

A meta-analysis of 12 randomised controlled trials showed that corticosteroids reduced the number of patients without clinical improvement at 30 days (odds ratio 0.6, range 0.42-0.85) but did not result in long-term improvement of visual outcome even in patients with severe visual loss (Brusaferri and Candelise, 2000).

The report of the Quality Standards Committee of the American Academy of Neurology states that the decision to use higher dose oral or parenteral methylprednisolone should therefore be based on factors such as quality of life, visual function in the fellow eye or other situations, e.g. in the case of severe or bilateral visual loss (Kaufman et al., 2000).

Acute immunomodulatory therapy

Intravenous immunoglobulin has not been shown to have a beneficial effect in the treatment of optic neuritis. Two randomised controlled trials looking at the efficacy of IVIG in the treatment of optic neuritis did not demonstrate any difference in visual or MRI outcome or subsequent demyelinating events at 6 months (Noseworthy et al., 2001; Roed et al., 2005).

Plasmapheresis

Evidence is currently from observational cohort studies of patients with steroid resistant demyelinating optic neuritis and may be beneficial if instituted early. In a case series of 23 patients (10 with RRMS) 70% improved with plasmapheresis given after two cycles of intravenous methylprednisolone (Roesner et al., 2012).

2.3.2 Long-term immunomodulatory therapy

Guidelines on the use of immunomodulatory therapy after CIS vary internationally. In the US DMD therapy is discussed with patients after an episode of demyelinating optic neuritis that have at least two typical demyelinating white matter lesions on MRI. However, in the UK DMDs are generally only used if a second clinical attack occurs within 2 years of the optic neuritis.

Three trials have investigated the efficacy of beta interferons in reducing the risk of developing MS after a clinically isolated syndrome.

The CHAMPS study (Jacobs et al., 2000) was a randomised placebo controlled trial comparing early treatment with intramuscular interferon beta-1a 30 µg once a week versus placebo. 383 patients were randomised (50% with isolated optic neuritis). All patients had two or more typical demyelinating lesions on MRI scan. Patients received treatment with intravenous methylprednisolone within 14 days of symptom onset and were randomised to commence intramuscular interferon beta-1a/placebo within one month.

The study was terminated early because the cumulative probability of developing clinically definite MS was 35% in the treated group compared to 50% on the placebo group (p=0.002). There was also a reduction in new T2 weighted lesions and T1 gadolinium enhancing lesions on MRI at 18 months in the treated group.

In the ETOMS (Comi et al., 2001) 308 patients were randomised within three months of their first clinical demyelinating event to receive either interferon beta-1a 22µg once a week or placebo. All patients had at least four white matter lesions or three with at least one that enhanced with gadolinium. 35% of patients had an acute optic neuritis. At two years the proportion of patients who had developed clinically definite MS was 34% in the active group versus 45% in the placebo group. Amongst those patients who did develop clinically definite MS, onset was delayed in the active versus placebo group (569 days versus 252 days (30^{th} centile)). Additionally there was a reduction in the new T2 weighted lesions in the treatment group.

More recently the BENEFIT trial randomly assigned 487 patients with clinically isolated syndromes to receive ether interferon-1b 250µg once every other day or placebo. The results were consistent with the CHAMPS and ETOMs trials with a reduction in the risk of developing clinically definite MS in the treatment group (28% versus 45% in the placebo group) as well as reducing the amount of disease activity as measured by new T2 weighted lesions at 2 years (Kappos et al., 2006).

These results are consistent with the effects of DMDs in relapsing remitting MS where they reduce the number of relapses by a third.

In addition to these trials the PreCISe study investigated the effect on glatiramer acetate on conversion to clinically definite MS. 481 with a unifocal clinically isolated syndrome and two or more T2 weighted brain lesions were randomly assigned to receive glatiramer acetate 20mg od or placebo for up to 36 months. The risk of developing clinically definite MS was reduced by 45% compared to placebo and for those who did convert the time clinically definite disease was prolonged from 366 (placebo) to 722 days (glatiramer acetate) (Comi et al., 2009).

Some of the newer oral therapies have also been trialed in CIS. The TOPIC study assessed the efficacy and safety of teriflunomide in patients with a first clinical episode suggestive of MS. A double blind-placebo controlled trial that compared teriflunomide 14mg and 7 mg to placebo taken for up to 18 weeks. Teriflunomide significantly reduced the risk of a MS-defining relapse both at 7mg and 14mg ($p=0.0271$ and $p=0.0087$ respectively). Similarly, Teriflunomide at both doses significantly reduced the risk of relapse or a new MRI lesion compared to placebo (14mg, $p=0.0003$, 7mg $p=0.0020$)(Miller et al., 2014).

Oral cladribine at 5.25mg/kg and 3.5 mg/kg has also been shown to reduce the risk of time to conversion to clinically definite MS when compared to placebo ($p=<0.0001$ and $p=<0.0001$ respectively) (Leist et al., 2014).

When interpreting the results of these trials it is important to highlight that in the ONTT 40% of patients with abnormal scans had not progressed to clinically definite MS after 10 years.

Therefore, there is a risk of committing patients with a benign course to expensive long-term therapy that is not without side effects. In addition these therapies are only partially effective and according to the analysis of one study, in order to prevent one relapse a patient needs to be treated for approximately six years (Shams and Plant, 2009). Also there is some evidence that the prognosis for patients presenting with optic neuritis as a first manifestation of MS is relatively good (Ramsaransing et al., 2001). In the ONTT only 17 of the 105 patients who developed clinically definite MS had an EDSS of 3 or more after 5 years (Optic Neuritis Study Group, 1997).

2.4 Neuroprotective and remyelinating trials

Current treatment of optic neuritis with corticosteroids does not improve visual outcome and permanent visual disability after optic neuritis is largely due to axonal loss, as is discussed in more detail in section 2.11 In this context neuroprotection remains a major unmet need and identifying neuroprotective agents to prevent axonal loss along with strategies to induce remyelination (which itself may be neuroprotective) is a key area of therapeutic research. Several trials targeting potential mechanistic pathways of neuroaxonal loss including sodium channels, acid sensing channels, NMDA receptors (see Table 2-5) are underway or have been completed. Additionally an antibody against LING01, a CNS protein that down regulates oligodendrocyte precursor differentiation has been developed and has the potential to promote CNS remyelination. Trials are currently underway in acute optic neuritis and MS patients.

Table 2-5: Neuroprotective and remyelinating trials in optic neuritis

(Adapted from Table 2, Balcer et al., 2015)

Agent	Mechanism of action	Trial design	Outcome measures	Results
Simvastatin (Tsakiri et al., 2012) n= 64	Neuroprotective	Placebo-controlled Simvastatin 80mg od for 6mths Endpoints measured at 6 mths	Contrast sensitivity Visual acuity Colour vision VEPs	Borderline improvement contrast sensitivity (p=0.06) Significant improvement in VEP latency+ amplitude (p=0.01)
Erythropoeitin (Suhs et al., 2012) n=40	Neurotrophic	Placebo controlled 33000 IU/day erythropoietin for 3days Endpoints measured at 16 wks	Change between baseline at 16 wk RNFL thickness (affected eye) Visual acuity VEPS Optic nerve MRI	Reduced RNFL thinning(p=0.04) Reduced optic nerve atrophy(p=0.01) Reduced VEP latency (p=0.001)
Memantine (Esfahani et al., 2012) n=60	Neuroprotective	Placebo controlled Memantine 5mg/day for 1wk, 10mg/day for 2 wks Endpoints measured at 3 months	Change between baseline and 6mth RNFL thickness (affected eye) Visual acuity Contrast sensitivity Visual fields VEPs	Reduced RNFL thinning (p=0.01) No improvement in visual function/VEP measures
Anti-Lingo antibody (Cavidad et al., 2015 n=82)	Remyelination	Placebo controlled Anti-lingo 100mg/kg mthly for 20 wks Endpoints	Whole field VEP latency at 24wks Adjusted for baseline unaffected eye	No significant difference in VEP latency ITT analysis (p=0.33) but significant difference in

		measured at 24 weeks	measurement RNFL thickness GC/IPL thickness Low contrast acuity	per protocol analysis (p=0.05)
Amiloride (46)	Neuroprotective	Placebo controlled Amiloride 10mg of for 5 mths Endpoints measured at 6 mths	SLP +OCT RNFL thickness at 6mths adjusted for baseline unaffected eye Low contrast visual acuity Colour vision VEPs DWI posterior visual tracts MRS visual cortex	Trial in progress
Erythropoeitin (Phase 3) n=100	Neurotrophic	Placebo controlled Erythropoietin 33,000 units for 3days Endpoints measured at 6 mths	Low contrast visual acuity RNFL thickness Visual acuity Visual fields VEPs	Trial in progress

2.5 Recovery

Visual recovery usually commences within 2-4weeks and in the ONTT 93% of patients showed signs of improvement within the first five weeks (Optic Neuritis Study Group, 1991). Visual recovery can occur over months and in some patients can continue up to a year after the initial episode of optic neuritis. In the ONTT at 1 year 93% of patients had a visual acuity

of 20/40 or better and only 5% of patients had a visual acuity of 20/200 or worse (Optic Neuritis Study Group, 1997).

In the ONTT the best predictor of poor visual outcome was lower visual acuity at baseline. Despite this, 64% of patients with a visual acuity perception of light or worse recovered vision to 20/40 or better (Optic Neuritis Study Group, 1997).

Other prognostic indicators include lesion length in the optic nerve as measured with MRI with more elongated lesions being associated with poorer visual outcome. Lesions occurring in the optic canal are also associated with a worse visual prognosis (Hickman et al., 2004b).

Visual recovery may be worse in patients with MS than those without and in the ONTT older age was also associated with a slightly worse visual outcome (Optic Neuritis Study Group, 2008).

Hickman et al., 2004 found that the factors associated with a better prognosis included having a shorter enhancing lesion on triple dose gadolinium enhanced MRI, higher VEP amplitudes on follow up VEPs and a steeper gradient of initial visual improvement. They proposed that the crucial period of recovery appeared to be in the first 2 months

No other demographic factors are predictive of visual outcome.

Even with a good visual recovery in terms of visual acuity it is common for patients to continue to report subjective symptoms (Frederiksen et al., 1997). Patients often experience residual symptoms of reduced vision in bright light and glare, visual fading and Uhtoff's phenomenon.

Optic atrophy occurs in virtually all patients, even those with good visual recovery, with temporal pallor developing between four to six weeks (Shams and Plant, 2009).

VEP latencies remain delayed in most patients even with visual recovery and 80% remain abnormal at two years. However progressive latency shortening probably occurs for at least 2 years after presentation suggesting some degree of remyelination does occur for a

prolonged period of time (Brusa et al., 2001) although a small amount of shortening of latency might conceivably arise from central adaptation through synaptic plasticity.

The RAPD in the affected eye may disappear if vision recovers fully.

2.6 Recurrence

In the ONTT the rate of recurrence of optic neuritis was 19% in the affected eye, 17% for the fellow eye and 30% for either eye (Optic Neuritis Study Group, 1997). Recurrences occurred more frequently in patients who subsequently went on to develop clinically definite MS. Similarly patients with recurrent optic neuritis have a greater risk of developing MS (Beck et al., 2003). Recovery after recurrent optic neuritis is more variable than after isolated episodes.

In one study, 20-30% of patients with recurrent optic neuritis will develop seropositivity for NMO after a follow up period of up to 12 yrs. (de Seze et al., 2008)

2.7 Association with Multiple Sclerosis

The risk of developing clinically definite MS after an isolated episode of optic neuritis increases over time. In the ONTT the five-year proportion of patients diagnosed with MS was 30% and this increased to 50% at 15 years (Optic Neuritis Study Group, 2008) and the median time to diagnosis of MS was three years. Other studies similarly report a 25-35% risk of developing MS after an episode of demyelinating optic neuritis (Nilsson et al., 2005; Rodriguez et al., 1995)

Females are more likely to develop MS than males. In one study by (Rizzo and Lessell, 1988) 74% of women and 34% of men developed MS 15 years post optic neuritis. In adults, younger age at the time of the optic neuritis attack is associated with an increased risk. Ethnicity also seems to play a role with Caucasians being at increased risk (14% versus 5% non-Caucasians in the ONTT (Beck et al., 1993). Other factors that confer an increased risk of subsequent MS include evidence of retinal periphlebitis (57% of patients with periphlebitis developed MS at 3.5 year follow up in one study by (Lightman et al., 1987;

Compston, 1978) and unmatched oligoclonal bands on CSF examination and positive typing for HLA BT101 (Compston, 1978). The presence of HLA DR2 antigen may also be associated with increased risk of conversion to MS and is over-represented in certain MS populations (Hely et al., 1986).

The strongest predictor of future risk of MS is the presence of asymptomatic demyelinating lesions on brain MRI (Miller et al., 1988b). In the ONTT the risk of MS was 72% amongst patients with one or more lesions on MRI versus 25% among those with no lesions at 15 years. (Optic Neuritis Study Group, 2008). The location of the lesions also appears to be important with infratentorial lesions conferring a higher risk (Miller et al., 2005).

The presence of asymptomatic spinal cord lesions in addition to brain lesions is associated with an increased risk of early MS at 1 year as is the appearance of new T2 weighted lesions and gadolinium-enhancing lesions on repeat imaging at three months (Brex et al., 1999) .

Lesion load on MRI can also be predicative of future disability. In one CIS study baseline lesion volume and change in lesion volume in the first five years correlated with future disability (Brex et al., 2002). In another prospective study of patients presenting with optic neuritis the presence and number of infratentorial and spinal cord lesions was predicative of disability in those who subsequently developed MS (Swanton et al., 2009).

In 2001 the McDonald criteria for the diagnosis of MS were published to allow earlier diagnosis of MS based on MRI evidence of dissemination in time and space before a second clinical attack has occurred. When applied to a cohort of CIS patients with repeat imaging at 3 months the criteria had a specificity of 93% and a positive predicative value of 83% for developing clinically definite MS at 3 years (Dalton et al., 2002).

Normal MRI brain, male gender, onset in childhood, simultaneous bilateral optic neuritis, papillitis (particularly if severe), and peripapillary haemorrhage are associated with a lower risk of developing MS (Beck et al., 2003)

2.8 Pathology and Pathophysiology of optic neuritis

Pathology of optic nerve in optic neuritis and MS

There are very few studies on the pathological findings in the optic nerves of isolated acute optic neuritis. This is primarily due to the fact that the condition typically afflicts a young patient group that naturally will not die until many years afterwards and only then offer the possibility of post mortem data (biopsy of the acute lesion is not reasonable because of the potential risk of visual damage in a condition that normally has a good visual recovery).

Data from pathological studies of the optic nerve in acute and advanced MS patients have demonstrated that the demyelinating plaques are similar to those found elsewhere in the brain in MS. MS lesions in the optic nerves are found in approximately 94-99% of autopsy cases. Optic nerve lesions have been described as more diffuse and less well demarcated than brain lesions and are often associated with atrophy. Lesions may affect the whole cross section of the optic nerve or partial sections (Lumsden, 1970). The optic chiasm is often involved. Lesion lengths of 3- 30 mm have been reported in pathological studies. (McDonald, 1986).

Evangelou et al., 2001 measured axonal loss and neuronal size changes in the anterior visual pathways of eight patients who had died of MS and compared them to controls. They found that the optic nerves from MS brains had a trend towards smaller mean cross-sectional area and estimated total axon counts were reduced by 45% when compared to controls. In MS brains the parvocellular cells of the lateral geniculate nucleus were significantly smaller than controls and this correlated with the axonal loss in the optic nerves. This was not true of the magnocellular cells that were similar in MS brains and controls. They concluded that there appears to be selective atrophy of smaller neurons in the parvocellular nucleus as a result of transynaptic atrophy preferentially affecting smaller axons.

Gartner, 1953 examined 14 eyes from 10 patients with advanced MS. They found optic atrophy predominantly in the temporal portion of the optic nerve with the papillomacular bundle predominantly affected in the retina. There was an increase in glial cells in the optic nerve and gliosis of the optic discs. As mentioned in Chapter 1 this has implications for

follow up retinal nerve fibre layer measurements which may not just be measuring axonal loss but also gliosis (that could 'falsely' increase RNFL thickness measurements giving the impression of axonal preservation).

Histopathological studies of EAE models of optic neuritis in animals have demonstrated inflammatory infiltrate, extensive demyelination and axonal loss in the affected optic nerves (Rao et al. 1977; Hayreh et al., 1981)

The Pathology of the acute active plaque in MS

It is believed that most plaques begin with the margination of activated autoreactive CD4+T cells across breaches in the blood brain barrier.

Although patients with MS appear similar to healthy controls in the number of T cells that react to myelin in their peripheral blood, they appear to be qualitatively different. Myelin reactive T cells in MS patients exhibit an activated phenotype compared to a naïve phenotype in healthy controls. There are also significant differences in the cytokines they release with myelin reactive T cells in MS patients being relatively more inflammatory (Frohman et al., 2006).

The existence of several putative myelin and non-myelin target antigens including myelin basic protein, myelin-associated glycoprotein and αB crystallin have been proposed. This is followed by amplification of the immune response after recognition of target antigens on antigen presenting cells and the release of proinflammatory cytokines. Lymphocytes and macrophages form perivascular cuffs around capillaries and venules. There is diffuse parenchymal infiltration by inflammatory cells and oedema with loss of oligodendrocytes and myelin. Demyelination may be due to an anti-myelin antibody that enables phagocytosis by macrophages in the presence of complement (Frohman et al., 2006).

There is inflammation, demyelination with variable gliosis and relative axonal preservation. Although there is relatively less axonal injury it does occur and is most pronounced during active inflammatory demyelination (Trapp et al., 1998).

Early MS lesions demonstrate marked heterogeneity in their pathological appearance and four distinct immune-pathological patterns have been characterised (Lucchinetti et al., 2000). Lucchinetti et al found that a single lesional type was common to all active plaques in the same patient but there was major variation in the pathological appearance of plaques in different patients. Others have not consistently confirmed this finding but it does suggest that there are a variety of different immunological mechanisms and targets responsible for inflammation and demyelination in MS and these may vary from patient to patient. The 4 types are therefore summarized below.

Type I – characterised by active demyelination on a T lymphocyte and activated macrophage/microglia inflammatory background with a lack of immunoglobulin and complement deposition. There is variable oligodendrocyte loss most marked at the active lesional border. There is a high incidence of remyelination (15% of active MS lesions).

Type II – characterised by active demyelination associated with immunoglobulin and complement deposition on myelin and macrophage phagocytosis of myelin debris on an inflammatory background. There is variable oligodendrocyte loss at the active border with a high incidence of remyelinated shadow plaques. (58% of MS patients)

Type III – ill-defined lesions show active demyelination with oligodendrocyte apoptosis and preferential loss of periaxonal myelin components. Loss of oligodendrocytes is most prominent at the active plaque border but extends into the normal appearing white matter. The inactive plaque centre is also devoid of oligodendrocytes with no remyelination shadow plaques (26% of MS patients biopsied).

Type IV lesions were very rare and exhibited profound oligodendrocyte loss in periplaque white matter.

Barnett and Prineas, 2004 challenged this classification in their series of patients who died during or shortly after and acute relapse. They propose that lesion heterogeneity is related to differences in lesion age rather than inter patient differences.

2.9 Pathophysiology of optic neuritis

To some extent we are able to visualise the pathology of the lesion in optic neuritis in vivo with MRI studies. Gadolinium enhancement occurs where there is a breakdown in the blood brain barrier and likely represents inflammation occurring in the acute lesion. Gadolinium enhancement of the optic nerve is a sensitive (94%) finding in acute optic neuritis and does not occur with old lesions (Kolappan et al., 2009). This sensitivity is increased further by using triple dose gadolinium (96%). (Hickman et al., 2004b) found that the acute enhancing lesion length using triple dose gadolinium was associated with both baseline visual acuity and final visual outcome. Duration of enhancement was not predictive of final visual outcome.

Imaging studies have correlated breakdown of the blood brain barrier and optic nerve inflammation with the initial clinical presentation. (Youl et al., 1991) demonstrated that gadolinium leakage was a consistent early feature of the optic nerve lesion and lasted a mean of 31.2 days. Gadolinium enhancement in the optic nerve lesion was associated with the symptoms and signs of an optic neuropathy as well as prolonged latency and reduced amplitude on VEPs. Conversely disappearance of gadolinium leakage was associated with recovery of VEP amplitude to a mean of 50% of the unaffected eye as well as clinical improvement. Youl et al did not find a correlation between VEP changes acutely and lesion length but follow up VEP amplitude was found to correlate inversely with lesion length. They concluded that inflammation and oedema are crucial factors in determining the reversible element of conduction block and visual impairment.

Demyelination also occurs during the active inflammatory phase. Halliday et al observed delayed pattern evoked VEP responses in eyes affected by optic neuritis with a mean latency of 155ms +/- 20.0ms compared to 121.1 +/- 5.9 in healthy controls due to demyelination and slowing of conduction in the affected optic nerve (Halliday et al., 1972) Other studies have also demonstrated that reduced amplitude and prolonged latency occurs acutely during an episode of optic neuritis.

It is therefore likely that an important cause of functional loss in the initial presentation of optic neuritis is axonal conduction block. Conduction block occurs at the site of

inflammatory demyelination but is unimpaired on either side of this. The likelihood of conduction block depends on the amount of myelin that is lost. In experimentally demyelinated central axons conduction block invariably occurs if a whole internode of myelin is lost and lasts for several days (Smith and McDonald, 1999).

Demyelination widens the nodal distance thereby increasing the electrical capacitance of the node that reduces its safety factor for conduction (Smith and McDonald, 1999). In normal axons the safety factor of nerve conduction is around 3-5 times greater than required to produce an impulse. Demyelinated axons have an inherently lower safety factor that is typically near unity. As such even small changes in environment can have significant effects on axonal conduction and clinical symptoms.

Inflammation may play also contribute to conduction block via proinflammatory cytokines e.g. tumour necrosis factor-*a,* interferon–*y,* which are potent stimulators of the inducible form of nitric oxide synthetase. Nitric oxide has been shown to induce conduction block in demyelinated axons within minutes and its effects can last for hours (Smith and McDonald, 1999). This may be due to an effect on sodium channels and mitochondrial metabolism (Bolaños et al., 1997).

In addition to the resolution of inflammation, restoration of current along the demyelinated axon may also contribute to resolution of symptoms. In experimental models of demyelinated central axons current can be restored within 2-3 weeks of demyelination even in the absence of remyelination (Felts et al., 1997). There is evidence to suggest that functional recovery is possible despite complete demyelination of axons within plaques (Wisniewski et al., 1976) and normal visual acuity can be preserved in MS patients despite significant delays in VEP latency (Halliday et al., 1972)

Restoration of current involves upregulation of sodium channels along the demyelinated segment and the adoption of a microsaltatory mode of conduction. Although conduction is restored across the demyelinated segment it is not as fast as normal resulting in increased latency of conduction. Remyelination may not play a big role in the initial stages of recovery.

Fading of Vision

The ability of demyelinated axons to conduct trains of impulses is restricted due to the gradual accumulation of the refractory period between repeated activation. This means that the maximum frequency of conduction of action potentials can be quite significantly reduced after relatively short periods of activity. This phenomenon is likely to contribute to the fading of vision in bright environments that sometimes occurs after an episode of optic neuritis.

Uhtoff's Phenomenon

This symptom was initially described by Uhtoff (1890) as the transient deterioration in vision that occurred during exercise in patients with optic neuritis. Young and Bennett first described the exacerbation of visual symptoms by increased temperature. It is a common symptom after optic neuritis and can occur in up to 33% of patients (Perkin and Rose, 1976). Although it can be apparent acutely during optic neuritis it is generally characteristic of the recovery phase. It can occur for several months to years after an episode of optic neuritis and its resolution may suggest remyelination. In a study by (Selhorst et al., 1982) VEP amplitude was found to be reduced or absent during exercise in 4 patients following optic neuritis and this was accompanied by a reduction in visual acuity. Vision recovered within 5-15 minutes after exercise cessation and was accompanied by a return in VEP amplitude to pre-exercise levels.

Uhtoff's Phenomenon can be explained by the reduced safety factor in demyelinated axons that renders them susceptible to increases in temperature with transient conduction block. Conversely ingestion of ice and reduced temperature has been shown to transiently improve symptoms.

Phosphenes

This is a perception of flashes of lights provoked by eye movements. They are believed to be the optical equivalent of Lhermitte's phenomenon. Their pathophysiology can be explained by the electrophysiological properties of demyelinated axons that render them hyper

excitable to mechanical stimuli generating spontaneous bursts of spurious (ephaptic) impulses.

Pulfrich's Phenomenon

This is the anomalous perception of the directionality of the movement of an object that occurs after an episode of unilateral optic neuritis. It is due to the asymmetry in the conduction velocity of the optic nerves that leads to a difference in latency of the cortical response to stimulation in the two eyes. In clinical practice it usually occurs in the recovery period after optic neuritis but is not as common as Uhtoff's phenomenon.

2.10 Remyelination.

Initially thought not to take place, it is now well established that extensive remyelination may occur within plaques in optic neuritis and MS. This is particularly true in early MS lesions occurring within the first few years of disease onset (Lassmann, 1998). It accounts for the appearance of shadow plaques (completely remyelinated plaques). The mature nervous system retains a pool of undifferentiated oligodendrocyte precursors. These precursor cells are recruited to the site of tissue injury and surround lesions in MS and new myelin is formed. Remyelinated plaques are characterized by decreased myelin thickness to axonal diameter ratio with short internodal distances (Bogdan et al. 2013). Oligodendrocytes expressing myelin proteins in their cytoplasm are found in close proximity to these myelin sheaths. Remyelination may be complete or incomplete. If incomplete it mostly occurs at the lesion edge. Shadow plaques are characterized by sharply circumscribed areas of myelin pallor in the normal appearing white matter. The timing of remyelination is unknown but demyelination and remyelination may occur at the same time and the two processes may occur in a dynamic equilibrium. The extent to which remyelination occurs is thought to depend upon the availability of oligodendrocyte progenitor precursor cells as well as the pro or anti-inflammatory balance and may vary from patient to patient (Bogdan et al. 2013). The degree of axonal loss and glial scar formation may also be important factors. Remyelinated plaques may be more susceptible to second hit inflammatory demyelination. Remyelination of MS lesions may have important functions including protection of axons and restoration of conduction velocity.

Remyelination is thought to occur after an episode of optic neuritis as suggested by the progressive shortening of VEP latency over time. Normalisation of VEP latency has been shown to occur in up to 38% of cases after optic neuritis. Brusa et al., 2001 demonstrated that VEP latency decreased significantly for the first year post optic neuritis and less strikingly during the second year. The most marked reduction in VEP latency occurred between 3 and 6 months. This was not accompanied by a significant functional improvement. They postulated that remyelination was the most likely cause for the progressive shortening although reorganisation of ion channel distribution and synaptic plasticity may also contribute. They suggested that the dissociation between VEP latency and visual function is that final visual outcome is dependent on axonal loss rather than remyelination.

Non-conventional MRI techniques have been used to image the extent of myelination within the optic nerve after optic neuritis in vivo. Magnetisation transfer indirectly measures the amount of macromolecular structure, e.g. myelin that is present in the tissue (Kolappan et al., 2009). Thorpe et al., 1995 demonstrated that MTR was significantly reduced in the affected optic nerves of 20 patients with optic neuritis when compared to controls. MTR reduction was negatively correlated with VEP latency suggesting it might be an indicator of demyelination. Inglese et al., 2002 measured MTR in the whole optic nerves in a cohort of patients with previous optic neuritis. Mean MTR correlated with visual acuity and was significantly reduced in the optic nerves of patients with worse visual outcome compared to those with good recovery. MTR values did not correlate with VEP latency. This may have been because the cohort of patients studied was biased towards poorer vision with more pronounced axonal loss. In a study of serial MTR imaging in acute optic neuritis (Hickman et al., 2004b) found that the mean MTR of the affected nerve lesion progressively decreased until reaching a nadir at 240 days with a minimum value of 44 pu. After this point mean the mean MTR of the affected optic nerve increased to a value of 45 pu at 1 year. Time averaged MTR and mean VEP latency was related. The subsequent rise in MTR may be attributable to remyelination.

2.11 Axonal loss

Axonal loss is now recognised as a major cause of irreversible disability in MS and impaired visual function after optic neuritis. Axonal transection and degeneration occur in the setting of acute inflammatory demyelination and the extent of axonal loss correlates with the magnitude of inflammation (Trapp et al., 1998). Axonal loss also occurs as a result of chronic demyelination (Ganter et al., 1999). It is likely that progression in MS is due to cumulative axonal loss.

Various mechanisms for axonal loss have been proposed including:

Acute

1) Proteolytic enzymes, cytokines and free radical produced by activated immune and glial cells

2) Cytotoxic CD8+ T cells

3) Oxidative stress due to nitric oxide and mitochondrial dysfunction

Sub acute

4) Glutamate excitotoxicy

5) Alterations in the expression or activity of axonal ion channels

Chronic

6) Lack of trophic support from myelin and oligodendrocytes

7) Wallerian degeneration

MRI studies have correlated axonal loss with a reduction in N-acetyl aspartate and hypo intensity on T1 weighted images (T1 black holes) and brain atrophy (Bjartmar et al., 2000; van Waesberghe et al., 1999).

Alterations in axonal cytoskeleton and fast axonal transport have been used to indirectly demonstrate pathology in demyelinated axons. Amyloid precursor protein is transported by fast axonal transport and accumulates when this is disrupted. Ferguson et al., 1997 demonstrated accumulation of APP in active MS lesions, particularly occurring in terminal axonal swellings suggesting axonal transection. They were found to correlate with the degree of inflammation. Trapp et al., 1998 demonstrated that acute lesions contained more than 11,000 transected axons per mm^3 compared to 1 transected axon per mm^3 in controls.

Despite the fact that axonal loss is extensive in acute lesions the plasticity of the CNS may compensate for this and in the early stages of MS axonal loss may not associated with significant disability initially. However, cumulative loss of axons over time as a result of inflammatory demyelination is likely to lead to irreversible disability. There may be a threshold of axonal loss beyond which the brain can no longer compensate that marks the transition from the relapsing to the progressive phase of MS.

After optic neuritis several studies have demonstrated that VEP amplitude correlates with visual outcome (Halliday et al., 1973). This suggests that amount of axonal loss after an episode of optic neuritis is predictive of visual outcome although a component of reduced VEP amplitude may reflect conduction block due to demyelination.

Quantifying atrophy of the optic nerve using MRI gives an indication of axonal loss after optic neuritis, although atrophy of tissue in MS could potentially result from demyelination or axonal loss. However, axons contribute twice as much bulk to white matter than myelin (Miller et al., 2002) and are therefore likely to be the important determinant of atrophy.

In a cross-sectional study of 17 patients with a previous episode of unilateral optic neuritis, Hickman et al., 2001 were reliably able to demonstrate optic nerve atrophy following optic neuritis. A subsequent serial MRI study in acute optic neuritis found initial optic nerve

swelling at baseline that was followed by progressive atrophy over time. At 52 weeks the mean cross-sectional are of the affected nerve was 11.3 mm^2 compared to 13.1 mm^2 in controls. They found that there was an association with baseline optic nerve mean area (when there was swelling of the nerve reflecting inflammation) and logMAR visual acuity but there was no evidence of an association at 1 year (Hickman et al., 2004b). However, in a different study of a cohort of patients with more severe visual loss, visual acuity was associated with the degree of optic nerve atrophy as well as reduced VEP amplitudes (Hickman et al., 2002a). Inglese et al., 2002 imaged the optic nerves of thirty MS patients with a previous episode of unilateral optic neuritis and found that optic nerve volume on T1 weighted images correlated with visual acuity and VEP latency.

Henderson et al., 2011 looked at early factors associated with axonal loss after optic neuritis as measured by RNFL thickness on OCT. They performed clinical, electrophysiological and MRI assessments at baseline and 3 months. They found only VEP latency and colour vision at baseline and 3 months were significantly and independently associated with RNFL thinning.

Even though most patients make a good recovery there is an average a 20% reduction of RNFL thickness in the affected eye following an episode optic neuritis (Henderson et al., 2010). Similarly, normal visual acuity is possible despite an abnormal VEP. This may be explained by a redundancy of axons in the optic nerve. A threshold level of axonal loss may be required to produce clinically significant visual loss. In a study by Frisen and Quigley (1984) nerve fibre counts were obtained from the temporal quadrants of optic nerve with optic atrophy. They found that normal visual acuity is possible despite loss of 40% of neural substrate (Frisen and Quigley, 1984).

Visual acuity depends on the quality of the optics of the eye and the processing of the image in the neural pathway from the retina to the brain. Altered optics of the eye can degrade the quality of the image, the retina has anatomical and physiological limits, and higher order neural processing can alter the perception of an image (Amesbury and Schallhorn, 2003). Consequently visual acuity depends not only on the number of functioning neural channels but is also significantly limited by other factors such as the optics of the eye and spacing of

photoreceptors. It is therefore not surprising that acuity presents a relatively insensitive and pathologically nonspecific measure of visual dysfunction after optic neuritis.

Another factor that may contribute to visual recovery after optic neuritis despite structural damage is cortical adaptation. Werring et al (2000) demonstrated extra-occipital activation, suggesting functional reorganisation of the cerebral response to a photic stimulus, after optic neuritis in patients with a good visual recovery (normal visual acuity and colour vision) when compared to normal controls. They suggested that the change in distribution of cortical activation, with activation of areas involved in visual processing and multimodal sensory integration, occurred in response to persistently abnormal afferent input to the visual cortex and could possibly have contributed to visual recovery. They postulated that activation of multimodal regions could contribute to suppression of abnormal input from the affected eye or alternatively could reflect increased attention and perhaps perceptual enhancement of a pathogically degraded stimulus (Werring et al., 2000).

Toosy et al (2005) prospectively performed functional MRI on 20 patients with acute optic neuritis at baseline, 1, 3, 6 and 12 months and correlated it with clinical function and optic nerve function. They found that baseline gadolinium enhanced lesion length was associated with lower functional activation within the visual cortex and worse vision. They also found significant fMRI changes within the right peristriate cortex and bilaterally in the occipital cortices when either affected or unaffected eyes were stimulated at baseline even when accounting for confounding structural pathology. These changes subsided after a few months. They concluded that these findings were suggestive of cortical adaptation within the extrastriate areas occurring early on after optic neuritis (Toosy et al., 2005) .

In a longitudinal study of patients with acute optic neuritis over 12 months, Jenkins et al (2010) investigated the role of neuroplasticity in higher visual areas in recovery after acute optic neuritis. They found that greater baseline fMRI responses in the lateral occipital complex were predictive of better visual outcome and vice versa. This affect was independent of measures of demyelination and neuroaxonal loss. They concluded that early neuroplasticity in higher cortical areas appears to be an important determinant of visual outcome (Jenkins et al., 2010).

Chapter 3 Clinical, Imaging and Electrophysiological Methods of Assessing Anterior Visual Pathway in Optic Neuritis

3.1 Visual function

High contrast visual acuity (HCVA) refers to the spatial resolving ability of the eye and measures the smallest size black-on white letters that can be read. Although theoretically a test of foveal function, in reality it is reflective of the integrity of the entire anterior visual system and is in fact a very crude way of measuring visual function. The most commonly used HCVA charts in research are the early treatment diabetic retinopathy study (ETDRS) charts, the gold standard used in ophthalmology clinical trials. Unlike Snellen charts each line contains an equal number of letters and change between the lines occurs in equal logarithmic steps thereby providing continuous data in the form of LogMAR visual acuity that is amenable to statistical analysis. Although visual acuity provides a reasonable assessment of the quantity of vision it is not a good measure of the quality of vision.

3.2 Low contrast letter acuity

Contrast is defined as the quantity of lightness or darkness contained by an object with respect to its background. Contrast threshold is the smallest difference in lightness and darkness between an object and its background that can be distinguished. This is usually reported as contrast sensitivity that is the reciprocal of contrast threshold (Richman et al., 2013).There are numerous different charts available to assess contrast sensitivity but Sloan low contrast letter acuity charts are the main type used in MS and optic neuritis clinical trials.

Low contrast letter acuity (LCLA) is the identification of grey letters on a white background and is assessed using Sloan charts These charts have gray letters on a white background and have a standardized format based on ETRDS visual acuity charts. Each line of letters gets progressively smaller whilst the contrast remains the same. Patients are seated at 2 metres from the chart and asked to read as many letters as they can from top to bottom. Charts at varying contrast levels are available e.g. 1.25%, 2.5%. Letter scores indicate the number of letters at a particular contrast level the patient can identify correctly with a maximum score of 70. This method of assessing contrast sensitivity has advantages in that it is easily

administered, time efficient and inexpensive. It is however important to control for factors that can affect LCLA assessment including refractory error and lighting levels of the testing environment. (Balcer et al., 2015).

Figure 3-1: Low contrast letter acuity chart

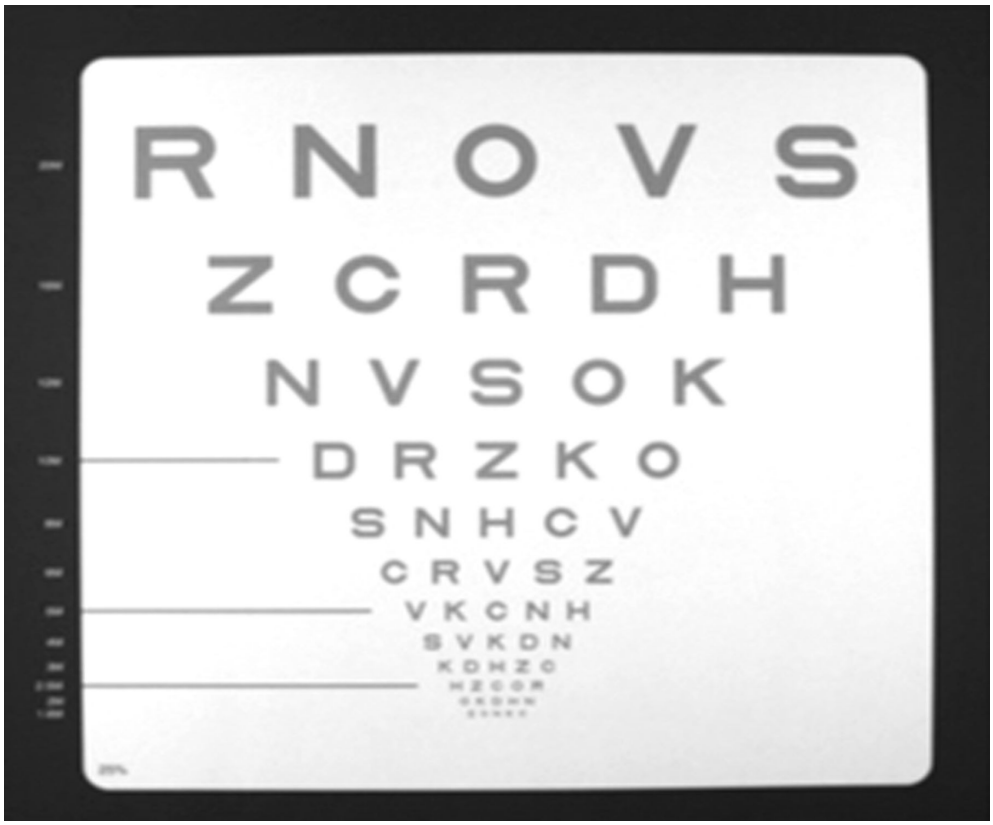

Measures of low contrast vision in optic neuritis and MS have been shown to be reliable and sensitive to visual impairment even among patients with good high contrast visual acuity (Balcer and Frohman, 2010). Low contrast letter acuity is more sensitive to subjective visual complaints and is predictive of 'real world' visual tasks such as reading rate and facial recognition (Sakai et al., 2011).

The Optic Neuritis Treatment trial was important in establishing the role of low contrast vision as an outcome measure after optic neuritis. It demonstrated that contrast sensitivity was able to elucidate persistent visual abnormalities despite recovery of high contrast vision (Beck et al., 2004). Subsequently, low contrast letter acuity was incorporated into several MS trials as

an exploratory outcome measure and visual function is now recognized as an important aspect of outcome assessment in MS trials.

A substudy of the IMPACT trial (which evaluated the efficacy and safety of interferon-1b in patients with secondary progressive MS) demonstrated that mean low contrast acuity scores were lower in MS patients than normal controls (Baier et al., 2005). This and other studies of patients with RRMS and secondary progressive MS also demonstrated that LCLA correlates with MSFC (positively) and EDSS (negatively). In the IMPACT trial the use of LCLA imparted additional value to the MSFC with regards to predicting changes in EDSS (Balcer et al., 2003).

In addition to disability, LCLA scores have been associated with T2 lesion volume and in one study for every one line (5 letters) worsening of LCLA was associated with a 3 mm^3 increase in whole brain T2 lesion volume (Wu et al., 2007).

Fischer et al found that there was a modest but highly significant correlation between mean RNFL thickness and visual function (p=0.0001); after adjusting for age there was a 3-4 μm decrease in RNFL thickness for every 1 line reduction in LCLA (Fisher et al., 2006) .

In another study by Talman et al (2010), 2.5% LCLA was significantly associated with RNFL thinning. Scores from 1.25% chart correlated less well. They postulated that floor effects may limit the capacity of 1.25% chart to capture changes in acuity as many MS patients had zero or close to zero scores limiting their capacity to demonstrate change over time. This may also be because the amount of variability in this measurement means it lacks precision. In addition they suggested that changes in LCLA at 1.25% contrast level might be more reflective of disease in the brain and posterior visual pathway (Talman et al., 2010). When considering the advantages of 2.5% versus 1.25% Sloan charts it is important to consider potential ceiling and floor effects.

Table 3-1 Mean reference values for visual and OCT assessments in MS (Taken from Sakai et al 2011, table 1)

	Disease-Free Controls	All MS	MS, No History of ON	MS, History of ON	References for Data*
High-contrast VA, ETDRS, number of letters correct	64 ± 5 (n = 61 eyes)	59 ± 8 (n = 239 eyes)	60 ± 6 (n = 150 eyes)	58 ± 9 (n = 87 eyes)	103* (22,47,56,81,84)
Binocular testing	66 ± 5 (n = 324 pts)	62 ± 8 (n = 1,007 pts)	63 ± 7 (n = 544 pts)	61 ± 10 (n = 463 pts)	56* (7–10,51)
Low-contrast letter acuity (2.5%), number of letters correct	34 ± 8 (n = 61 eyes)	26 ± 11 (n = 239 eyes)	28 ± 9 (n = 150 eyes)	22 ± 12 (n = 87 eyes)	103* (22,47,56)
Binocular testing	43 ± 6 (n = 324 pts)	36 ± 10 (n = 1,007 pts)	38 ± 9 (n = 544 pts)	35 ± 11 (n = 463 pts)	56* (7–10,51)
Low-contrast letter acuity (1.25%), number of letters correct	25 ± 7 (n = 61 eyes)	16 ± 10 (n = 239 eyes)	18 ± 10 (n = 150 eyes)	11 ± 11 (n = 87 eyes)	103* (22,47,56,81,84)
Binocular testing	34 ± 8 (n = 324 pts)	24 ± 11 (n = 1,007 pts)	26 ± 11 (n = 544 pts)	22 ± 12 (n = 463 pts)	56* (7–10,51)
NEI-VFQ-25 composite score, best score = 100	96 ± 4 (n = 31 pts)	88 ± 13 (n = 122 pts)	90 ± 12 (n = 111 pts)	85 ± 14 (n = 51 pts)	103* (49–51,56)
10-Item Neuro-Ophthalmic Supplement to the NEI-VFQ-25, best score = 100	97 ± 3 (n = 31 pts)	87 ± 13 (n = 122 pts)	88 ± 12 (n = 111 pts)	83 ± 14 (n = 51 pts)	103* (49–51,56)
TD-OCT					
Peripapillary RNFL thickness, µm	104.5 ± 10.7 (n = 219 eyes)	92.5 ± 16.7 (n = 1,058 eyes)	95.6 ± 14.5 (n = 730 eyes)	85.7 ± 19.0 (n = 328 eyes)	81* (20–22,47,70–84)
Total macular volume, mm^3	6.84 ± 0.36 (n = 219 eyes)	6.54 ± 0.51 (n = 1,058 eyes)	6.63 ± 0.48 (n = 730 eyes)	6.36 ± 0.53 (n = 328 eyes)	81* (20–22,70–84)
SD-OCT					
Peripapillary RNFL thickness, µm	92.9 ± 10.0 (n = 61 eyes)	84.3 ± 12.8 (n = 239 eyes)	87.6 ± 11.1 (n = 150 eyes)	78.4 ± 13.6 (n = 87 eyes)	103* (96,105)
GCL+IPL, µm	88.9 ± 6.9 (n = 61 eyes)	84.1 ± 8.4 (n = 239 eyes)	87.0 ± 6.6 (n = 150 eyes)	79.7 ± 9.2 (n = 87 eyes)	103* (96,105)
Macular RNFL, µm	29.6 ± 6.0 (n = 61 eyes)	23.5 ± 8.2 (n = 239 eyes)	25.5 ± 7.1 (n = 150 eyes)	20.0 ± 9.0 (n = 87 eyes)	103* (96,105)

*Reference with asterisk is source of data presented in table; references that contain similar data are in parentheses.
pts, patients; SD, spectral-domain (Cirrus platform); TD, time-domain (OCT-3 platform).

Several phase III trials in MS have shown that LCLA was able to demonstrate treatment affects. In the AFFIRM trial of natalizumab versus placebo for RRMS binocular low contrast letter acuity was measured using 1.25 and 2.5% charts Sloan charts. Patients in the active group demonstrated a reduction of cumulative probability of sustained visual loss (47% p=<0.001 at 2.5%) in addition to a sustained clinically meaningful improvement in vision (57% p=0.01). No treatment effect was demonstrated for high contrast visual acuity (Balcer et al., 2007; Balcer et al., 2012). Similar treatment effects on LCLA were shown in the SENTINAL trial (natalizumab plus IFNB-1a versus placebo plus IFNB-1a).

Measuring patient reported vision related quality of life can provide evidence for the clinical meaningfulness of structural and functional measurements. The NEI-VFQ-25 is a well validated vision related quality life measure and has been supplemented with a 10-item Neuro-opthalmic questionnaire specifically designed for MS patients for use in clinical trials (Ma et al., 2002; Raphael et al., 2006)

The issue of defining what is a 'clinically significant' improvement or deterioration of LCLA has been tackled recently and it is now well established that reductions in LCLA are reflected in worse vision-related quality of life scores (Mowry et al., 2009). Balcer et al looked at the inter-rater and test-retest reliability of LCLA and demonstrated that 7 letters corresponds to two standard deviations of difference (Balcer et al., 2000). A 7-letter reduction in LCLA IS associated with significant worsening of NEI-VFQ-25 scores as well as RNFL thickness by OCT (Talman et al., 2010) and was used in the AFFIRM trial to define clinically meaningful improvement or deteri oration (Balcer et al., 2007).

More recently measures of visual function have been used as the primary outcome measure in trials assessing potential neuroprotective therapies to improve visual recovery following optic neuritis (Tsakiri et al., 2012).

3.3 Colour Vision

Colour vision involves the detection of different spectra of light by colour sensitive cones (red, green, blue light) these project to the retinal ganglion cells. Colour vision is mainly served by the macula. RGC axons then project to the parvocellular and koniocellular

neurons in the LGN. In primate optic nerves, small axons transmit colour information. Smaller axons are concentrated in the fovea and larger axons extrafoveally

Acquired dyschromptopsia can result from injury anywhere along the visual system from photoreceptors to the visual cortex. Most standard bedside tests in neurology are optimized for detection of congenital colour deficits. Given the complexity of colour vision, methods have been developed for converting colour vision performance using the organization of coloured caps into a quantitative score. The Farnsworth Munsell 100 hue test is an example. The patient is asked to place 85 coloured caps in perceived order of hue and an error score is calculated.

Abnormalities in colour vision are common in MS in particular following optic neuritis. Even without a history of optic neuritis deficits in colour vision can be detected in up to 70% of MS patients (Gundogan et al., 2013).

Although traditionally optic neuritis has been thought to cause defects in red/green discrimination the optic neuritis treatment trial showed that no single type of colour vision defect was consistently associated with ON (Beck et al., 1992b). Katz et al analysed the raw colour vision data from the optic neuritis treatment trial. They suggested that the spatial organization of the visual field defect might be the primary determinant of the type of colour vision defect present. Central field defects were more likely to cause red/green dyschromatopsia and patients with preserved central vision more likely to have blue green dyschromatopsia (Katz, 1995)

A study by Villoslada et al confirmed and extended observations on abnormalities of colour vision in patients with MS. They were present in all disease subtypes but more severe in patients with progressive disease and visual function was weakly correlated with disease duration. They found a strong correlation between colour vision and mean RNFL thickness, temporal quadrant RNFL thickness and macular volume. Colour vision measurements were more strongly associated with OCT scores than other measurements of visual function (HCVA/LCLA).

They found colour visual function tests were strongly correlated with OCT measures at all stages of the disease strongly suggesting colour vision impairment in MS is a consequence of injury to the anterior visual pathway rather than post chiasmatic or posterior visual pathway structures. Different visual outcomes (HCVA, LCLA and colour vision) were partially but not completely correlated suggesting they may measure different aspects of the anterior visual pathway function but this could equally be due to the imprecision of measurements of visual function (Villoslada et al., 2012).

Martínez-Lapiscina et al found impaired colour vision in MS eyes without a history of ON was associated with increased disability in addition to OCT (RNFL thickness and macular volume) and MRI measures (normalized brain parenchymal volume and normalized grey matter volume) of neuroaxonal loss. Interestingly they found that inflammatory disease activity did not differ between patients with colour vision abnormalities and those without perhaps suggesting that colour vision abnormalities are more indicative of diffuse neuroaxonal loss than inflammatory activity (Martínez-Lapiscina et al., 2014).

In support of this Henderson et al found that colour vision at baseline and three months after optic neuritis were independently associated with the final degree of RNFL thinning as measured by OCT. They suggested that neurons with small axons in the parvocellular pathway are selectively vulnerable to damage after demyelinating optic neuritis (Henderson et al., 2011). This is consistent with the study by Evangelou et al that found selective atrophy of smaller neurons in the parvocellular layer of the LGN in a pathology study of 8 patients with MS (and is discussed in more detail in sections 2.8) (Evangelou et al., 2001). Post mortem studies examining the spinal cord In MS patients have also demonstrated that small axons of < 3 μm^2 are particularly affected with large fibres remaining relatively intact (DeLuca et al., 2004; Lovas et al., 2000)

This is in accordance with the findings by Flanagon et al (2005) who demonstrated that MS/ON selectively affects processing in colour pathways rather than the magnacellular pathway and within colour pathways neurons with opposed L- and M- cone inputs are more damaged than neurons from S cones. (Flanagan and Markulev, 2005).

3.4 Visual Evoked Potentials

Electrophysiological measures allow us to assess the function of the anterior visual pathway. Visual evoked potentials (VEPs) have been shown to be highly sensitive but not specific test for optic neuritis (Petzold, 2014). Conventional VEPs measure the cortical response to monocular stimulation with a single checkerboard pattern in the central 30 degrees of the visual field. The major component of the VEP is the large positive peak at about 100 milliseconds (P100) and is reliable between individuals and stable between the ages of 5 and 60. The amplitude of the P100 peak can also be measured.

Demyelination causes delay of VEP latency and conduction block. VEP amplitude is generally preserved but a reduction in amplitude acutely can reflect conduction block and later on axonal loss. The P100 amplitude may also remain attenuated due to temporal dispersion.

A positive P100 elicited by pattern reversal stimulation has been shown to originate from the V1 striate visual cortex by the combined activity of postsynaptic potentials. The magnitude of the VEP reflects the number of functioning afferents that reach the striate cortex. VEPs test pathway function with a temporal precision of milliseconds.

Small check sizes preferentially stimulate the fovea and activate mostly contrast channels. Large check sizes stimulate the fovea and extrafoveal region and activate a mixture of contrast and luminance channels.

Halliday et al were the first to demonstrate a delay in pattern reversal VEPs after optic neuritis and that the delay persisted for many years after the attack (Halliday et al., 1972). A normal VEP during acute optic neuritis has been reported in up 23% of patients (Frederiksen and Petrera, 1999).

Within a month of onset of optic neuritis visual symptoms, remyelination by oligodendrocytes commences at the edges of the plaque this is compatible with the subsequent shortening of P100 latency. In a longitudinal study by Brusa et al, VEP latency decreased significantly during the first year post ON with the most marked reduction occurring between 3 and 6 mths, and continued for up to 2 yrs. This was not, however

accompanied by a significant functional improvement (Brusa et al., 2001).

Youl et al demonstrated that gadolinium enhancement of the optic nerve lesion on MRI was associated with prolonged VEP latency and reduced amplitude and that its subsequent resolution coincided with a recovery of VEP amplitude (but not VEP latency) and visual function. They concluded that inflammation was a crucial factor in the reversible element of conduction block and and visual impairment and that functional recovery can occur in the presence of demyelination (Youl et al., 1991a).

Hickman et al in a serial longitudinal study of 22 patients after optic neuritis did not find an association between any of the baseline VEP variables and final visual outcome. Average vision scores over the follow up period tended to be better in patients with higher time averaged whole and central field VEP amplitudes and higher VEP amplitudes were associated with a better prognosis (Hickman et al., 2004b).

Several studies have demonstrated an association between VEP amplitude and RNFL thickness (Trip et al., 2005; Klistorner et al., 2008), and in a study by Henderson et al looking at early factors associated with axonal loss after optic neuritis VEP latency at baseline and 3 months was significantly and independently associated with RNFL thinning. They postulated that more extensive and prolonged demyelination leads to a greater propensity to inflammatory-mediated axonal damage (Henderson et al., 2011).

3.4.1 Pattern electroretinogram

The ERG provides a measure of functional integrity of the retinal photoreceptors and ganglion cells. The PERG is the electrophysiological response obtained by stimulation of the central retina and provides an objective measure of macular function. The PERG has two components a positive response at about 50ms referred to as P50 and a later negative response N95 at approximately 95 ms. Current data suggests that the N95 component of the human PERG is a contrast related component generated by the retinal ganglion cells. The P50 is in part ganglion cell derived but also has retinal origins distal to the ganglion cells (although these have yet to be fully elucidated, (Holder et al., 2010)).

Optic disc oedema spreading in to the macula can affect ganglion cell function and the PERG P50 and N95 waves can be reduced acutely in optic neuritis. During the recovery phase P50 amplitude recovers to within normal limits but this may not be the case for the PERG N95 wave. Selective reduction of PERG N95 wave at 4-6 weeks after optic neuritis can reflect retrograde degeneration of retinal ganglion cells. PERGs are abnormal in approximately 40% of eyes with optic nerve demyelination and in 85% of these the abnormality is a reduced N95 (Brecelj, 2014). PERG P50 amplitudes at presentation may have prognostic significance after optic neuritis as in a case series of 17 eyes with acute optic neuritis the two eyes with poor visual recovery (≤ 6/12) had PERG P50 amplitudes of < 0.5*u*V at presentation. However larger series are required to confirm this (Holder, 2001).

3.4.2 Multifocal VEP

Due to cortical overrepresentation the full field VEP is greatly dominated by the macular region. They do not provide topographical detail of optic nerve dysfunction but rather a single global response. Multifocal VEPs allow the topographic study of optic nerve function with measurement of amplitude and latency from multiple locally derived VEP responses. Averaged multifocal VEPs have a significant contribution from the peripheral part of the visual field and take recordings from 60 locations simultaneously over 44 degrees of the visual field (Laron et al., 2010). They therefore allow for assessment of a much larger cross-sectional area of the optic nerve. Multifocal VEPs have been found to correlate with visual field perimetry results. In a study of patients with recovered optic neuritis, 73 % of the affected eyes were identified as abnormal according to the VEP P100 amplitude and/or latency, while 89% had abnormal multifocal VEPs, which revealed superior performance in detecting small or peripheral defects (Klistorner et al., 2008). Responses from peripheral areas can be recorded on multifocal VEPs even when the central field has no signal on conventional VEPs.

Multifocal VEPs demonstrated a strong topographical association between RNFL thickness and VEP amplitude in the affected eye after optic neuritis. The largest reduction of RNFL thickness was seen in the temporal sector and this corresponded with the biggest reduction of mfVEP amplitude in the central part of the visual field. Superior and inferior RNFL sector thinning also correlated highly with the mfVEP derived from the corresponding areas of the

visual field (Klistorner et al., 2009).

The same group identified electrophysiological evidence of heterogeneity of lesions in optic neuritis. They performed mfVEPS in 27 pts at 1, 3, 6 and 12 months post optic neuritis and found two distinct subgroups in terms of recovery of mfVEP latency with 63% of patients demonstrating significant latency shortening over the follow up period and 37% of patient whose latency remained unchanged. They suggested that this difference in recovery may be attributable to the different histopathologic patterns of MS lesions that have previously been described, postulating that the 63% of patients with the subsequent shortening of VEP latency had type 1 and 2 lesion patterns of demyelination/remyelination and those with little or no recovery of latency had type 3 and 4 (Klistorner et al., 2007).

Multifocal VEP latency has also been shown to correlate negatively with total and temporal RNFL thickness in MS patient without a history of optic neuritis suggesting that patients with subclinical ON demyelination also have RNFL thinning (Sriram et al., 2014).

3.5 Optic Nerve Magnetic Resonance Imaging

3.5.1 Conventional Imaging

Although MRI of the optic nerve is not routinely used for the diagnosis of optic neuritis it has been used in research studies to identify and monitor the evolution of the lesion in the optic nerve as well as performing atrophy measurements. Imaging of the optic nerve is difficult because of its small size and mobility, which means that high-resolution images are essential. In addition to this, artifacts caused by surrounding CSF and orbital bone and fat due to its anatomical location are problematic.

Pathological studies have demonstrated that demyelinating optic nerve lesions are more diffuse and less well demarcated than brain lesions and are often associated with atrophy (Rocca et al., 2005). Lesions may be complete are partial in cross-section often sparing a peripheral ring.

The most effective MR imaging sequences of the optic nerve are short tau inversion recovery, (STIR) fast spin echo T2 weighted fat suppressed images and spin echo T1 pre and

post Gad fat-suppressed sequences. Periorbital fat gives a high signal on FSE images that are not heavily T2 weighted and a very high signal on T1 weighted images.

The first MRI studies in optic neuritis used short tau inversion recovery sequences (STIR) to null the signal from orbital fat. In a study of 37 patients with acute optic neuritis, STIR sequences detected 84% of lesions in the symptomatic eye (Miller et al., 1988a). Subsequently faster imaging techniques with the addition of fat saturation impulses (to suppress the signal arising from orbital fat) were developed. Fast spin echo sequences allow increased resolution with reduced acquisition times when compared to spin echo imaging. FSE images have been shown to be superior in detecting optic nerve lesions than STIR (Gass et al., 1996).

On FSE and STIR sequences CSF gives a high signal possibly obscuring signal from the optic nerves. With fluid attenuated inversion recovery (FLAIR) imaging it is possible to suppress the signal from CSF and can be combined with other sequences to allow more accurate optic nerve cross-sectional area measurements High signal in the optic nerve persists despite visual recovery. However unlike the brain, T1 hypointense lesions are not seen in the nerve; this may be due to the different architecture of the optic nerve compared to the white matter in the brain.

Gadolinium enhancement in the optic nerve occurs due to breakdown of the blood brain barrier in association with acute optic neuritis and is a consistent feature during the acute phase (Kupersmith et al., 2002). Hickman et al demonstrated that dilatation of the optic sheath immediately posterior to the globe and optic nerve sheath enhancement are also common but not specific findings on conventional MR sequences in acute optic neuritis (Hickman et al., 2005).

The disappearance of gadolinium enhancement after around 4 weeks coincides with visual recovery and an increase in VEP amplitude (Youl et al., 1991a). A study by Kuppersmith et al (2002) demonstrated that abnormal enhancement of the affected optic nerve is a sensitive finding in acute optic neuritis and was present in 94.4% of patients. There was no enhancement in clinically unaffected optic nerves, nor was enhancement seen in chronic

lesions of the optic nerve. The length of gadolinium enhancement was correlated with baseline visual function and canilicular lesions were associated with worse baseline colour vision (Kupersmith et al., 2002). Hickman et al (2004) used triple dose gadolinium in a prospective cohort of 22 patients with acute optic neuritis. They found an association between baseline gadolinium enhanced lesion length and visual outcome and reported a worsening of 0.02 logMAR units for every additional 3mm increase in baseline gadolinium–enhancing lesion length (Hickman et al., 2004b). Neither the Kupersmith nor Hickman studies found an association between the gadolinium enhanced lesion length and final visual recovery.

Quantifying atrophy of the optic nerve using MRI gives an indication of axonal loss. Hickman et al were reliably able to demonstrate atrophy of the intraorbital segment of the optic nerve using fat saturated sTE-FLAIR sequences, allowing cross-sectional area measurements using a semi-automated contouring technique (Hickman et al., 2001). In a subsequent serial MRI study in acute optic neuritis there was initial optic nerve swelling followed by progressive atrophy. At 52 weeks the mean cross-sectional area of the affected eye was 11.3 mm^2 compared to 13.1 mm^2 in controls. They found an association between baseline optic nerve mean cross-sectional area and logMAR visual acuity but there was no evidence of an association at 1 year (Hickman et al., 2002a).

Trip et al (2005) studied a cohort of patients with incomplete recovery after an episode of optic neuritis. Optic nerve cross-sectional area was reduced by 30% when compared to controls and correlated with affected eye RNFL thickness and macular volume as measured by OCT. Optic nerve cross-sectional area was also correlated with measures of visual function and whole field VEP amplitude (but not latency). The correlations with VEP amplitude and OCT measures would suggest optic nerve atrophy on MRI is reflective of axonal loss (Trip et al., 2005).

3.5.2 Non-conventional imaging – Magnetisation transfer ratio

Magnetisation transfer ratio (MTR) is a measure of the degree of proton exchange between free water and macromolecules and indirectly measures the amount of macromolecular

structure, e.g. myelin, that is present in tissues. As would be expected, MTR is higher in white matter than grey matter and is reduced in acute MS plaques.

Thorpe et al (1995) demonstrated that MTR was significantly reduced in the affected optic nerves of 20 patients with optic neuritis compared to controls. MTR was negatively correlated with VEP latency suggesting it may be an indicator of demyelination (Thorpe et al., 1995).

Inglese et al (2002) measured MTR in the whole optic nerve in a cohort of patients with previous optic neuritis. Mean MTR correlated with visual acuity and was significantly reduced in the optic nerves of patients with worse visual outcome compared to those with good recovery (Inglese et al., 2002).

In a longitudinal study of patients with acute optic neuritis, Hickman et al found that MTR values were initially unchanged during the acute phase and then subsequently declined until it reached a nadir at 8 months. After this point the mean MTR began to increase but had not returned to normal at 1 year. They suggest the increase in MTR after 8 months may be due to remyelination (Hickman et al., 2004a).

In their cohort of patients with incomplete recovery post optic neuritis, Trip et al (2005) demonstrated that whole nerve affected eye MTR and lesional nerve MTR were reduced compared to the fellow eye and controls. Mean whole nerve MTR and lesional MTR were significantly correlated with central field VEP latency as well as RNFL thickness suggesting that MTR is a measure of both axonal loss and demyelination (Trip et al., 2005).

This was supported by a study by Wang et al who found that affected nerve MTR was significantly reduced compared to the unaffected eye at three, 6 and 12 months after optic neuritis. 3 and 12 month MTR was associated with RNFL thinning at 12 months suggesting a reduction in MTR is associated with axonal loss (Wang et al., 2012).

Further studies are required to elucidate the exact contribution of axonal loss and demyelination to reduced MTR.

Ongoing developments in optic nerve imaging including increased field strengths (7 Tesla MRI), surface coils adjacent to the optic nerves and faster acquisition times may in future enable higher resolution images, with increased signal to noise ratio and reduction in motion artifact improving the quality of these images

3.6 Optical coherence tomography

Optical coherence tomography (OCT) was first described by Huang *et al*. in 1991 and was first used to image the retina in 1991 (Huang et al., 1991). OCT technology has evolved rapidly enabling the production of in vivo high-resolution cross-sectional and three-dimensional images of the retinal microstructure in real time. These OCT images closely reflect histological sections of the macula and fovea, hence the term "optical biopsy."(Blumenthal et al., 2009)

The technique was initially used for the diagnosis and management of ophthalmological diseases but over the last decade has been increasingly recognized for its applications in multiple sclerosis.

3.6.1 Basic principles of OCT

OCT is the optical analogue of B mode ultrasound, except that instead of using acoustic waves it uses light reflections to acquire images. A broad band width laser or super luminescent diode low coherence light source is scanned across the retina and the magnitude and echo time delay of backscattered light is measured. In contrast to standard ultrasound, direct detection of light echoes is not possible because of their high speed. A correlation technique is therefore required and OCT systems are based on the principle of low coherence tomography that was first described by Sir Isaac Newton. Acquisition of the OCT signal is based on splitting of the coherent light beam into two parts: a sample and a reference beam which are the same length but follow two different paths. When reflected light from each of the two paths reaches the detector at the same time they induce an interference signal. The image is acquired by measuring the amplitude of this interference signal.

3.6.2 Spectral Domain OCT

The first retinal images with spectral domain OCT were reported in 2002 and the technique became commercially available in 2006. Imaging is approximately 60-110 times faster than time domain OCT with an acquisition speed of approximately 25,000 axial scans per second and an axial image resolution of approximately 5-7µm. There is also a significant reduction of artifact from ocular movements. Spectral domain also exceeds time domain OCT in its ability to form 3 dimensional maps of the retina and optic nerve.

It is based on fast Fourier transformation and it allows all echoes of light from the different retinal layers to be measured simultaneously and the interference signal is a function of their wavelength. This eliminates the need for a moving reference mirror.

New spectral domain OCT devices include automated eye centering, longitudinal co-registration and correction for eye movements allowing for increased reproducibility of measurements.

Figure 3-2: Schematic diagram demonstrating basic principles of OCT

Taken from (Frohman et al., 2008)(Figure 1)

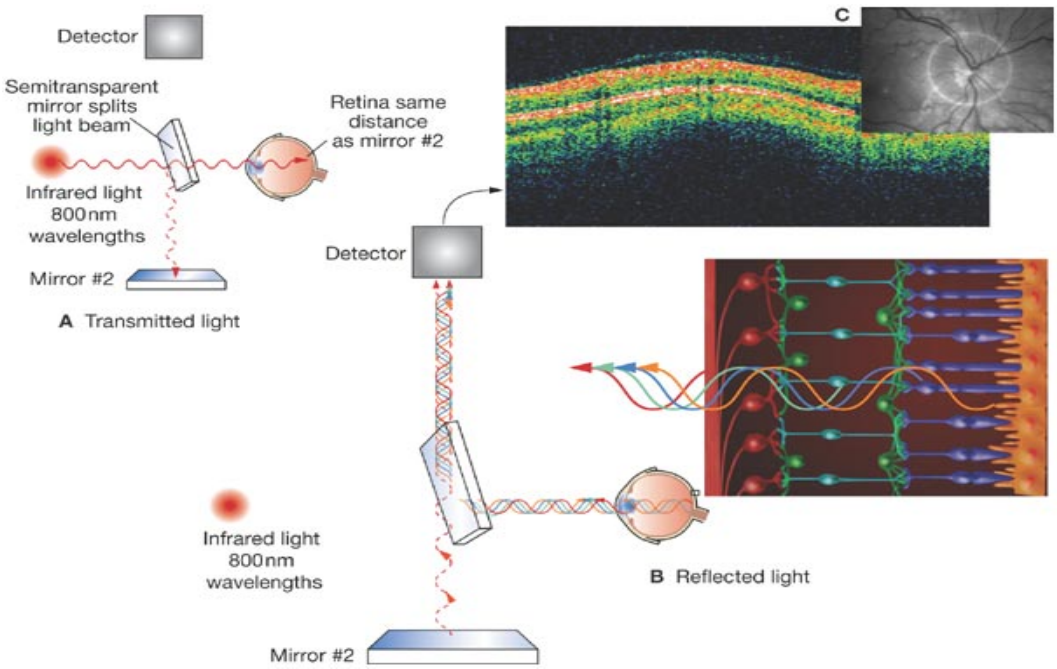

A: Low coherence infrared light is transmitted into the eye through the pupil

B: Near infra red light is scanned across the retina and the magnitude and echo time delay of backscattered light is measured from the interference signal

C: An algorithm mathematically transforms this information into a grey scale image

The first applications of OCT were in ophthalmology and it is now validated for the longitudinal assessment of glaucoma and macular degeneration. However, over the past 15 years there has been an exponential increase in the literature on its application in MS.

3.6.3 Optical coherence tomography in Optic Neuritis and MS

The retina has often been described as the window into the CNS and the afferent visual system represents an exciting prospect for MS researchers specifically with regards to the processes of neurodegeneration and repair. This is because the retina is unique in the CNS

in that it contains unmyelinated axons, which comprise the retinal nerve fibre layer (RNFL), the most proximal part of the afferent visual system and therefore thinning of the RNFL primarily represent axonal loss. OCT measurements of RNFL thickness in MS have been shown to be reliable and reproducible (Cettomai et al., 2008; Syc et al., 2010).

The anterior visual system is a frequent target of the disease process in MS. When an acute lesion affects the optic nerve during an episode of optic neuritis there is transection of axons followed by retrograde axonal degeneration culminating in loss of retinal ganglion cells and axons in the RNFL, which manifests as loss of macular volume and RNFL thinning (Figure 3-3). RNFL thinning and reduced macular volume can also occur as a result of trans-synaptic retrograde degeneration from lesions in the posterior visual pathway. In reality it is likely that axonal injury always leads to bi-directional trans-synaptic axonal degeneration (Petzold et al., 2010).

Figure 3-3: Schematic diagram demonstrating mechanisms of RNFL thinning

(Taken from Petzold et al 2010 (Figure 6))

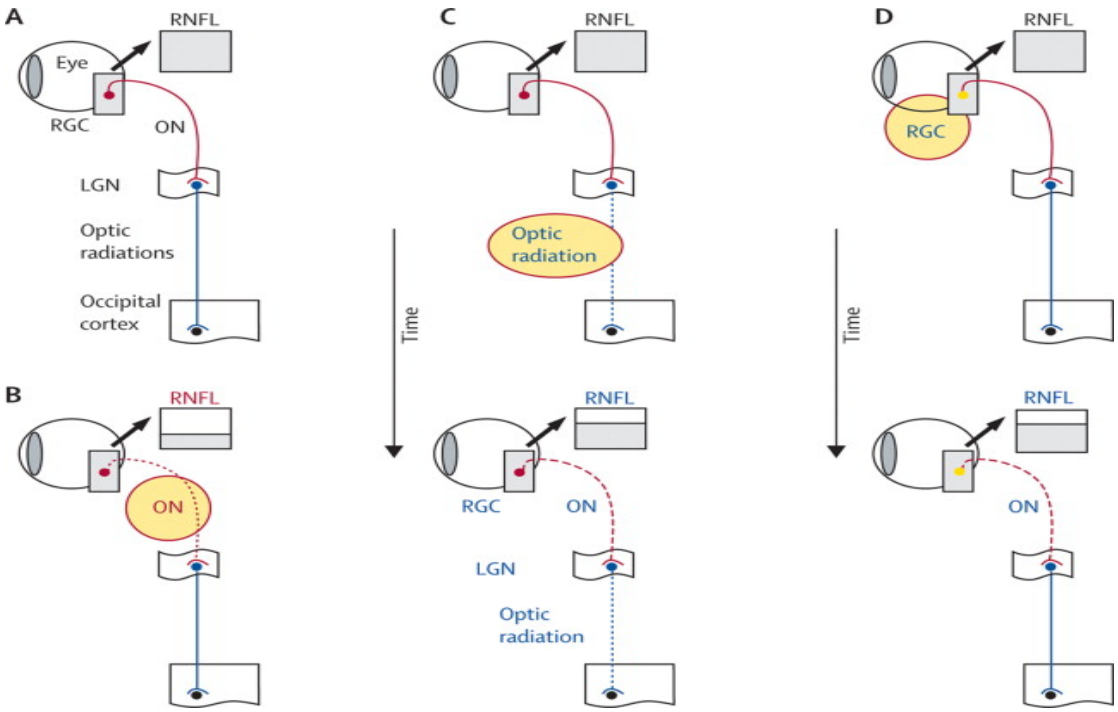

A: Schematic diagram of normal visual pathway in humans

B: Optic neuritis causes acute axonal loss within the optic nerve (red dotted line) leading to RNFL thinning

C. In MS lesions with the optic radiations can cause transynaptic axonal loss through the LGN that eventually over time leads to RNFL thinning.

D In MS chronic subclinical changes in the anterior visual system can lead to a small amount of RNFL thinning.

OCT provides a non-invasive means of quantifying the structural effects of an inflammatory lesion in the optic nerve that can be compared to functional outcomes to construct a structural-functional paradigm of CNS injury. In this way it is hoped that the neurodegenerative process occurring in the retina can be extrapolated to the processes occurring in the rest of the brain and spinal cord in patients with multiple sclerosis. This would allow the retina to be used as a biomarker for monitoring neurodegeneration in MS and also for measuring the therapeutic efficacy of neuroprotective drugs.

Parisi et al reported the earliest study of OCT in MS. They demonstrated that RNFL thickness was 46% lower in 14 MS eyes with a prior history of optic neuritis compared to controls. Importantly they also demonstrated even in MS eyes without a history of optic neuritis RNFL thickness was 26% lower than controls (Parisi et al., 1999). This innovative work was the catalyst for further OCT studies in optic neuritis and MS.

Subsequently Trip et al. investigated 25 patients after a single episode of optic neuritis (with an intentional bias towards poor visual recovery) in a retrospective cross-sectional study. The mean RNFL thickness and total macular volume of affected eyes was reduced by 33% and 11% respectively compared with controls. Greater RNFL thinning predicted worse LogMAR visual acuity, visual field abnormality, colour vision and visual evoked potential (VEP) amplitudes, consistent with axonal degeneration (Trip et al., 2005). The group also looked at the cross-sectional area of the optic nerve as measured by magnetic resonance imaging (MRI) and found that the optic nerve area of the affected eye was significantly

reduced when compared with fellow eyes and controls and that the RNFL and macular volume of the affected eye correlated significantly with optic nerve area.(Trip et al., 2006)

In 2006 Costello et al reported that 75% of patients with MS will sustain 10-40 μm of RNFL loss within a period of 3-6 months following acute optic neuritis (AON) (Costello et al., 2006).

Subsequently in a meta-analysis by Petzold including the results from 12 studies there was an estimated average loss of -20.38 μm (CI -22.86 to -17.91) in MSON eyes compared to controls (Petzold et al., 2010). This is particularly striking as the general population, (without concomitant eye disease) will only lose about 0.017% per yr or approximately 10-20 μm over 60 yrs. (Sakai et al., 2011).

Figure 3-4: RNFL thickness of MSON eyes versus controls

(Taken from metanalysis by Petzold et al 2010, Figure 3)

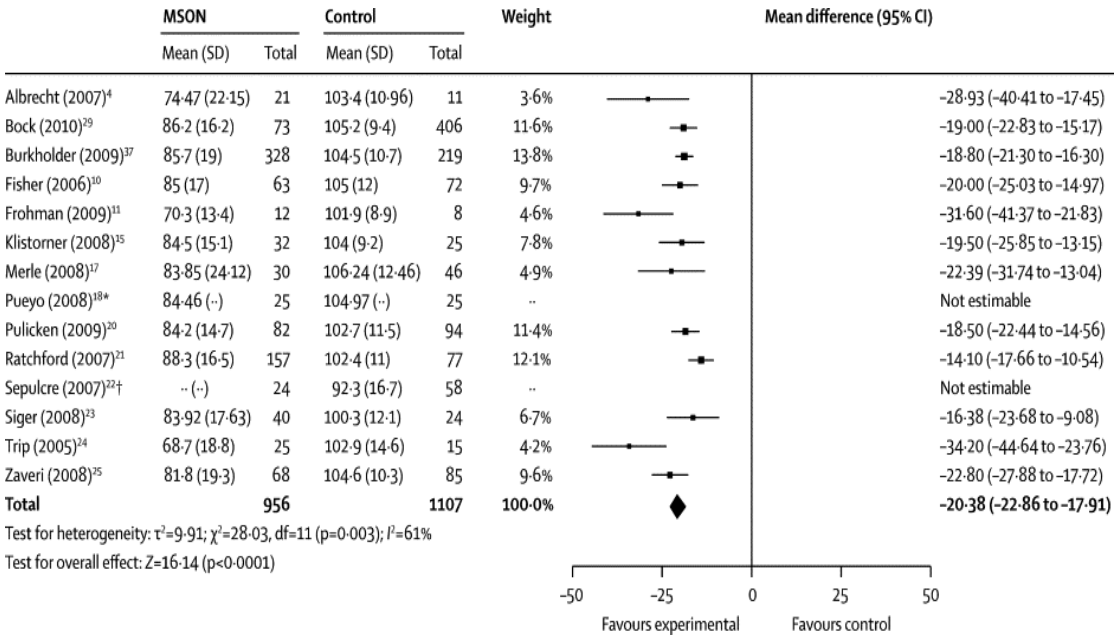

In the same meta-analysis, 15 studies comparing MS eyes without a history of optic neuritis to controls the mean estimated RNFL loss was -7.8 μm (CI -8.65 to -5.52) (Petzold et al., 2010).

Figure 3-5: RNFL thickness of MS non-ON eyes versus controls

(Taken from Petzold et al 2010, Figure 4)

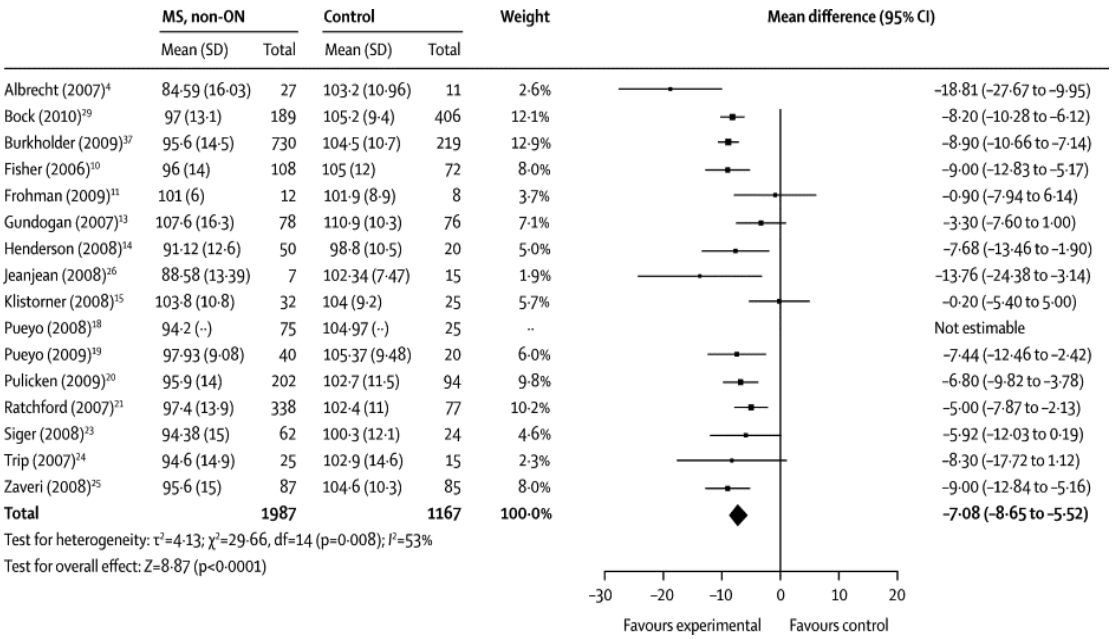

In a 12-month longitudinal study, Costello *et al*. demonstrated that 74% of patients had RNFL thinning after acute optic neuritis and the majority of this occurred within the first three to six months, the temporal sector being the earliest involved at two months (Costello et al., 2008). The temporal sector of the RNFL receives fibres from the papillomacular bundle and is reduced by 25-34% compared to controls Noval et al (Noval et al., 2011).

The development of validated measures of visual functioning has greatly facilitated the exploration for a structural biomarker for neurodegeneration and one of the most important findings from OCT in studies of patients with MS is the correlation between RNFL thickness and visual function.

3.6.4 RNFL thickness and visual function

In a cross-sectional study Fisher *et al*. demonstrated low contrast letter acuity scores were significantly correlated with average RNFL thickness and every one line decrease in low contrast letter acuity was associated with an average 4 μm thinning of the RNFL (Fisher et al., 2006).

This finding was also confirmed in a cohort of patients with MS by a longitudinal study by Talman et al.. They found a significant association between low contrast letter acuity at 2.5% and RNFL thickness (Talman et al., 2010).

Costello et al recruited 54 patients with acute unilateral optic neuritis within 1 month of symptom onset and performed assessments including Humphrey visual fields (using 30-2 full threshold strategy testing) as well as RNFL measurements at 3 monthly intervals over the period of a year. Regression analyses were performed to assess the relationship between mean RNFL thickness and visual field mean deviation (VFMD, (dB)) as well mean RNFL thickness and logMAR visual acuity in 54 patients. Two regression lines were fitted using RNFL to predict visual field function. The RNFL measure of 75 μm was used as the cut off between the two regression lines because above this level the predictive effect of RNFL thickness on VFMD was not significant. Below this level there was a significant association between RNFL thickness and VFMD such that for every 10 μm reduction in RNFL thickness there was a 6.46 dB reduction in VFMD. For logMAR visual acuity the cutoff point was 70 μm below which RNFL thickness was significantly associated with logMAR visual acuity. Costello et al suggested that a threshold RNFL thickness of 75 μm needs to be reached before visual function, as measured by automated perimetry, declines linearly. They reasoned that this was due to the 'functional reserve" of the visual system whereby that visual function is preserved until a critical level of axonal loss is reached (Costello et al., 2006).

However others have argued against the concept of 'functional reserve' reasoning that the impression of functional reserve is due to the logarithmic nature of of the decibel scale VFMD and that there is actually a linear relationship between RNFL thickness and the anti-log of VFMD. In addition they argue that the structural test (e.g. RNFL thickness) can show a statistically significant reduction before functional tests (e.g. VFMD) due to the smaller

confidence intervals of structural measures that have less variability than functional tests (Hood and Kardon, 2007; Garway-Heath et al., 2002).

3.6.5 RNFL thickness and MS subtypes and disability

Several studies have shown that average RNFL thickness can differentiate between MS subtypes with lower values in progressive forms of MS when compared with patients with clinically isolated syndromes suggestive of MS (Costello et al., 2010; Pulicken et al., 2007). The lowest values may be in patients with SPMS. (Costello et al., 2010; Pulicken et al., 2007)
In a study by Burkholder et al a 10 μm reduction in peripapillary RNFL was associated with a $0.2mm^2$ reduction in macular volume. Total macular volume differed for different sub groups of patients with lower values in secondary progressive MS than PPMS. Reductions in inner total and outer macular volumes were associated with lower high and low contrast letter acuity scores. Inner macular volume remained a significant predictor of visual loss even when peripapillary RNFL thickness was taken into account suggesting that neuronal loss is associated with impaired visual function. These findings are significant because tracking macular volumes in ON patients may help determine the temporal relation between primary neuronal cell death and axonal loss after a CNS inflammatory event (Burkholder et al., 2009).

There are conflicting data on the correlation between overall disability, as measured by the expanded disability status scale and RNFL thickness. In a meta-analysis by Petzold et al of 12 studies investigating the relationship between RNFL and EDSS an inverse correlation was reported in 6. Findings from these trials were consistent with two further studies which described a reduction of RNFL thickness with EDSS percentiles (Petzold, 2014). The strongest relationships appear to be in cohorts of patient with relapsing remitting MS and generally low EDSS and is has been proposed that OCT is more reflective of pathology in early MS (Noval et al., 2011).

Figure 3-6: RNFL thickness and EDSS

(Taken from Fischer et al 2006, Figure 3)

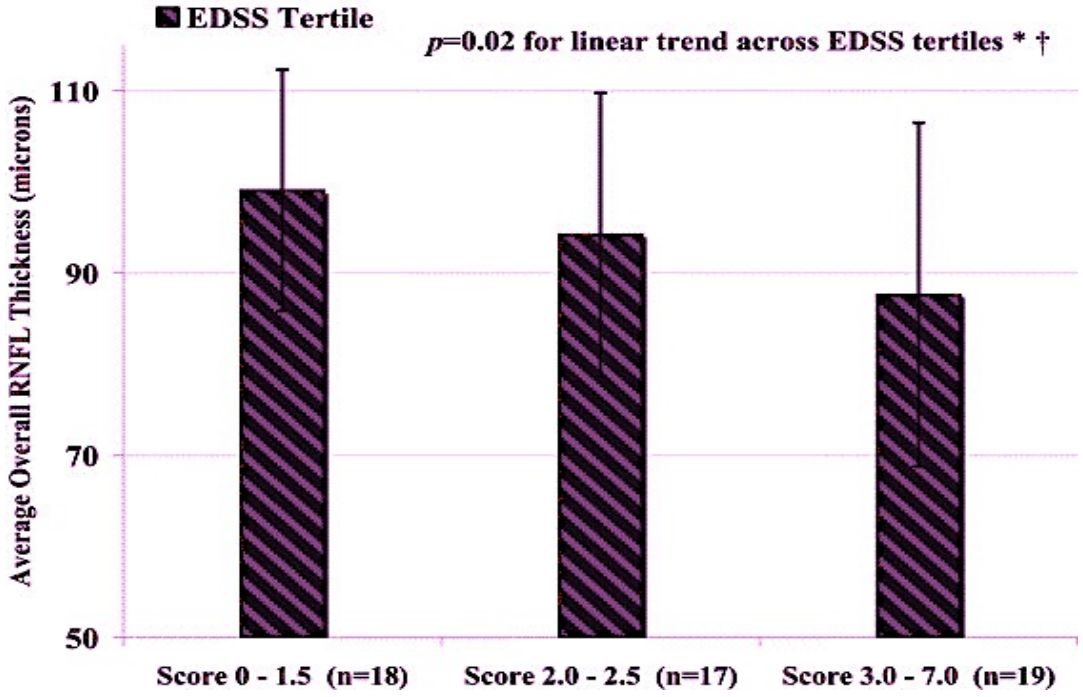

In a longitudinal study of 299 MS patients with and without a prior history of optic neuritis (median follow up of 18 months) Talman et al demonstrated a reduction of RNFL thickness from baseline of 1.7% at 1-2yrs, 3.2% at 2-3yrs and 6.7% at >3yrs of follow up This was in contrast to mean RNFL loss of 0.5% over 3 yrs in disease free control eyes. (Talman et al., 2010).

Sepuclre et al found a decrease in average RNFL thickness of 4.8 μm after 2 yrs in a cohort of MS patients with early- intermediate disease. Patients with more active disease had more temporal sector RNFL atrophy than patients who were clinically stable (Sepulcre et al., 2007).

3.6.6 RNFL thickness and brain atrophy

Significant correlations between RNFL thickness and brain global and regional atrophy have also been demonstrated (Gordon-Lipkin et al., 2007; Saidha et al., 2013). It is important to note that a previous history of optic neuritis may interfere with the correlations between MRI parameters and RNFL thickness in patients with MS (Zimmermann et al., 2013).

3.6.7 Establishing the time course of axonal loss after optic neuritis for neuroprotection trials

Establishing the time course of axonal loss after optic neuritis is important for future neuroprotection trials and OCT has helped to elucidate this in detail. In 2010, Henderson *et al*. performed a prospective study on 23 patients with acute unilateral optic neuritis within a median of 16 days from onset. Patients underwent OCT, visual assessments and VEPs at 3, 6, 12 and 18 months. The evolution of retinal nerve fibre layer changes over time fitted well with an exponential model (Figure 3-7) with RNFL thinning appearing a mean of 1.6 months from symptom onset (compared to the baseline unaffected eye). They found that 90% of the retinal nerve fibre degeneration occurred within a mean 2.38 months from onset of the disease and that poorer visual function was associated with greater decline in RNFL thickness during the first three months. They also performed sample size calculations for placebo-controlled trials of acute neuroprotection. They found that smaller numbers of patients were required after 6 months follow up than three and study power was improved by investigating differences between affected and fellow eyes rather than changes in RNFL thickness of the affected eye alone due to swelling of the affected eye at baseline. (Henderson et al., 2010)

This study has paved the way for future neuroprotection trials using OCT as a primary outcome measure

Figure 3-7: Affected minus baseline fellow eye RNFL thinning over time after demyelinating optic neuritis

(Taken from Henderson et al 2010, Figure 2)

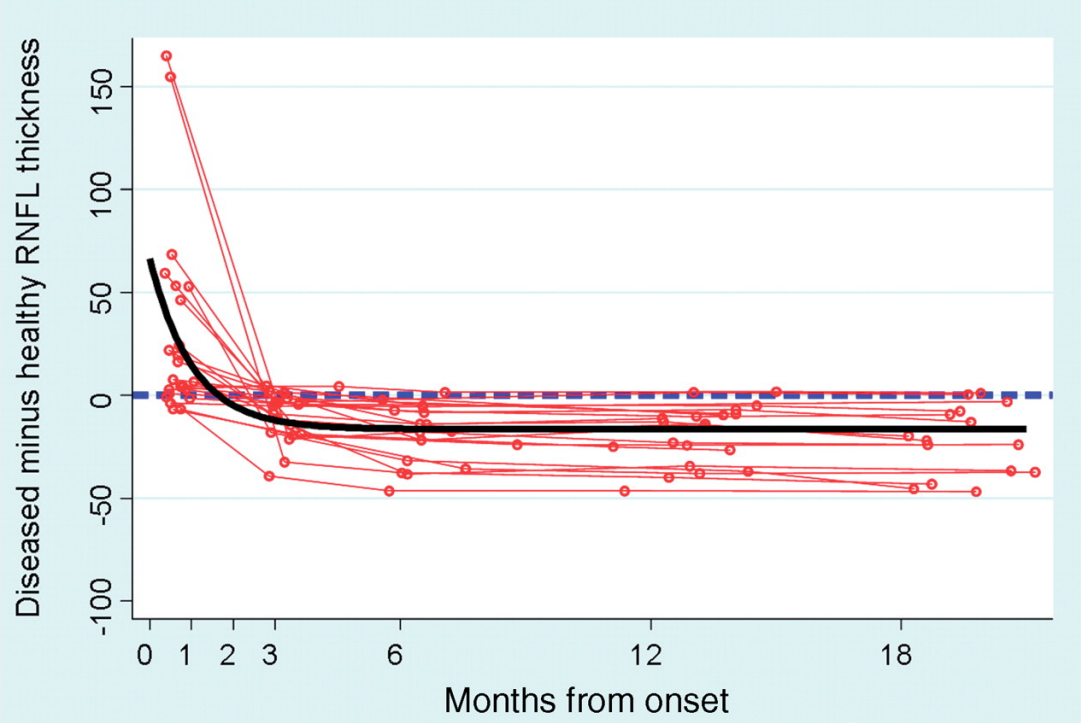

.

3.6.8 Retinal Segmentation in optic neuritis and MS

With the introduction of high resolution, spectral domain OCT images and novel analysis techniques it is now possible to segment and quantify individual retinal layers. The macular is neuronally enriched and 34% of its volume consists of RGCs and their axons. Given that neuronal loss is recognized as an important cause of disability in MS measurements of retinal ganglion cell layer thickness have emerged as a potential biomarker. Post mortem ganglion cell drop out is described in >70% of MS patients (Kerrison et al., 1994). A recent pathology study on eyes of 82 patients with MS demonstrated atrophy of retinal ganglion cells and their axons as well as of the inner nuclear layer (Green et al., 2010). Subsequently retinal ganglion cell layer loss has been demonstrated in vivo using OCT both in acute optic neuritis and in MS.

In a longitudinal study of 20 acute optic neuritis patients recruited within 4 weeks of visual symptoms there was no significant difference in ganglion cell/inner plexiform layer (GC/IPL) thickness when compared to the fellow eye at baseline whereas average retinal nerve fibre layer thickness was significantly higher in the affected eye. There was no significant difference in any of the other retinal layers compared to the fellow eye. At three months there was significant thinning of the GC/IPL and the RNFL compared to baseline and the fellow eye. GC/IPL and RNFL thinning then remained stable throughout the 12 month follow up period and there were no changes in any of the deeper retinal layers. The authors suggested that as there was no demonstrable oedema of the GC/IPL during the acute phase of optic neuritis that it could be a superior outcome measure for neuroprotection trials than RNFL thickness as it would allow true measures of the baseline affected eye instead of surrogate measures of the contralateral eye (Syc et al., 2012).

In support of this Saidha et al demonstrated a superior structure-function correlation between GC/IPL thickness and other measures of visual function suggesting that it may be a superior biomarker to assess the processes of neurodegeneration. They suggested that astrogliosis may contribute to falsely increased measures of RNFL thickness (Saidha et al., 2011a) and this is supported by pathological studies as discussed in section 1.2.

Walter et al found that clinically meaningful reductions in high and low contrast letter acuity were associated with thinning of peripapillary and macular RNFL and GC/IPL. They found that retinal GC/IPL thickness was most strongly related to visual dysfunction and QOL in MS (Walter et al., 2012).

Tatrai et al recruited 39 patients with relapsing remitting MS and found a strong correlation between EDSS and peripapillary nerve fibre layer and GC/IPL. There was no correlation between any of the other retinal layers. Peripapillary RNFL correlated strongly with GC/IPL in the macula. They demonstrated that macular GC/IPL measurements had the highest sensitivity and specificity to detect axonal loss independent of optic neuritis (Tatrai et al., 2012)

Garcia Martin et al evaluated 204 patients with relapsing remitting multiple sclerosis and compared them to healthy controls; they obtained automated segmentation of 10 retinal layers using a single parafoveal scan. They found reduced thickness in all retinal layers in the MS patients when compared to controls. The inner retinal layers (RNFL, GC/IPL and INL) were significantly thinner in patients with a history of optic neuritis than those without but a history of optic neuritis had no significant effect on the outer retinal layers. RNFL and GC/IPL correlated inversely to EDSS (Garcia-Martin et al., 2014).

Albrecht et al (2012) segmented retinal layers on high resolution, horizontal and parafoveal scans on 41 RRMS, 42 SPMS and 12 PPMS patients. GC/IPL thickness was reduced in all subgroups of MS patients when compared to controls. INL thickness was only significantly reduced in PPMS patients. This was independent of a history of optic neuritis and they postulated may represent primary retinal pathology. They found no significant difference in ONL/OPL thickness between any of the MS groups and controls. They found significant correlations of mean RNFL, macular and OPL thickness with EDSS. Interestingly in contrast to RNFL and macular thickness, OPL thickness was positively correlated with EDSS. They suggested that thickening of this layer occurs due to reorganization following degeneration of other retinal layers (Albrecht et al., 2012).

3.6.9 Microcystic macular oedema

It has been reported that approximately 5% of patients with early MS will have evidence of microcystic macular oedema (MME) and inner nuclear layer thickening. MME is defined as two or more limited, insular and cystoid areas of hyporeflectivity in two or more consecutive B scans. Shadowing in the retinal layers below the cystoid areas may occur. The pathophysiology of MME is unknown and inflammatory processes, retrograde degeneration of inner retinal layers and vitreous traction have been postulated to play a role. In MS the presence of microcystic macular oedema and INL thickening are associated with increased inflammatory disease activity, including gadolinium-enhancing lesions and new T2 lesions on brain MRI and relapses (Gelfand et al., 2012; Saidha et al., 2012)

However, microcystic macular oedema might not be specific to MS but may be optic neuritis dependent. Kaufhold et al (2013) found that MME was associated with a history of optic

neuropathy (of any cause) in 95 % of cases Eyes with MME had reduced RNFL and macular volume and reduced visual acuity compared to eyes unaffected by MME. Eyes with an RNFL thickness below the first quartile categorised as having a history of severe optic neuritis were at greatest risk for development of MME odds ratio=13.6. SLO images showed dark, dotted patterns in the ocular fundus of all patients affected by MME and generally presented in a crescent shape around the fovea. They found that MME was more common in patients with NMO and CRION than MS and suggested a strong pathophysiological correlation between the development of MME and the extent of optic nerve damage (Kaufhold et al., 2013).

Another study by Abegg et al also demonstrated that MME is not specific for demyelinating disease. They found that MME was restricted to retinal areas with nerve fibre layer and ganglion cell loss and hypothesized that MME is caused by retrograde degeneration of the inner retinal layers resulting in impaired fluid resorption (Abegg et al., 2014). .

3.6.10 Macular thinning predominant phenotype

Saidha et al (2011) described a group of macular thinning predominant (MTP) patients defined as having a macular thickness of < 5^{th} percentile, ipsilateral normal average RNFL thickness and in the absence of a history of acute optic neuritis. In MTP patients all retinal layers were lower when compared to controls. Compared to other MS patients without MTP, MTP patients had significantly reduced INL and ONL thickness. They found that average MS severity score was significantly higher in patients with MTP and it appeared to be associated with a more aggressive form of MS. In the MTP patients, multifocal ERG, which predominantly reflects the function of the outer retina, was diffusely abnormal with attenuated amplitudes of the P1 waveform. The authors suggest that patients with the MTP phenotype may have a distinct pathological process of primary neuronal loss. These findings have not been replicated by other studies (Saidha et al., 2011b).

Table 3-2: Methods for assessment of the anterior visual system in MS.

(Adapted from Frohman et al 2006, Table 2)

	Information	Limitation
Visual acuity	Global high-contrast acuity	Crude measure of visual function Insensitive to other visual system abnormalities
		Subjective
		Subject cooperation
		Potentially affected by fatigue, temperature and other factors such as infection, stress
Low-contrast letter acuity/sensitivity	Sensitive measure of visual function that relates to physiological and structural changes	Subjective
	Predictive of 'real world' tasks	Subject cooperation
		Potentially affected by fatigue, temperature and other factors such as infection, stress
Colour vision	Cone vision	Subjective
	Small axons of parvocellular pathway selectively affected by demyelination	Subject cooperation
	Correlates with structural changes	Potentially affected by fatigue, temperature, and other factors such as infection, stress
Visual Evoked potentials	Transmission characteristics of anterior visual system	Potentially affected by temperature, infection
	Provides measure of magnitude and latencies of responses, reflecting axonal and myelin integrity	Cortical overrepresentation
MRI techniques	Structural measures of tissue architecture. Sensitive to changes in myelin, axons, gliosis, and inflammation	Long imaging times Requires high resolution images Image quality limited by motion artifact Not as reproducible as OCT
		Not entirely specific for each pathological process
OCT	Measures retinal architecture. RNFL	

	contains axons and glia but no myelin	Dependent on accurate disc centering and adequate signal strength
	Non invasive, sensitive and reproducible Fast acquisition times	Patients cooperation + must be able to fixate Different instruments have different measurement techniques and analysis protocols

Chapter 4 A Phase II Placebo Controlled Trial of Neuroprotection with Phenytoin in Optic Neuritis

4.1 Background and rationale for neuroprotection with sodium channel blockade

Acute demyelinating optic neuritis is a common, often presenting manifestation of Multiple Sclerosis (MS). During long term follow up around 75% of patients presenting with clinically isolated optic neuritis go on to develop multiple sclerosis (MS)(Beck et al 1993). The acute inflammatory lesion in the optic nerve resembles the demyelinating plaques elsewhere in the CNS.

Although in general visual recovery after a single episode of optic neuritis is good, 10-15% of patients will be left with significant permanent visual deficits (Beck et al 1993). Axonal loss and subsequent neurodegeneration is now recognized as a major cause of persistent disability both in optic neuritis and multiple sclerosis. Imaging of the retinal nerve fibre layer (RNFL) with optical coherence tomography (OCT), and of the optic nerve with MRI both demonstrate significant tissue loss which correlates with impaired visual function after optic neuritis (Kolappan et al., 2009).

As with other MS relapses, corticosteroids have no or little impact on the extent that vision recovers, nor do they prevent optic nerve atrophy on MRI or improve VEP latency after an attack of optic neuritis (Spoor and Rockwell, 1988; Beck et al., 1992b; Kapoor et al., 1998). Also, immunomodulation with disease modifying therapies has been only partially successful in preventing disability in MS that occurs following relapses. With this background, neuroprotection remains a major unmet need. Treatments that protect against acute neuroaxonal loss should not only prevent disability after optic neuritis but also by implication, relapses of MS in general.

Optic neuritis represents an attractive model to investigate the effects of potential neuroprotective treatments in MS as 1) it occurs in a structurally eloquent region of the CNS that is commonly affected by the disease process; 2) it presents with a clinical syndrome

which is relatively easy to recognize (although acutely this can be more challenging when symptoms/signs have not fully developed) and prompts patients to seek help early; 3) it can be reliably studied with a combination of validated clinical, electrophysiological and imaging techniques thereby allowing a structure-function paradigm of CNS injury to be constructed; 4) the lesion in the optic nerve leads to retrograde degeneration of the retinal nerve fibre layer (RNFL), a relatively pure compartment of unmyelinated axons the thickness of which can be measured sensitively and noninvasively using optical coherence tomography (OCT); 5) the natural history of optic neuritis has been well defined.

Progress in the development of potential neuroprotective therapies in optic neuritis and MS relies upon the identification of key mechanisms and treatment targets. Amongst the possible mechanisms, there is growing evidence for the role of sodium channels in neurodegeneration in multiple sclerosis.

Pathological studies have demonstrated that significant axonal loss occurs even in the early stages of MS and the extent of axonal loss correlates with the magnitude and severity of inflammation at different sites within the CNS (Trapp et al., 1998; Bitsch et al., 2000). Early axonal transection is thought to be due to the vulnerability of demyelinated axons to inflammation. The extent of axonal degeneration in MS lesions is partly related to the number of cytotoxic T cells and activated macrophages that can be found in close opposition with injured axons (Smith and Lassmann, 2002). Thus inflammatory mediators, particularly nitric oxide, may play a key role in the mechanism of injury. In support of this the production of nitric oxide is significantly raised within MS lesions and its expression in EAE models coincides temporally and quantitatively with clinical signs (Smith and McDonald, 1999). Moreover, nitric oxide can promptly and reversibly cause conduction block and demyelinated axons are particularly vulnerable to this effect (Redford et al., 1997). The mechanisms by which NO can cause conduction block are not entirely clear but it is thought that NO can directly impair the function of sodium channels

The ‘sodium hypothesis’ postulates that axonal injury results from a combination of 1) excessive energy demands from ionic imbalances due to increased sodium loading in partially demyelinated axons and (Waxman, 1998; Craner et al., 2004; Bechtold and Smith,

2005)and 2) from inhibition of mitochondrial respiration by inflammatory mediators such as NO (Bolaños et al., 1997; Smith et al., 2001; Garthwaite et al., 2002).

To expand these points: demyelinated axons exhibit increased expression of Na channels along the denuded axolemma that is an adaptive response to allow restoration of current along the demyelinated segment. Specifically, studies have demonstrated upregulated expression of Na_v 1.2 and Na_v 1.6 along extensive regions of demyelinated axons in EAE and in acute MS plaques (Craner et al., 2004). Na_v 1.6 channels produce a persistent current as well as rapidly activating -inactivating currents.

Whereas in normal myelinated axons action potential generation is confined to nodal zones some chronically demyelinated axons develop a continuous mode of action potential supported by a more diffuse distribution of channels.

Figure 4-1: Diagram illustrating sodium channel reorganisation in the demyelinated axon

Taken from Waxman 2006 (Figure 1)

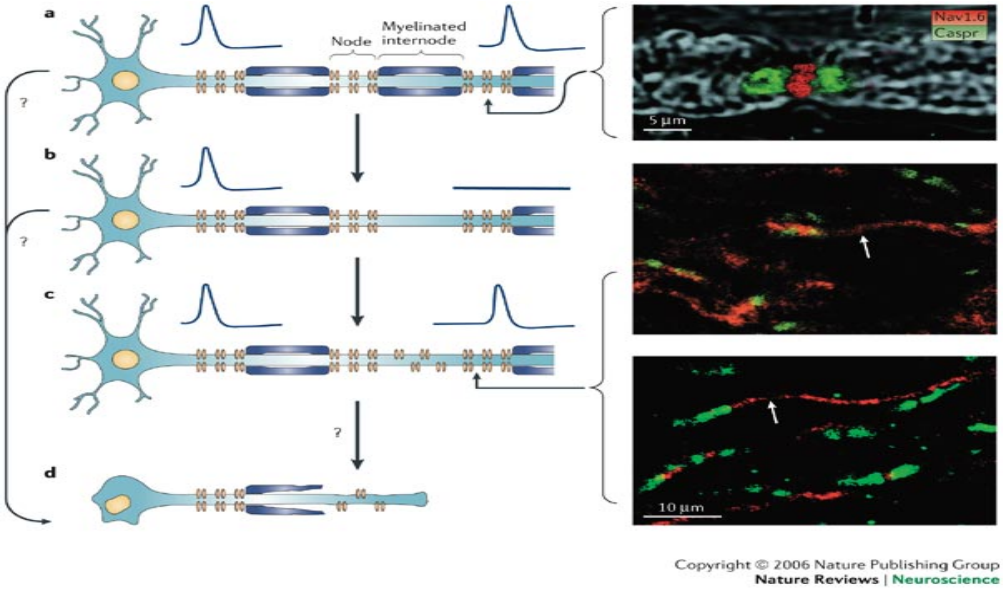

[a] In normal myelinated axons there is clustering of Na_v 1.6 channels at the nodes of Ranvier

[b] The acutely demyelinated axon has a low Na^+ channel density due to their scarcity in the exposed internodal region this leads to conduction failure

[c] Demyelinated axons exhibit increased expression of Na channels along the denuded axolemma, an adaptive response to allow restoration of current

[d] Chronically demyelinated axons can develop a continuous mode of conduction that can lead to sodium overloading and axonal degeneration

This leads to excessive intraxonal sodium loading thereby increasing the energy demand required to operate the NA+/K+ ATPase to allow repolarization (Bostock and Sears, 1978; Foster et al., 1980). This mismatch between energy supply and demand in demyelinated axons creates a state of 'virtual hypoxia' (Stys et al., 1992).

Because Na/K ATPase is required for extrusion of Na+ an inadequate supply of ATP may be expected to exacerbate the effects of persistent Na+ influx.

Nitric oxide is known to impair mitochondrial metabolism reducing ATP production leading to energy failure. Axons are particularly vulnerable to the effects of nitric oxide if they are electrically active (Smith and Lassmann, 2002; Kapoor et al., 2003).

This energy failure inhibits the activity of the Na+/K+ATPase to extrude sodium which in turn leads to the reverse operation of the Na+/Ca+ exchanger promoting injurious levels of intraxonal calcium, thereby activating degradative enzymes and promoting axonal degeneration (Kapoor et al., 2003).

Na_v 1.6 has been shown to be coexpressed with the Na/Ca2+ exchanger along degenerating axons in EAE (Craner et al., 2004) and would be expected to predispose demyelinated axons to import injurious levels of Ca2+.

Figure 4-2: Schematic diagram of the role of sodium channels in axonal degeneration in multiple sclerosis (taken from Raftopoulos and Kapoor, 2013 Figure 1)

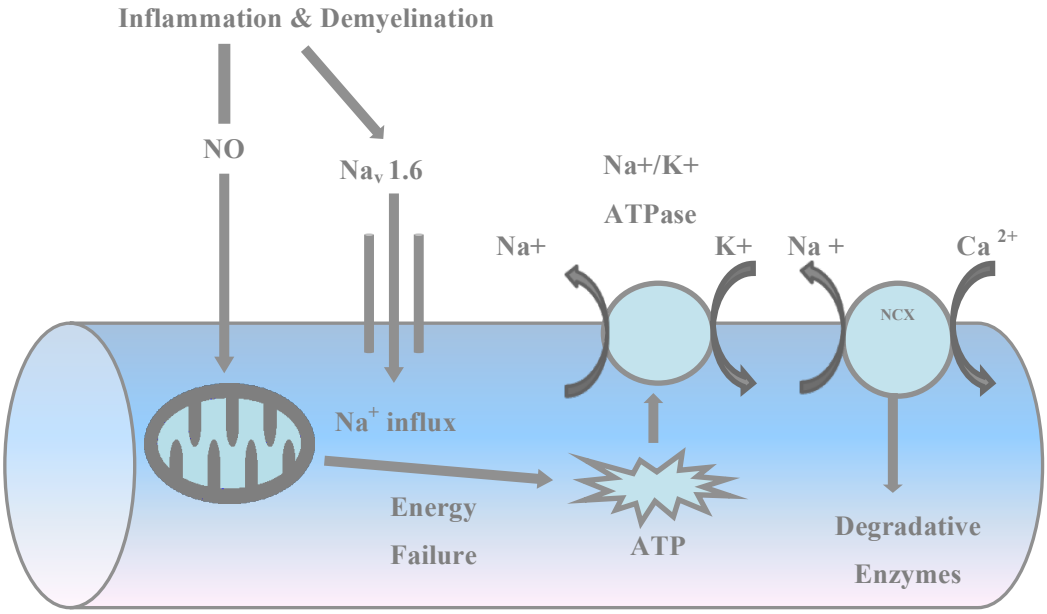

Nitric oxide production impairs mitochondrial metabolism leading to reduced ATP production and energy failure. This, in turn leads to failure of the sodium/potassium ATPase and reduced ability to extrude sodium with subsequent depolarisation and inability to maintain transmembrane ion gradients. Depolarisation activates voltage gated sodium channels that provide a conduit for persistent sodium influx. This subsequently drives the reverse operation of the sodium/calcium exchanger leading to injurious levels of intraxonal calcium and axonal degeneration

The premise that sodium loading may be an important cause of axonal degeneration raises the possibility that axons may gain protection from partial sodium channel blockade. Indeed partial sodium channel blockade has been shown to be neuroprotective in several experimental models of inflammatory axonal injury. For example, Garthwaite et al (2002) demonstrated partial blockade of sodium channels prevented nitric oxide mediated axonal degeneration in rat optic nerves (Garthwaite et al., 2002). Subsequently Lo et al (2003) demonstrated that oral phenytoin taken for a 28-30 day period in CF7B1 mice with EAE was protective against axonal loss and improved clinical outcome. Importantly neuroprotection with sodium channel blockade could be achieved at concentrations that didn't compromise the conduction of action potentials (Lo et al., 2003).

Sodium channels also occur in cells in the immune system and may have a regulatory effect on their function and the subsequent immune response. Na_v 1.6 sodium channels are present in macrophages and microglia within acute MS lesions and their expression is up regulated when these cells are activated. Macrophages and microglia are closely associated with degenerating axons in MS and produce axonal injury via CD4+T cell proliferation, production of inflammatory cytokines and NO. In one study sodium channel blockade with phenytoin reduced inflammatory infiltrate in EAE by 75% (Craner et al., 2005). The expression of Na_v 1.6 channels has also been shown to be upregulated in macrophages and microglia upon activation in acute MS lesions (Craner et al., 2005). Sodium channel blockade may therefore have immunomodulatory effects in addition to the directly protective effects on axons described above.

In EAE models the sudden withdrawal of phenytoin resulted in acute clinical deterioration in association with an increased CNS inflammatory infiltrate and ultimately death in over 50% of mice. (Black et al., 2007). There is currently no evidence that this occurs in humans.

4.2 The Lamotrigine Trial in Secondary Progressive Multiple sclerosis

The experimental evidence in animal models of a neuroprotective effect of sodium channel blockade led to a clinical trial of lamotrigine trial in secondary progressive MS. 120 patients were randomly assigned to receive lamotrigine or placebo for two years. The primary outcome measure was the rate of reduction in central cerebral volume over two years and the trial was powered to detect a 60% treatment effect. The prediction was that lamotrigine would preserve brain volume, but in fact the opposite effect was observed, at least in the first year of treatment, when loss of partial and whole brain volume occurred at a greater rate in the active arm. Specifically, the mean change in central cerebral volume was -3.8mls in the lamotrigine group and -2.48 mls in the placebo group. The volume loss was partly reversible after treatment was withdrawn. The trial was therefore regarded as having a negative outcome (Kapoor et al., 2010).

Figure 4-3: Mean central cerebral volume in the lamotrigine and placebo groups measured at 6-monthly intervals over a 2- year period (Taken from Kapoor et al 2010, Figure 2)

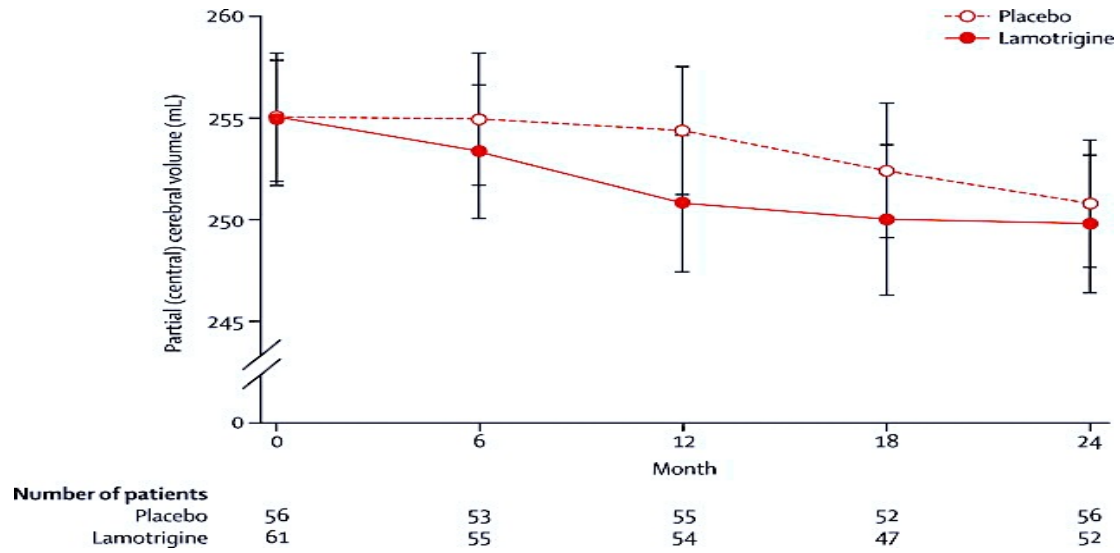

The interpretation of these findings was complex, partly due to the possible reversible treatment effects on fluid shifts and a reduction in inflammation (so called pseudo-atrophy). Also non–adherence in the lamotrigine group approached 50% as the drug was poorly tolerated. This may be because the significant pre-existing level of disability in secondary progressive MS patients renders them particularly susceptible to axonal block due to reduced conduction of sodium channels in chronically demyelinated axons.

Despite these limitations, some potentially positive treatment effects emerged. Namely, the rate of decline of walking speed, a secondary outcome measure, was halved in the active group compared to placebo and the active group had significantly lower serum concentrations of neurofilament (Gnanapavan et al., 2013) a potential biomarker of axonal degeneration.

Consideration of the trial design suggested a number of weaknesses, including limited compliance with treatment due to poor tolerability of sodium channel blockade in secondary progressive MS, and a premature read out which may have missed the

emergence of a beneficial effect of treatment on brain atrophy after the first year of treatment. Moreover, the wrong disease subtype may have been targeted given that neuroprotection may be more effective in relapses than in progressive MS because the higher level of inflammation in the acute plaque is closer to the experimental models from which the sodium hypothesis arose (Kapoor et al., 2010). Additionally a study by Black et al looked at the expression of Na_v 1.2 and Na_v 1.6 channels and the sodium calcium exchanger (NCX) in chronic MS plaques. Unlike in acute lesions, axonal injury, as evidenced by *B*- APP accumulation, did not occur at sites of coexpression of Na_v 1.6 and NCX and there was no expression of Na_v 1.2 channels along demyelinated axons. They suggested therefore that different mechanisms underlie axonal degeneration in chronic plaques and this may account for the lack of efficacy of sodium channel blockade in secondary progressive MS (Black et al., 2007).

We believe the limitations of the lamotrigine trial have been addressed in the design of this trial of neuroprotection with phenytoin in optic neuritis. Namely that treatment was commenced at an early stage of the evolution of an acute inflammatory lesion (in the optic nerve), which is more comparable to the experimental models on which the theory is based, and was continued beyond the resolution of inflammation.

Secondly, the trial targets people with isolated optic neuritis or early multiple sclerosis, in which sodium channel blockade is likely to be much better tolerated. This, in addition to the shorter trial design increased the likelihood of adherence.

Thirdly, Henderson et al (2010) demonstrated mean time to 90% loss of RNFL thickness after an episode of acute optic neuritis was 2.38 months and that the earliest detectable atrophy in the affected compared to the baseline fellow eye was 1.64 months. Therefore, the readout of the trial, which was timed at three months after cessation of treatment (and 6 months after onset of optic neuritis), allows the resolution of any treatment related volume changes, and incorporates the delay that occurs in the development of atrophy in the optic nerve and retina after the onset of inflammation (Henderson et al., 2010).

Finally the anterior visual system presents an opportunity to implement a sensitive and clinically relevant measure of neuroprotection, by using OCT to quantify the thickness of the retinal nerve fibre layer, in which thinning primarily reflects axonal loss.

Table 4-1: Advantages of the neuroprotection with phenytoin in acute optic neuritis over the lamotrigine trial in SPMS patients

Lamotrigine Trial (SPMS)	Phenytoin Trial (Acute Optic Neuritis)
Significant pre-existing disability renders patients particularly sensitive to axonal conduction block with Na channel blockade	CIS or early MS patient less disabled. Na channel blockade likely to be better tolerated.
Lower levels of inflammation, no longer actively relapsing.	Early inflammatory lesion more comparable to EAE model.
Cerebral volume changes confounded by reversible fluid shifts and reduced inflammation.	Clinically significant primary outcome measure in the retina which primarily reflects axonal loss
Premature read out time may have missed emergence of beneficial treatment effects after the first year	Delayed read out time, three months after cessation of treatment, to incorporate lag in RNFL atrophy
Longer trial design with poor compliance	Shorter trial design increases likelihood of compliance

4.3 Trial objectives

We undertook a phase II double blind placebo controlled trial of neuroprotection with phenytoin in acute demyelinating optic neuritis.

The primary aim of the trial was to determine whether immediate and sustained sodium channel blockade with phenytoin is neuroprotective in acute optic neuritis (given that phenytoin is a selective sodium channel inhibitor in the concentrations used in the trial (Yaari et al., 1986)).

Secondary aims were to assess whether sodium channel blockade with phenytoin improves visual outcome and promotes remyelination of the optic nerve. Additionally, we assessed

the safety profile of phenytoin in acute demyelinating optic neuritis and the occurrence of any unexpected adverse events.

4.4 Trial design

This investigator led trial had a multi-centre double blind, parallel group, randomized controlled design. There were two trial sites in London and Sheffield.

Patients aged between 18- 60 years were eligible if they had a clinical diagnosis of acute unilateral optic neuritis (confirmed by a neuro-ophthalmologist) with a visual acuity of ≤ 6/9 (and ≥ 6/6 in the fellow eye) and an interval of ≤ 14 days between onset of visual loss and randomization. Patients with a previous diagnosis of relapsing MS were eligible if they had ≤ 10 years of disease duration and an EDSS of ≤ 3. Prior or ongoing treatment with glatiramer acetate and *B* interferon was permitted and the decision to administer corticosteroids for treatment acute optic neuritis was left to the discretion of the treating physician.

Patients were excluded if they had a history of previous optic neuritis (in either eye) or any co-morbid ocular disease, clinical or biochemical evidence of cardiac, hepatic or renal abnormalities, contraindications to phenytoin use (including pregnancy) and disabling temperature dependent MS symptoms.

Patients were also excluded if they had taken drugs that block sodium or calcium channels in the preceding two weeks and if corticosteroids (with the exception of for treatment of their optic neuritis) or any other immunomodulatory drugs had been taking in the preceding two months.

The study was approved and by the London-South East UK Research and Ethics Committee and was monitored by an independent data monitoring and ethics committee. The trial is registered with Clinical.Trials.gov (NCT 01451593) and with EUDRACT. All patients gave written informed consent before entry.

Figure 4-4: Inclusion criteria

- Acute unilateral demyelinating optic neuritis
- ≤ 14 days since onset of visual loss (since axonal injury is dependent on coincident inflammation neuroprotection most likely to be effective if commenced as soon as possible)
- Age 18-60 (upper limit chosen to avoid including patients with cerebrovascular disease on MRI)
- Visual acuity ≤ 6/9 in the affected eye
- A pre-existing diagnosis of relapsing MS were eligible within 10 years of disease onset providing they had an EDSS of ≤ 3. (Patients with early MS are less disabled and more likely to tolerate sodium channel blockade)

Figure 4-5: Exclusion criteria

- Previous history of optic neuritis or ocular disease in either eye (as this would interfere with outcome assessment)
- Use of sodium channel or calcium blockers in the previous two weeks
- Use of corticosteroids in the previous two months (with the exception of for treatment of the optic neuritis)
- Clinical or biochemical evidence of cardiac, hepatic or renal abnormalities
- Contraindications to phenytoin (including pregnancy and breast feeding

4.5 Screening assessments

Participants were referred from a number of patient identification centres across the country. In particular, ophthalmologists in eye casualties were included in the trial infrastructure. Each participating centre was visited to increase awareness of the trial and encourage referrals. Each centre was provided with posters outlining the main inclusion and exclusion criteria and the contact details of the trial team.

Potential trial participants were screened clinically at one of the two trial sites for a diagnosis of acute optic neuritis. A full medical history and ophthalmological examination

was undertaken. Screening investigations included full blood count, urea and electrolytes and liver function tests, aquaporin 4 antibodies, urinalysis and urinary pregnancy test, ECG and OCT to ensure that phenytoin could be given safely. Eligible patients were provided with a detailed patient information leaflet and were given adequate time to consider participation in the trial. Appropriate follow up was arranged for patients who were either ineligible or declined to participate in the trial.

Participants who were randomised and enrolled but later found not to have optic neuritis and those with positive aquaporin 4 antibodies were withdrawn from the trial and excluded from the ITT cohort.

188 patients were screened in total across the two sites (157 London and 31 Sheffield). The tables below outline the reasons for screening failure.

Table 4-2: Reasons for screening failure

Reason for screening failure	Number of patients
Visual acuity 'too good'	28
Declined	25
Alternative diagnosis (see table below)	20
>14 days since onset of visual loss	11
Bilateral optic neuritis	5
Previous history of optic neuritis	3
On long term immunosuppression	1
Diagnosis unclear	4
Other	5

Table 4-3: Alternative diagnoses

Central serous retinopathy	1
Migraine with aura	2

Optic nerve meningioma	1
Cavernoma compressing optic chiasm	1
Posterior scleritis	2
Sarcoidosis	3
Uveitis	1
Leber's hereditary optic neuropathy	2
Toxic optic neuropathy	1
Neuroretinitis	1
Optic disc drusen	1
Functional visual loss	4

4.6 Randomization and Procedures

Patients were randomly assigned (1:1) to phenytoin or placebo via a website (www.sealedenvelope.com) by minimization, with time from onset (≤7 days, >7 days), Center (London, Sheffield), prior MS diagnosis (yes/no), disease modifying treatment (yes/no), and corticosteroids for optic neuritis (yes/no), as binary minimization variables. Patients were allocated a randomization code that was matched to a confidential treatment list by the study pharmacist to assign patients either to phenytoin or placebo (which were identical in appearance) for 3 months. Throughout the study only the pharmacist was aware of treatment allocation. Treating and assessing physicians as well as patients remained masked to treatment allocation.

Patients were loaded with a total dose of 15mg/kg divided in three equal doses, each rounded up to the nearest 50mg, over three days. A daily maintenance dose (4mg/kg, rounded up to the nearest 50mg, with a maximum of 350mg) was given for 13 weeks, increased to 6 mg/kg from at the recommendation of the DMEC due to sub-therapeutic serum phenytoin levels, the protocol was amended from 17 July 2013. Patients were recruited between February 2012 and May 2014. 58 participants were randomised before 17 July 2013, 29 of whom were assigned to the lower daily maintenance dose of phenytoin

and 28 were randomised after this date 13 of who were assigned the higher daily maintenance dose. Final assessments were performed in December 2014.

The rationale for the timing and duration of treatment was that because axonal injury may be driven both by inflammation and by increased expression of axonal sodium channels, neuroprotection would be expected to be most effective if treatment is commenced as soon as possible after the onset of a relapse and continued until after inflammation (as inferred by presence of gadolinium enhancement of the lesion) and axonal membrane readaptation has subsided. In support of this Al-Izki et al (2013) found Na_v blocking compounds were most effective during lesion formation and periods of blood barrier breakdown in an EAE model of optic neuritis. Beyond this once the natural regulatory mechanisms were initiated, Na_v blockage failed to improve recovery (Al-Izki et al., 2014). In view of this patients were recruited and treatment commenced in ≤ 14 days from onset of visual symptoms and continued for 3 months. During this period there was also a possibility that surviving axons undergo a degree of remyelination providing further protection from longer-term injury.

A treating physician assessed patients after 1 and 3 months, when blood samples were obtained to measure phenytoin concentrations, blood counts and liver function tests.

4.7 Study end points

The primary outcome measure was active versus placebo difference in mean retinal nerve fibre layer thickness in the affected eye at 6 months, adjusted for the corresponding baseline measurement in the unaffected eye. Mean retinal nerve fibre layer thickness (RNFL) was chosen as the primary outcome measure due to the large body of data supporting its use as a surrogate outcome measure of axonal loss in multiple sclerosis and optic neuritis (Petzold et al., 2010; Balcer et al., 2015; Henderson et al., 2010). RNFL measurements have been shown to correlate with measures of visual function in patients with and without a history of optic neuritis as well as more general disability (Fisher et al., 2006), brain atrophy and T2 lesion load in patients with MS (Saidha et al., 2013). Additonally the timeframe of RNFL loss after optic neuritis has been well defined. For these reasons it was felt that RNFL thickness measurements would provide information about clinically relevant treatment effects within feasible a timeframe for a clinical trial. At the time of

designing the trial relatively little data was available on the use of ganglion cell layer thickness measurements as a surrogate outcome in neuroprotection trials. Also, at the time segmentation algorithms had yet to be fully optimized and were not commercially available.

Secondary imaging outcomes included macular volume as measured by OCT, and MRI measures including lesional optic nerve cross-sectional area and MTR (an indirect measure of optic nerve myelination) in addition to lesion length.

Visual function was not chosen as the primary outcome measure as the redundancy in the anterior visual system would make treatment effects more difficult to demonstrate.

Secondary clinical outcomes included affected eye visual function as measured by logMAR visual acuity, low contrast letter score (1.25% and 2.5% Sloan charts) and Farnsworth-Munsell 100 Hue test. In addition whole and central field VEP amplitudes and latencies were performed to give independent inferential measures of axonal conduction block/loss and demyelination/remyelination respectively of the optic nerve.

Primary and secondary endpoints were measured at baseline and 6 months later. The 3-month gap between cessation of treatment and this final assessment was designed to allow any artefactual effects of sodium channel inhibition (e.g. pseudoatrophy) to reverse before the final readout. Brain MRI sequences were obtained at baseline for patients without a prior diagnosis of multiple sclerosis. This was done to detect the presence of demyelinating lesions for prognostication or diagnosis of MS. MS was diagnosed using 2010 McDonald criteria (Polman et al., 2011).

Optical coherence tomography

OCT images were acquired with spectral domain OCT (Spectralis Heidelberg engineering, Germany, Software V 5.4B). Identical OCT protocols were performed at both sites by trained technicians blinded to treatment allocation.

Mydriatics were not used if pupils were large enough to permit scanning (>5mm). Automated real time a method for maintaining OCT B scan alignment and registration during image acquisition was employed.

Retinal nerve fibre layer measurements were performed using 3.45 mm diameter circle scan. The mean and sectoral (nasal, temporal, superior and inferior) RNFL measurements were recorded.

In addition a fast macular volume scan (20 x20° field, 25 horizontal B scans, ART 9) centered on the fovea was performed.

Internal fixation was used unless this was not possible due to poor visual acuity in which case an external fixation light using the unaffected eye was employed.

The software assisted retest function was applied to the baseline scans. This uses landmarks in the baseline image to re-centre the SD-OCT beam in the follow up scan to the previously scanned location.

Scans were excluded if they had a signal strength of <25 or violated international consensus quality control criteria (Schippling et al., 2015).

Low contrast letter scores

Low contrast letter scores were measured using retro-illuminated Sloan letter charts at 1.25%, 2.5% contrast levels for each eye at 2 meters (Precision Vision, La Salle, IL) using standard fluorescent office lighting. Numbers of letters identified were recorded for each eye.

LogMAR Visual Acuity

High contrast logMAR visual acuity was performed using retro-illuminated ETRDS charts at 4m. When no letters could be correctly identified a score of 1.7 was assigned. Standard lighting levels were established using fluorescent office lighting. Best-corrected acuities

were obtained with prescription spectacles and pinhole occluder. In addition to logMAR visual acuity taken at baseline and six months, Snellen visual acuity was also performed at one and three months for safety reasons (to ensure that treatment with phenytoin did not have a deleterious effect on vision)

Colour Vision

To assess colour vision the Farnsworth Munsell Hue 100 test was performed as previously described (Farnsworth, 1943). 85 coloured caps of different hues were presented under standard daylight conditions (colour temperature 6500K) in numerical order. Each eye was tested separately. Patients with a logMAR acuity of 1.0 or worse were deemed to have insufficient visual acuity to perform the test and were assigned an error score of 2000. Otherwise a computer program calculated the total error score.

Magnetic resonance imaging

MRI images were obtained on a two 3 T scanner and identical scanning protocols performed at both sites. Each optic nerve was imaged separately and for all acquisitions the imaging plane for the optic nerves was set orthogonal to the longitudinal axis of the optic nerve itself.

The following sequences were performed using identical scan geometry:

1) A multi-dynamic fat-suppressed heavily T2-weighted multi-slice "single-shot" two-dimensional (2D) turbo spin echo (TSE) with field of view (FOV) = 160 x 160 mm^2; repetition time (TR) = 16 s; echo time (TE) = 74 ms; voxel size = 0.5 × 0.5 × 3 mm^3; number of excitations (NEX) = 1; 20 contiguous slices; number of repeated dynamic scans = 15 (32s per dynamic scan; to minimize the effect of motion patients were asked to fixate on a marker attached to the coil; the individual volumes acquired were then co-registered and averaged to produce the final image, (Yiannakas et al., 2013).

2) A conventional fat-suppressed T2-weighted 2D-TSE with FOV = 160 x 160 mm^2; TR = 3 s; TE = 80 ms; voxel size 0.5 x 0.5 x 3 mm^3; NEX = 3; 20 contiguous slices; scan time 6 min 30 s

3) A T1-weighted fluid attenuated inversion recovery (FLAIR) 2D-TSE with FOV = 160 x 160 mm^2; TR = 2.1 s; TE = 10 ms; inversion time (TI) = 1 s; voxel size 0.5 x 0.5 x 3 mm^3; NEX = 2; 20 contiguous slices; scan time 6 min 26 s .

4) For MTR imaging, a 3D slab-selective FFE sequence with two echoes (TR = 49 ms, TE1/TE2 = 3.6/6 ms, flip angle α = 9°), performed with and without Sinc-Gaussian shaped MT saturating pulses of nominal α = 360°, offset frequency 1 kHz, duration 16 ms. Twenty slices were acquired with FOV = 160 × 160 mm^2; voxel size 0.75 × 0.75 × 5 mm^3 (reconstructed to 0.5 × 0.5 × 5 mm^3), NEX = 2, SENSE acceleration factor = 2, scanning time = 7 min.

Three independent assessors blinded to treatment allocation identified lesion length and position and patient identity using a combination of the conventional and multidynamic T2 weighted sequences.

The length of the lesion (in millimeters) was determined as the number of slices involved multiplied by 3.The globe–lesion distance (in millimeters) was calculated by multiplying the number of slices between the globe and the anterior edge of the lesion by 3.

A blinded assessor using semi- automated contouring technique on the T1 weighted images performed mean lesional cross-sectional area. A lesion mask was created on the baseline affected eye T2 images. Affected eye baseline T2 and 6 month T1 images were subsequently registered together. The T2 lesion mask was then applied to the registered 6 -month T1 images and mean 'lesional' cross-sectional area calculated. Measurements were then corrected for the corresponding baseline mean 'non –lesional' cross-sectional area in the unaffected eye (by applying the T2 lesion mask to baseline unaffected eye T1 images)

The MTR analysis was performed as follows:

Two MToff and two MTon images were acquired for each optic nerve within the same acquisition. MTon and MToff represent acquisitions with and without the pre-saturation pulse respectively.

Lesional MTR values for the affected optic nerves (corresponding MTR values for the unaffected nerves) were derived as follows for baseline and 6 month follow up MRI scans. FSL flirt was used for registration (http://fsl.fmrib.ox.ac.uk/fsl/fslwiki/FLIRT).

1) Calculation of optic nerve MTR maps

All four MT images were registered (using FSL) to one of the MToff images. The two MToff and two MTon images were respectively averaged to produce one MToff and one MTon image for each nerve. MTR optic nerve maps were calculated using the formula (MToff-MTon/MToff) x100.

2) Extraction of optic nerve MTR values

Jim (Xinapse systems) was used to delineate ROIs within the optic nerves. Initially, T1 optic nerve maps were registered to the MToff maps using FSL flirt. Circular ROIs (diameter 1.5mm, area 1.76 mm sq) were then applied to centres of the optic nerves on the registered T1 maps (using MToff and registered MTon maps as visual reference). The optic nerve MTR values were then extracted on a slice-by-slice basis for each optic nerve (left and right).

3) Determining lesion extent on optic nerve MTR map

The acute lesion was previously identified on the baseline optic nerve T2 images (e.g. the lesion could extend from slice numbers 4-8 inclusive). A crude baseline T2 lesion mask was created based on the longitudinal extent of the lesion. The baseline optic nerve T2 images were registered to baseline MToff space (this is in the same space as MTR) and the transformation matrix was applied to the T2 lesion mask to determine the MTR equivalent lesion mask at baseline. This was binarized with an intensity threshold of 0.9.

Baseline MToff images were registered to follow-up MToff images. A transformation matrix was applied to the baseline T2 lesion mask to convert it to follow-up MToff space. This transformed mask was binarized with an intensity threshold of 0.9. The baseline and follow-up MT lesion masks were overlaid onto the optic nerve MTR maps and the longitudinal slice extent of the lesion was recorded. A similar algorithm was followed for the unaffected optic

nerve with T2 lesion masks initially created for the unaffected side before being transformed into baseline and follow-up MT space. Hence the lesional MTR values could be determined for affected and fellow optic nerves and these were entered into statistical analysis.

Visual evoked potentials

VEPs were performed at both sites following International Federation of Neurophysiology guidelines (Holder et al., 2010) on a Synergy system. Monocular stimuli were applied using reversal of achromatic checks with a luminance of 61.2cd/m^2 (55.6cd/m^2 in Sheffield), (Michelson) contrast of 96.9% (93.1% in Sheffield), a reversal rate of 2.1/s (1.9/s in Sheffield) of a 32 x 32 array with a check size of 15.6' arc min/0.25° (18.0' arc min/0.3° in Sheffield) and a stimulus field of 15.6° (19.1° x 14.4° in Sheffield) in standard background office lighting. Responses were recorded from Oz using Fz as reference and Cz as ground at a sweep duration of 250 ms and filters at 1 Hz (high pass) and 100 Hz (low pass) without notch. At least 100 responses were averaged per trial using automatic artefact rejection and at least 2 replicates were obtained. Replicates were averaged and VEP latencies were measured to the nadir of the P100 and amplitudes from N75 to P100 to an accuracy of one decimal place.

Patients with absent VEP latencies or amplitudes were assigned a value of 200 and 0 respectively. At baseline 20 affected eyes in each group had their absent VEP latencies and amplitudes replaced this way (this was not used in the main analysis given that the baseline fellow rather than the affected eye measurements were used in the statistical analysis (see section 4.8) and none at baseline unaffected eye. At 6 months this replacement was made in three patients, all three in the active group. Although the 200 value is arbitrary, it is higher than the highest measured value in the study – 188. It is therefore conservative to include these values at 6 months rather than to exclude them that would have reduced the mean latency of the active group. Substituting values of 220 had no effect on the statistical significance level when comparing active vs. placebo difference.

Trained staff blinded to treatment allocation performed all outcome assessments.

4.8 Statistical analysis

The target sample size of 45 per arm was chosen to give 80% power to detect a treatment effect in RNFL thickness of 50% (inferred from a 50% reduction in the amount of RNFL loss compared to the fellow eye in a trial comparing active and placebo arms) at 5% significance level, whilst allowing for a 20% combined rate of loss to follow-up and non-adherence. Sample size was calculated from longitudinal OCT data on 23 patients with acute demyelinating optic neuritis using the mean follow up affected eye RNFL thickness adjusted for baseline fellow eye RNFL thickness (calculated using the follow up affected eye RNFL standard deviation (18.32) and the follow up affected versus baseline fellow eye Pearson correlation coefficient (0.63) (Henderson et al., 2010).

Adjusting for the fellow eye maximised power by overcoming the large inter-subject variability in normal RNFL thickness The fellow eye was chosen because acute swelling in the affected eye makes this eye a poor predictor of follow-up thickness, and makes affected eye change uninterruptable. Accordingly, an ANCOVA analysis method was used, using multiple linear regression of the follow-up affected eye RNFL on a trial arm indicator with the following pre-specified covariates: baseline fellow eye value, center (binary), days between onset and baseline assessment, and whether the patient was prescribed corticosteroids at the time of baseline assessment (3 categories: no/ 1-5 days prior to assessment/ 6-30 days prior). Two planned binary covariates were not used because of a pre-specified minimum of 10 for their smallest category: “Prior MS” (4 yes, 82 no) and “Prescribed disease-modifying treatment” (1 yes, 85 no). Secondary outcomes were analyzed similarly, with the corresponding baseline fellow-eye value and the same pre-specified covariates. An exception was lesion length, for which the baseline fellow eye was not specified as covariate; also, due to only 3 patients at one MRI site (Sheffield), center was not used as a covariate in the analyses.

The primary intention-to-treat (ITT) analyses included all randomized patients who were followed up. Secondary per protocol (PP) analyses, after excluding patients with a subsequent further episode of optic neuritis, compared all placebo patients with just adherent active patients, defined as having phenytoin present in their one-month blood.

Where regression residuals showed signs of non-normality and/or heteroscedasticity, p-values were calculated with a permutation test. Statistical significance, where referred to, indicates $p<0.05$ and all p-values refer to two-tailed tests.

Chapter 5 Baseline Results

5.1 Introduction

Optic neuritis is one of the most common causes of acute visual loss in young adults (Jin et al., 1998). It may occur in isolation, so called 'idiopathic optic neuritis' or in association with multiple sclerosis. It usually presents with subacute monocular visual loss associated with retro-orbital pain, dyschromatopsia and reduced low contrast vision.

At baseline visual evoked potentials typically demonstrate a delayed P100 latency and acutely amplitude may be reduced or there may even be complete conduction block. The lesion in the optic nerve may be visualized by orbital MRI using fat-saturated fast spin echo sequences and imaging of the retinal nerve fibre layer using optical coherence tomography may demonstrate RNFL swelling.

In this chapter I aimed to look at the baseline clinical, electrophysiological and imaging profile of our cohort of patients with acute optic neuritis recruited within 2 weeks of symptom onset and investigate whether there were any significant correlations with baseline visual function and RNFL swelling.

5.2 Methods

The baseline data of all 86 patients recruited into the study was analyzed. Clinical visual function testing, VEPS and optical coherence tomography measurements (RNFL thickness and macular volume) were performed within 2 weeks of symptom onset as described in Chapter 4.7. Orbital MRI was performed and optic nerve cross-sectional area measurements obtained as described in Chapter 4.7. Lesion length was obtained using the conventional fat suppressed T2 weighted 2D-TSE images by calculating the number of consecutive slices involved and multiplying by 3. The globe–lesion distance (in millimeters) was calculated by multiplying the number of slices between the globe and the anterior edge of the lesion by 3.

5.3 Summary of baseline results

86 patients were included in the baseline analysis, of these 63 were female (73%). The mean time from onset of visual loss to being enrolled into the trial was 8.2 days (+/- 3.2). The majority of patients (79%) were prescribed steroids as treatment for their optic neuritis. Only 4 patients had a pre-existing diagnosis of Multiple sclerosis and just one of these was prescribed a disease-modifying drug (B interferon).

A baseline brain MRI was performed in 80 patients. Three patients had a known diagnosis of MS and did not require brain imaging, two were lost to follow up before the MRI was performed and one was unable to have the scan due to metalwork.

At baseline 74% had ≥ 1 T2 hyper-intense lesions on brain MRI, 53% of patients satisfied McDonald's 2010 criteria for dissemination in space and 30% satisfied McDonald's 2010 criteria for MS.

81 patients underwent optic nerve imaging and the symptomatic optic nerve lesion visualized in all except three at baseline. Mean lesion length was 17.6mm (+/- 7.60). The majority of patients had involvement of the intra-orbital segment of the optic nerve (84%). Canalicular involvement was seen in 59% of patients and the intracranial segment was involved in 31% of patients. 25% of patients had long lesions involving all three segments of the optic nerve. Only 1 patient had involvement of the optic chiasm.

82 patients had baseline electrophysiology performed. VEPs were absent in the affected eye in 40 (49%) for the small check size and 35 (43%) for the large check size at baseline.

See Table 5-1 for a summary of baseline measurements:

Table 5-1: Baseline clinical, electrophysiological and MRI characteristics for all patients

	Affected eye measurements (n=86)	Unaffected eye measurements (n=86)
Age (yrs)	34 (8.7)	
Women	63 (73%)	
Days from onset to randomization	8.2 (3.2)	
Prescribed corticosteroids	68 (79%)	
Prior diagnosis of multiple sclerosis	4(5%)	
≥ 1 T2 hyperintense MRI brain lesions	64(74%)	
RNFL thickness affected eye (μm)	127.9 (44.9)	98.2 (11.0)
Macular volume (mm^3)	8.7 (0.5)	8.7 (0.4)
LogMAR visual acuity	1.09 (0.57)	-0.03 (0.09)
1.25% low contrast letter score	0.26 (1.74)	27.91 (10.13)
2.5% low contrast letter score	0.49 (2.53)	33.69 (9.76)
FM 100-Hue total error score	1103 (770.1)	89.54 (52.85)
VEP small check latency (ms)	167.7 (35.5)	104.4 (6.1)
VEP small check amplitude (μV)	2.9 (3.8)	10.5 (5.45)
Optic nerve cross-sectional area (mm^2)	7.54(1.49)	5.42 (0.82)
Lesion length (mm)	17.6 (7.6)	n/a

Data are mean (SD) for the affected eye, or number (%)

5.4 Statistical analysis

Univariable (pairwise) associations between baseline variables were assessed using Pearson correlation coefficients. In order to determine which measures were independently predictive of baseline visual function and RNFL swelling, multiple linear regressions were used, with visual function or RNFL as response (dependent) variables. Where normality of residuals could not be assumed, non-parametric, bias-corrected and accelerated bootstrap confidence intervals were obtained using 1000 replicates, to confirm or correct the regression results

5.5 Correlations with baseline visual function

Mean baseline corrected (with patients' spectacles and pin hole) logMAR visual acuity of the affected eye was not significantly correlated with mean lesion length or distance of the lesion from the globe (p=0.34, r=0.11 and p=0.53, r=0.07 respectively). There was no significant difference in baseline logMAR visual acuity in patients with long lesions of ≥ 17.5 mm and those with shorter lesions <17.5 mm (p= 0.28).

Likewise there was no significant association between baseline affected eye logMAR visual acuity and affected eye lesional optic nerve cross-sectional area.

Baseline mean lesional optic nerve cross-sectional area was significantly correlated with mean lesion length (p=0.005, r= 0.32).

Baseline low contrast letter score (1.25% and 2.5%) was not significantly associated with lesion length, distance of the lesion from the globe or optic nerve cross-sectional area. Similarly there was no significant association between baseline FM hue 100 score and lesion length and optic nerve cross-sectional area. However patients with long lesions of ≥ 17.5 mm had borderline significantly worse FM hue 100 error score than those with shorter lesions <17.5 mm (p=0.07)

There was a significant correlation between baseline corrected with patients' spectacles and pin hole) logMAR visual acuity and affected eye RNFL swelling (baseline affected eye RNFL thickness-baseline unaffected eye RNFL thickness0 (p=0.04, r=0.23) (Figure 5-1)

Figure 5-1: Baseline LogMAR visual acuity was significantly correlated with RNFL swelling

(in patients with recordable VEPs)

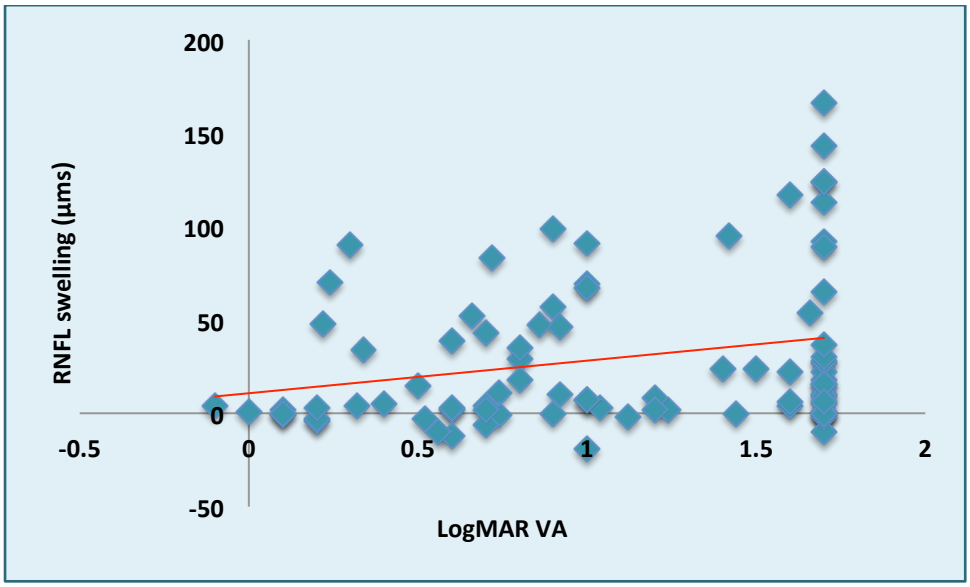

Similarly, baseline affected eye RNFL thickness was predictive of a higher (worse) baseline logmar when adjusted for the baseline unaffected eye RNFL thickness in a regression model (p=0.02)

There was no significant correlation between baseline corrected logMAR visual acuity and either affected eye macular volume or macular volume swelling (baseline affected eye macular volume- baseline unaffected eye macular volume) (p=0.23, r= -0.13 and p= 0.13, r= 0.17 respectively).

Patients with conduction block and absent affected eye VEPs (small check) had logMAR visual acuity 0.65 higher (worse) than those with recordable VEPs at baseline (p=<0.001).

Amongst patients with recordable VEPs a 1 ms increase in VEP latency (small check) was predictive of 0.008 increases in logMAR visual acuity (p=0.03) at baseline (See **Figure 5-2**)

There was no significant association between baseline logMAR visual acuity and VEP amplitude (small check) (p=0.09).

Figure 5-2: Baseline LogMAR visual acuity was significantly associated with VEP latency

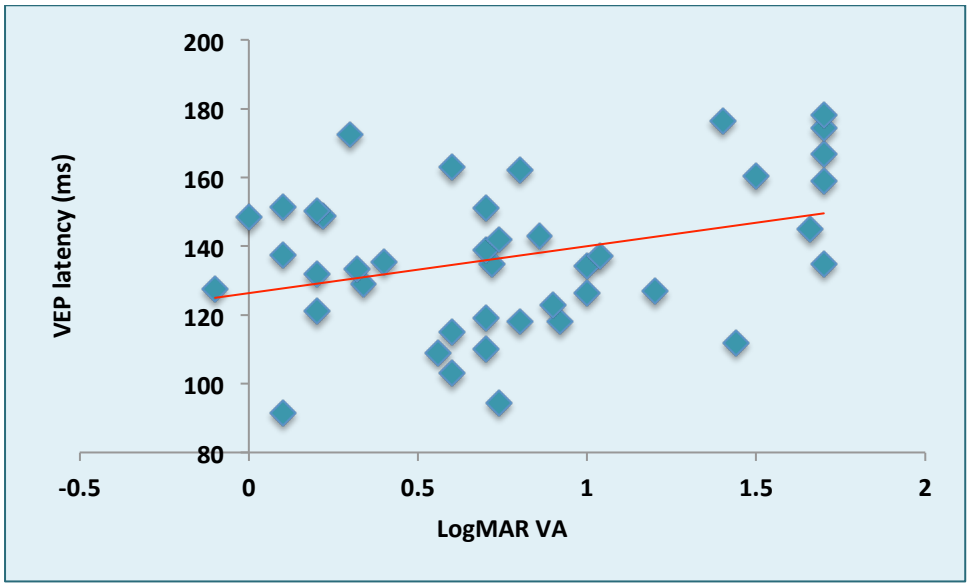

Table 5-2: Univariate correlations with best corrected LogMAR visual acuity (affected eye)

MRI measures	No.	P value	r =
Lesion length	78	0.34	0.11
Optic nerve cross-sectional area (mm^2)	73	0.48	-0.08
Globe lesion distance (T2weighted) (mm)	78	0.53	0.07
OCT measures			
RNFL thickness (µm)	86	0.08	0.19
RNFL swelling (µm)	86	0.04	0.23
Macula volume (mm^3)	86	0.23	-0.13
Macula swelling ($mm^£$)	86	0.13	0.17
VEP measures			
Small check VEP	42	0.03	0.11

latency* (ms)			
Small check VEP amplitude* (µV)	42	0.09	0.07
Absent VEPS	40	<0.001	0.31

- In patients with recordable baseline VEPs

Therefore, at baseline the predictors of logMAR visual acuity were baseline RNFL swelling and absent VEPs as well as prolonged VEP latency in patients with recordable VEPs.

When both baseline RNFL swelling and absent affected eye VEPs were included in a multivariate regression model only absent VEPs were independently predictive of logMAR visual acuity at baseline (p=<0.001).

Likewise when both baseline RNFL swelling and baseline VEP latency (small check) for those with recordable VEPs were included in the regression model, only VEP latency was independently predictive of logMAR visual acuity at baseline (p=0.04).

In the regression model absent VEPs (small check) explained 31% of the variability in LogMAR visual acuity at baseline where as VEP latency in those with recordable VEPs explained 11% of the logMAR variability suggesting that absence of VEPs are the better predictor of logMAR visual acuity at baseline.

There was no significant difference in low contrast letter scores (1.25% and 2.5%) between patients with absent and those with recordable VEPs. However mean affected eye FM-Hue-100 error score in patients with absent baseline VEPs was more than double that of patients with recordable VEPs at baseline (1554 versus 679, p=<0.001).

In patients with recordable VEPs there was a significant negative correlation between low contrast letter score at 1.25% (p=0.03, r=-0.33) and 2.5% (p=0.02, r-0.37) and VEP latency but no significant correlation with VEP amplitude.

Mean VEP latency and amplitude in patients with recordable VEPs were significantly correlated with FM-hue 100 error scores at baseline (p=0.008, r=0.41 and p=0.02, r-0.36 respectively).

5.6 Correlations with baseline RNFL swelling

There was a significant positive correlation between RNFL swelling with optic nerve lesion length and lesional optic nerve cross-sectional area at baseline (p= 0.001, r=0.36 and p=0.02, r=0.28 respectively) (See Figure 5-3 and Figure 5-5). Conversely, there was a significant negative correlation between baseline RNFL swelling and distance of the lesion from the globe (p=0.002, r=-0.34) (See Figure 5-4).

There was no significant association between baseline low contrast letter score (1.25% and 2.5%) and RNFL thickness/RNFL swelling/Macular volume. However, baseline FM-Hue error score was significantly associated with RNFL thickness and RNFL swelling (baseline affected eye RNFL thickness – unaffected eye RNFL thickness) (p=0.05, r=0.21 and p=0.03, r= 0.23 respectively).

Table 5-3: Univariate correlations with RNFL swelling (affected eye)

MRI measures	No.	P value	r =
Lesion length (mm)	81	0.001	0.36
Optic nerve cross-sectional area ($mm^{2)}$	73	0.02	0.28
Globe lesion distance (mm) (T2weighted)	81	0.002	-0.34
Visual function measures			
LogMAR visual acuity	86	0.04	0.23
2.5% low contrast letter score	86	0.40	-0.09
1.25% low contrast letter score	86	0.21	-0.14
FM-100 Hue total error	86	0.03	0.23

score			
VEP measures			
Absent VEPS	40	0.005	0.3

Figure 5-3: Baseline RNFL swelling was significantly associated with lesion length

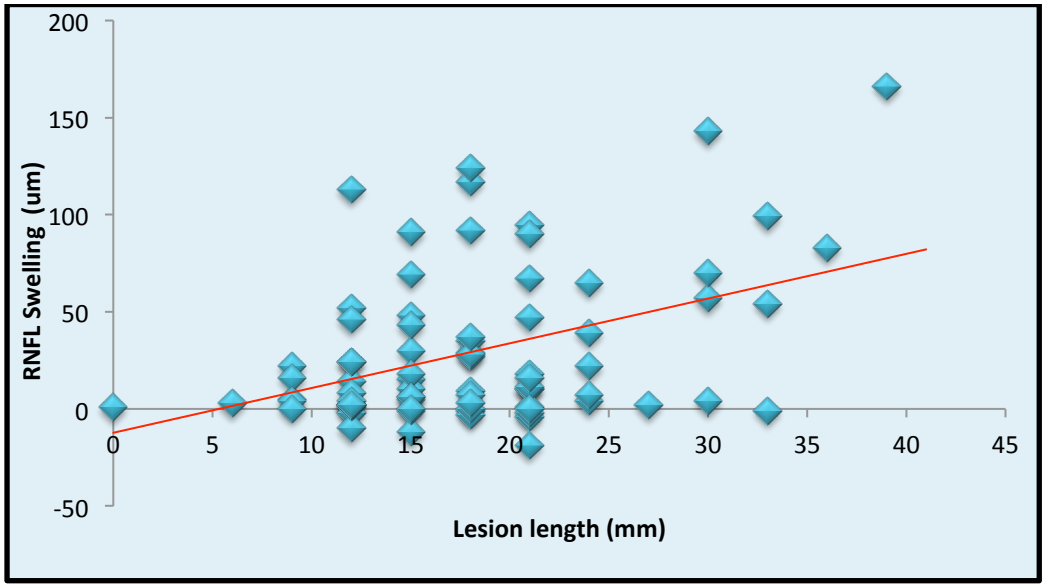

Figure 5-4: Baseline RNFL swelling was negatively associated with distance of the lesion from the globe

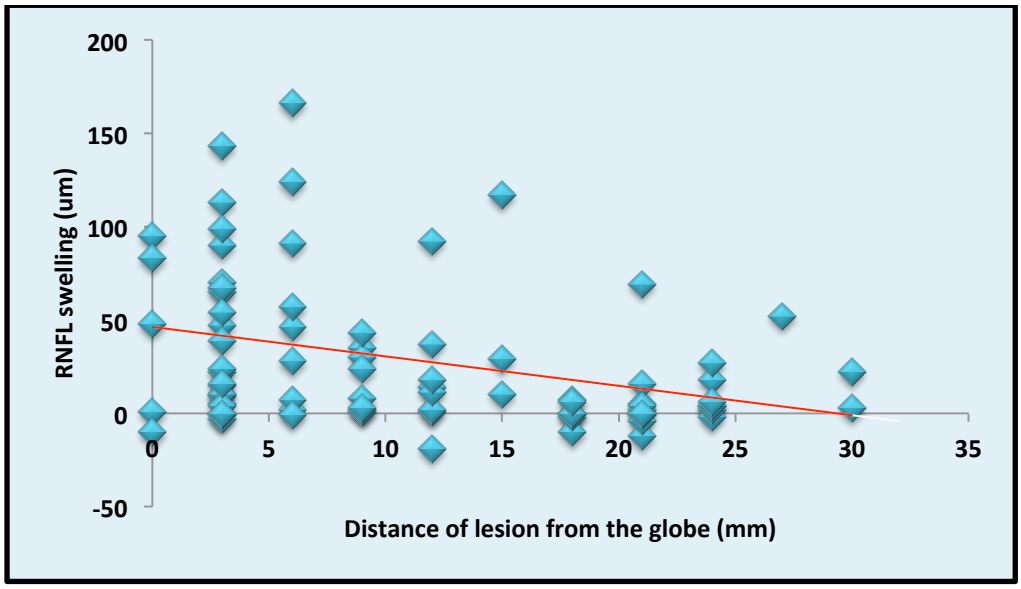

Figure 5-5: Baseline RNFL swelling was significantly associated with optic nerve cross-sectional area

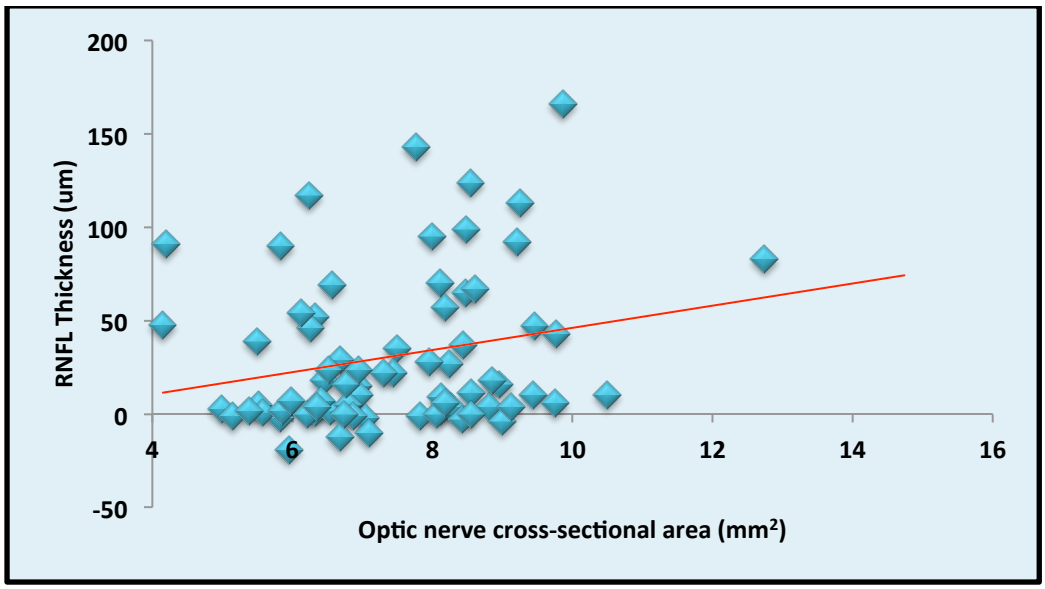

Patients with absent baseline VEPs (small check) had on average a 25 µms greater RNFL thickness than those with recordable VEPs (p=0.002) at baseline.

When lesion length, lesional optic nerve cross-sectional area, distance of the lesion from the globe and absent VEPs were all included in a multivariate regression model (adjusting for the unaffected eye) the strongest independent predictor of baseline RNFL swelling was lesion length (p=0.003 r=0.28). Distance of the lesion from the globe and absent VEPs was also independently predictive of RNFL swelling at baseline (p=0.02 r= -0.21 and p=0.05 r= 0.17 respectively).

Patients with absent VEPs at baseline had borderline significantly longer symptomatic optic nerve lesion by 3.2 mm than patients with recordable VEPs (p=0.06)

5.7 Discussion

Inflammation and conduction block appear to be the main determinants of visual loss at baseline in acute optic neuritis as suggested by the significant associations of both RNFL swelling and absent VEPs with logMAR visual acuity and FM-hue 100 error score in the

affected eye. The degree of demyelination also appears to be an important determinant of baseline visual function given the association between prolonged VEP latency in those patients with recordable VEPs and logMAR visual acuity and colour vision. The lack of any significant baseline associations between any of the MRI, OCT or VEP measurements and low contrast letter scores is likely due to the floor effect of performing these tests at baseline when visual function is most impaired. Conduction block on baseline VEP was the best independent predictor of visual loss at baseline explaining 31 % of the variability and is likely to be due to a combination of inflammation and inflammatory mediators as well as demyelination.

The results are supportive of the findings by Youl et al 1991 who found that inflammation - as demonstrated by Gd-DTPA leakage across the blood optic nerve barrier - was associated with conduction block and the clinical deficit (Youl et al., 1991a).

More surprisingly none of the MRI characteristics (including lesion length) were associated with baseline visual acuity although patients with longer lesions on MRI ($\geq$ 17.5mm) had borderline worse colour vision at baseline. It should be noted that in my study the lesion length was identified using a combination of the conventional fat-suppressed T2-weighted 2D-TSE images and multi-dynamic fat-suppressed heavily T2-weighted multi-slice "single-shot" two-dimensional TSE images rather than using gadolinium enhanced images of the optic nerves. Previous studies have demonstrated an association between lesion length as measured by the length gadolinium enhancement of the optic nerve and baseline visual acuity (Hickman et al., 2004b; Kupersmith et al., 2002). In concordance with my results Hickman et al 2004 did not find a significant association between lesion length on the baseline FSE images and logMAR visual acuity. In that study the median lesion length was 6 mm longer on the gadolinium-enhanced images than the FSE images perhaps suggesting that gadolinium enhancement of the optic nerve is a more sensitive method of imaging acute inflammation in the optic nerve. Gadolinium enhancement may also be more specific for inflammation and has been shown to correlate with the inflammatory infiltrate and expansion of the extracellular space (Guy et al., 1992); on the other hand, fat saturated T2 weighted images demonstrate high signal as a result not only of vasogenic oedema and inflammation but also axonal loss, extracellular water and gliosis.

The location of the lesion did not appear to be an important determinant of baseline visual loss as there was no association between distance of the lesion from the globe and baseline visual acuity.

Despite the lack of association between MRI characteristics and baseline visual acuity, longer and more anterior lesions on T2 weighted MRI were significantly associated with RNFL swelling at baseline. Longer lesions may be more likely to cause stasis of axoplasmic flow leading to RNFL swelling proximal to the lesion. Equally, the more proximal the lesion to the optic nerve head the more likely the extension of inflammation/oedema across the lamina cribrosa into the RNFL.

Conduction block on baseline VEPs was also significantly associated with RNFL swelling and there was also a borderline significant association with lesion length, again implicating the degree of inflammation in the acute lesion with loss of function and conduction block. The strongest independent predictor of RNFL thickness at baseline was lesion length, and the extent of the lesion was more important than its location in predicting RNFL swelling. This perhaps suggests that RNFL swelling is more often due to a secondary phenomenon (axoplasmic stasis) rather than direct spread of inflammation from the optic nerve to the retina.

Chapter 6 Trial results – Primary outcome measure

6.1 Patients

Patients were recruited between February 2012 and May 2014, and final assessments performed in December 2014. 86 patients were randomly assigned to receive phenytoin (n=42) or placebo (n=44)(Figure 6-1). The groups had similar baseline characteristics (Table 6-1) There were however a slightly higher proportion of patients in the active group who were prescribed corticosteroids. This may be due to the slightly worse baseline visual acuity in the phenytoin compared the placebo group. There were only four patients who had a pre-existing diagnosis of multiple sclerosis; 3 of these were in the placebo group. One patient from the placebo group was on disease modifying medication at the time of randomization. Amongst the remainder of patients similar proportions of patients had ≥ 1 T2 hyperintense MRI brain lesions in the phenytoin and placebo groups (73% and 76% respectively). 13 patients in the active group and 11 in the placebo group fulfilled McDonald 2010 criteria for the diagnosis of MS on presentation. A further 16 went on to have relapses during the trial follow up period (13 of these were MS defining (7 active, 9 placebo).

Only screening data was available for the patients who declined to participate in the trial. However they were of similar age (mean age 32) and sex (76% female) with comparable visual acuity in the affected eye (mean logMAR visual acuity 1.0) to the patients who were recruited into the trial. Given the similar screening characteristics it is likely that the findings of the trial are generalisable to all patients who matched the eligibility criteria.

The mean time from onset of visual loss to recruitment was 8.2 and 8.1 days respectively in the phenytoin and placebo groups respectively. Given the mounting evidence that vitamin D deficiency may be one of the environmental factors associated with an increased risk of developing MS (Martinelli et al., 2014), baseline vitamin D levels were taken in 41 patients (18 phenytoin and 23 placebo). Baseline mean vitamin D levels were 38.83 nmol/L (active) and 40.22 nmol/L (placebo) respectively.

Table 6-1: Baseline, clinical, structural and electrophysiological data

	Phenytoin (n=42)	Placebo (n=44)
Age (yrs.)	33 (8.2)	35 (9.1)
Women	31 (74%)	32 (73%)
Days from onset to randomization	8.2 (3.1)	8.1 (3.2)
Prescribed corticosteroids	35 (83%)	33 (75%)
Prior diagnosis of multiple sclerosis	1 (2%)	3 (7%)
≥ 1 T2 hyperintense MRI brain lesion	32 (73%)	32 (76%)
RNFL thickness affected eye (µm)	130.6 (46.4)	125.2 (43.4)
Macular volume (mm^3)	8.7 (0.5)	8.6 (0.4)
LogMAR visual acuity	1.11 (0.54)	1.07 (0.6)
1.25% low contrast letter score	0.07 (0.5)	0.45 (3.0)
2.5% low contrast letter score	0.21 (1.2)	0.77 (3.8)
FM 100-Hue total error score	1066 (764.6)	1139 (775.5)
VEP P100 latency[a] (Small check, ms)	167.9 (35.2)	167.6 (35.8)
VEP P100 amplitude[a] (small check, µV)	2.8 (3.8)	3.0 (3.8)
Optic nerve cross-sectional area (mm^2)	7.60 (1.55)	7.48 (1.43)
Lesion length (mm)	17 (8.1)	18 (7.1)

Data are mean (SD) for the affected eye, or number (%)

[a]Twenty subjects in each group had affected eye vision too poor to measure VEP, but the baseline affected eye VEP was not used in analyses.

5 patients were lost to follow up, leaving 81 who attended for assessment of the primary outcome at 6 months (39 phenytoin, 42 placebo). Of these, 10 in the phenytoin group were withdrawn from treatment due to rash after a mean of 18.4 (SD 14.98) days, but continued to be followed up (Figure 6-1). The remaining 29 in the phenytoin group were serum adherent (mean serum phenytoin concentration 8.57 (SD 5.40)mg/L). The combined overall rate of loss to follow-up, withdrawal from treatment and non-adherence was 19%.

Figure 6-1: Trial profile

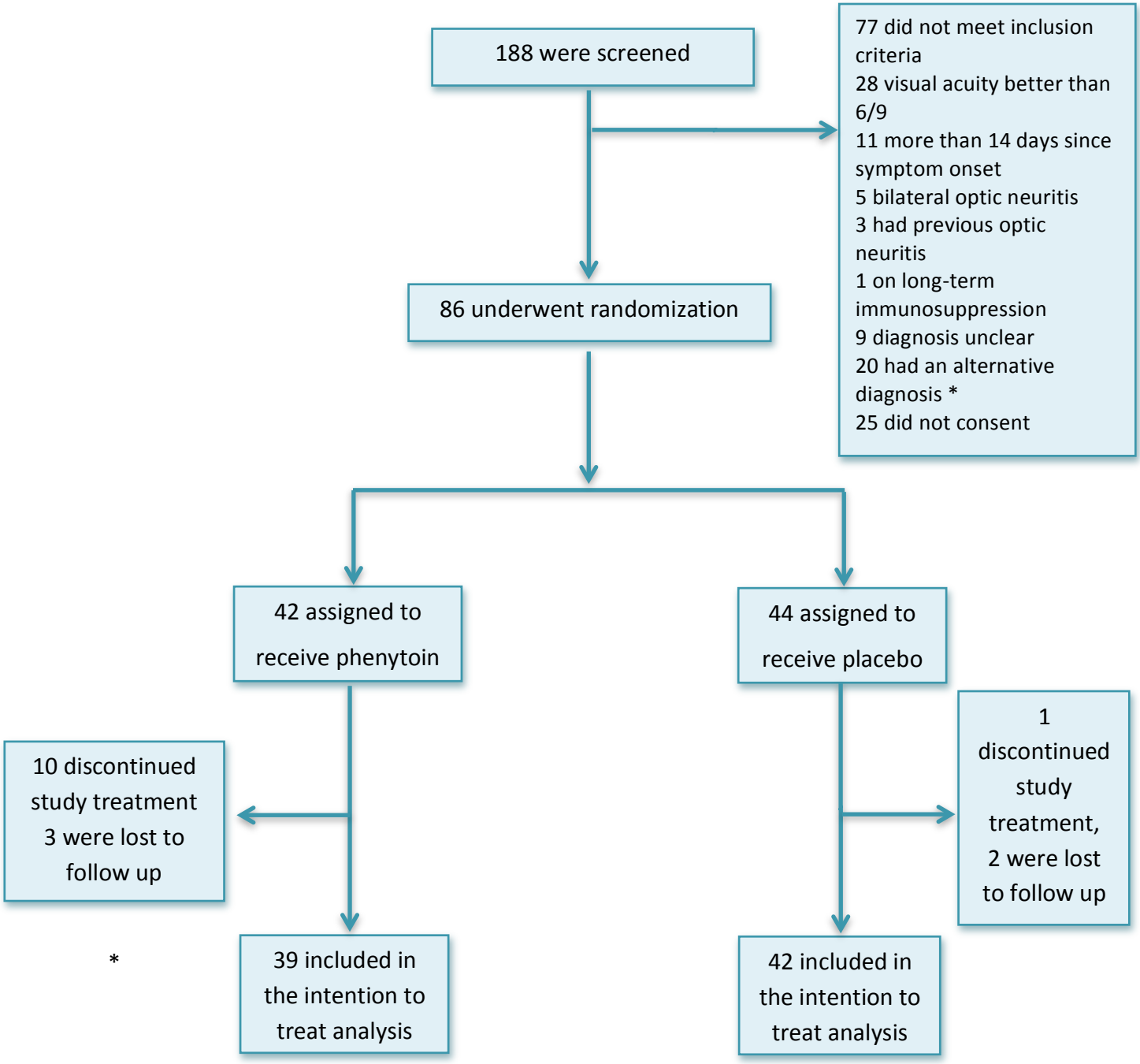

*

Alternative diagnosis were functional visual loss (n=4), sarcoidosis (n=3), migraine with aura (n=2), posterior scleritis (n=3), Leber hereditary optic neuropathy (n=2), compressive optic nerve lesions (n=2), uveitis (n=1), toxic optic neuropathy (n=1), neuroretinitis (n=1) central serous retinopathy (n=1) and optic nerve drusen (n=1)

6.2 Intention to treat comparison – Primary outcome measure

Measurements of the thickness of the RNFL and of macular volume remained stable in the unaffected eye, with no significant change between baseline and 6 months (Table 6-2)

Table 6-2: Stability of measurements in the unaffected eye in the phenytoin and placebo groups

	Phenytoin		Placebo	
	Baseline	6 months	Baseline	6 months
RNFL thickness (μm)	98.0 (11.1)	98.7 (11.6)	98.4 (11.0)	97.4 (13.2)
Temporal sector RNFL thickness	68.6 (11.6)	70.1 (11.6)	69.3 (11.5)	69.3 (14.3)
Nasal sector RNFL thickness	71.7 (17.1)	72.9 (17.2)	72.6 (17.2)	71.5 (13.8)
Superior sector RNFL thickness	120.1 (16.5)	120.7 (18.4)	120.3 (17.2)	119.2 (19.9)
Inferior sector RNFL thickness	131.2 (17.7)	129.9 (17.9)	133.1 (18.3)	129.2 (19.5)
Macular volume (mm^3)	8.7 (0.4)	8.7 (0.4)	8.6 (O.4)	8.6 (0.4)

Data are means and SD.

In the placebo group, the mean thickness of the RNFL in the affected eye fell by 24.1 μm (or 24%) after 6 months when compared with the baseline unaffected eye (Figure 6-2).

Proportionately, at 6 months, the temporal sector RNFL had the greatest reduction in thickness compared to the unaffected eye in the placebo group.

Figure 6-2: Atrophy of overall and sectoral RNFL thickness at 6 months in the affected eye (placebo arm only)

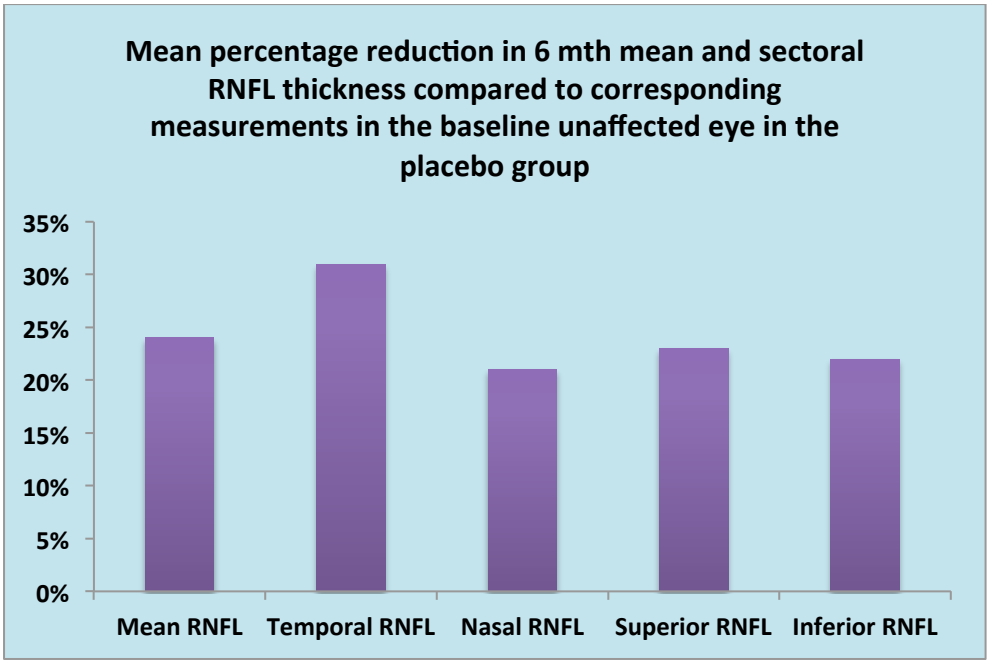

In the phenytoin group the mean affected-eye thickness fell 16.7 µm (17%) after 6 months compared with the baseline unaffected eye, giving a significantly higher mean 6-month affected eye RNFL thickness in the phenytoin group compared to placebo (Figure 6-3). The ITT adjusted phenytoin - placebo mean 6-month affected eye RNFL difference was 7.2 µm (95% confidence interval (CI) 1.1, 13.2; p=0.021), indicating a 30% beneficial treatment effect.

Figure 6-3: Scatter plots of RNFL thickness in the baseline unaffected eye and 6 month affected eye in the phenytoin and placebo groups

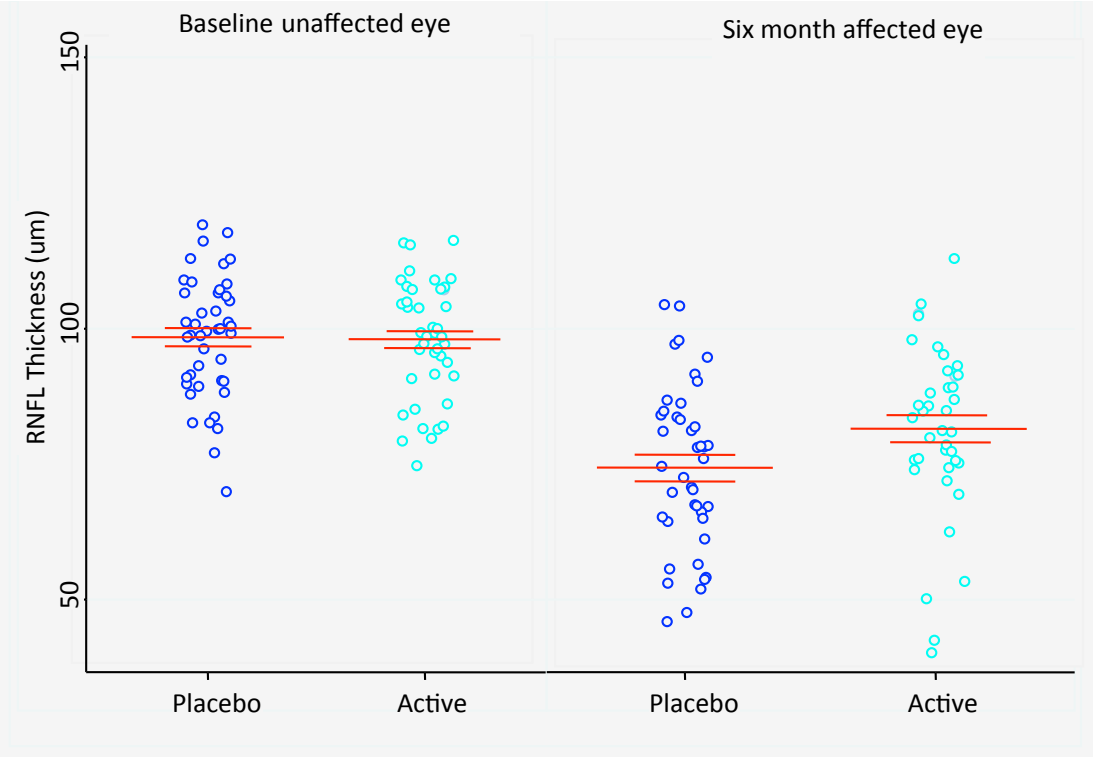

At 6 months superior and nasal sector RNFL thicknesses were significantly greater the active group (p=0.005 and p=0.058 respectively) There was no significant difference in the temporal sector or inferior sectors (p=0.39 and p=0.22 respectively (Table 6 -3)

Mean 6-month affected eye MV fell compared to the baseline unaffected eye by 0.6 mm^3 (7%) and 0.4 (4%) in placebo and phenytoin groups respectively, giving a significantly higher mean 6-month affected eye MV in the phenytoin group compared to placebo (Figure 6-4)

The ITT adjusted phenytoin-placebo mean 6-month affected eye difference in macular volume was 0.2 mm^3 (95% CI 0.1, 0.3; p=0.005), a 34% beneficial treatment effect. There was a significant phenytoin-placebo treatment effect on macular volume when adjusted for the baseline affected eye. Segmentation of the retinal layers had not been performed at the time of writing this thesis but will be performed retrospectively and will be the subject of future publications.

Figure 6-4: Scatter plots of macular volume in the baseline unaffected and 6 month affected eye in the active and placebo groups

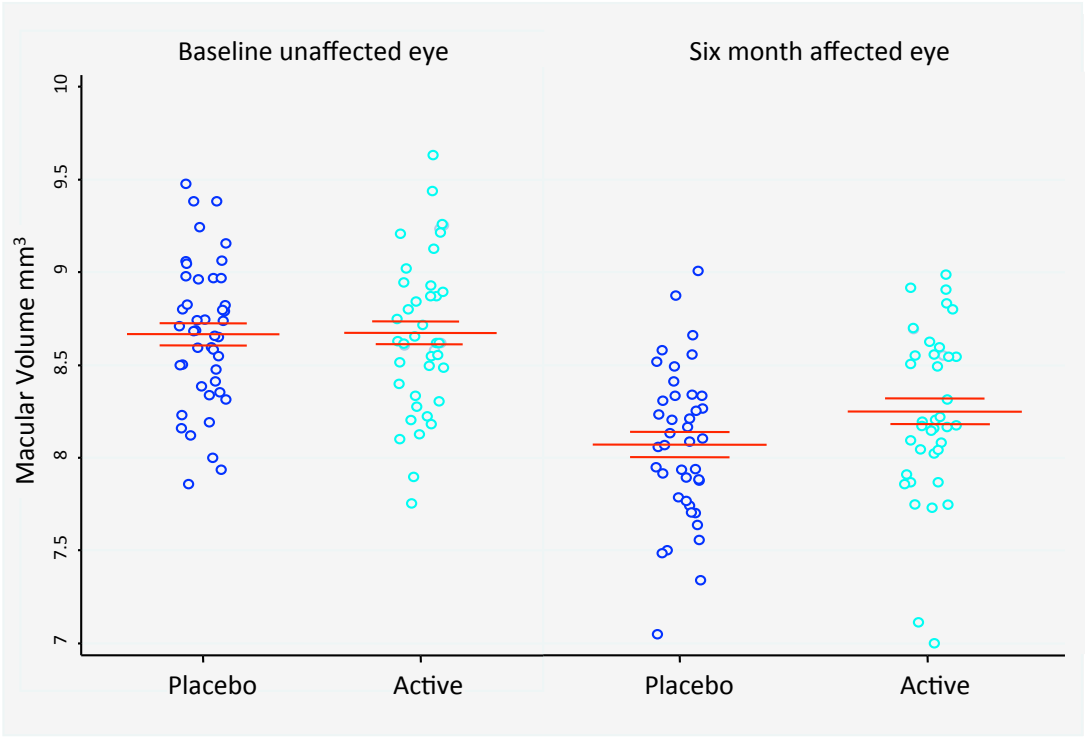

Exploratory analyses

Mean adjusted active-placebo difference in RNFL thickness in the affected eye was similar in patients who discontinued treatment due to rash compared to those who continued treatment for the full three months (8.3 µm, 95% CI 1.96,18.52).

There was no statistical difference in the treatment effect (on the primary analysis) between participants with normal (within normal limits for patient's age) and abnormal brain MRI (one or more demyelinating brain lesions) scans at baseline (p=0.629).

Table 6-3: Intention to treat comparison of primary endpoints at six months

	Active n=	Placebo n=	Adjusted active-placebo difference ¶ (95% CI)	p value
RNFL thickness (*µ*m)	81.5 (16.3) n=39	74.3 (15.1) n=42	7.2 (1.1,13.2)	0.02
Temporal sector thickness (*µ*m)	49.9 (13.8)	47.8 (14.0)	2.5 (-3.3,8.3)	0.39
Nasal sector thickness (*µm)*	62.3 (14.8) (n=39)	57.5 (15.5) (n=41)	5.2 (-0.2,10.6)	0.06
Superior sector thickness (*µm)*	105.5 (23.5) (n=39)	93.2(21.0) (n=41)	12.2 (3.9,20.6)	0.005
Inferior sector thickness (*µm)*	107.6 (23.0) (n=39)	100.8 (21.2) (n=41)	5.4 (-3.3,14.1)	0.22
Macular volume (mm^3)	8.3 (0.5) (n=39)	8.1 (0.4) (n= 41)	0.2 (0.5,0.3)	0.005

Data are mean (SD)

¶ Pre-specified adjustment for baseline unaffected value, centre, days between onset and baseline, days between steroid and baseline

6.3 Relapses

In the intention to treat comparison seven patients (17%) suffered a further demyelinating relapse during the 6-month follow up period in the phenytoin group and nine in the placebo group (21%). This difference was not statistically significant (p= 0.65). There was no significant difference in time to second demyelinating relapse between the two groups (logrank test p= 0.608) (Figure 6-5).

Figure 6-5: Kaplan Meier curves for time to second demyelinating relapse during the six month follow up period

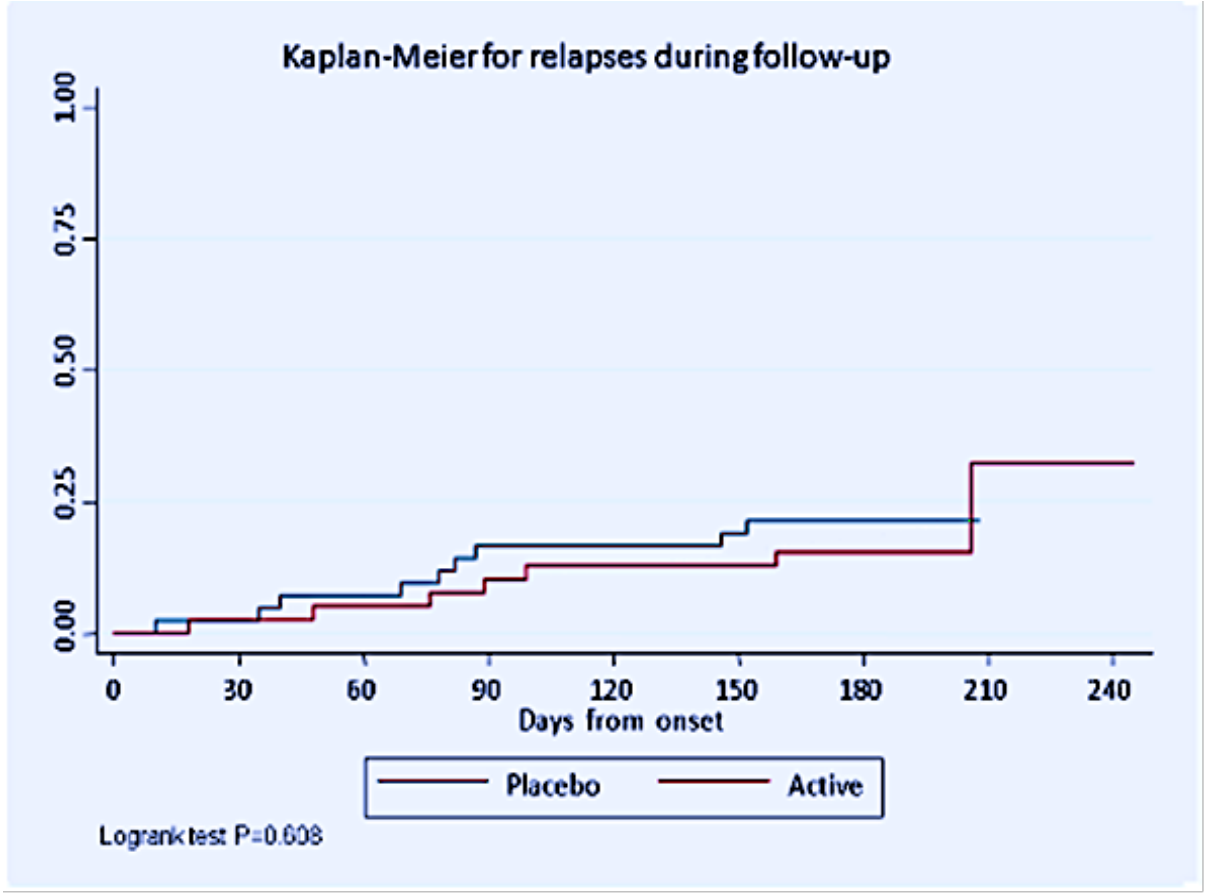

6.4 Per protocol comparison - primary end point

29 of the 42 patients in the phenytoin patients in the phenytoin group were serum compliant as defined by a 1 month serum phenytoin level of >0. For the 29 patients who were serum compliant the mean phenytoin concentration was 7mg/L, SD 5.9. Below is a histogram of serum phenytoin levels at 1 month.

Figure 6-6: Histogram of 1-month serum phenytoin levels in the active group

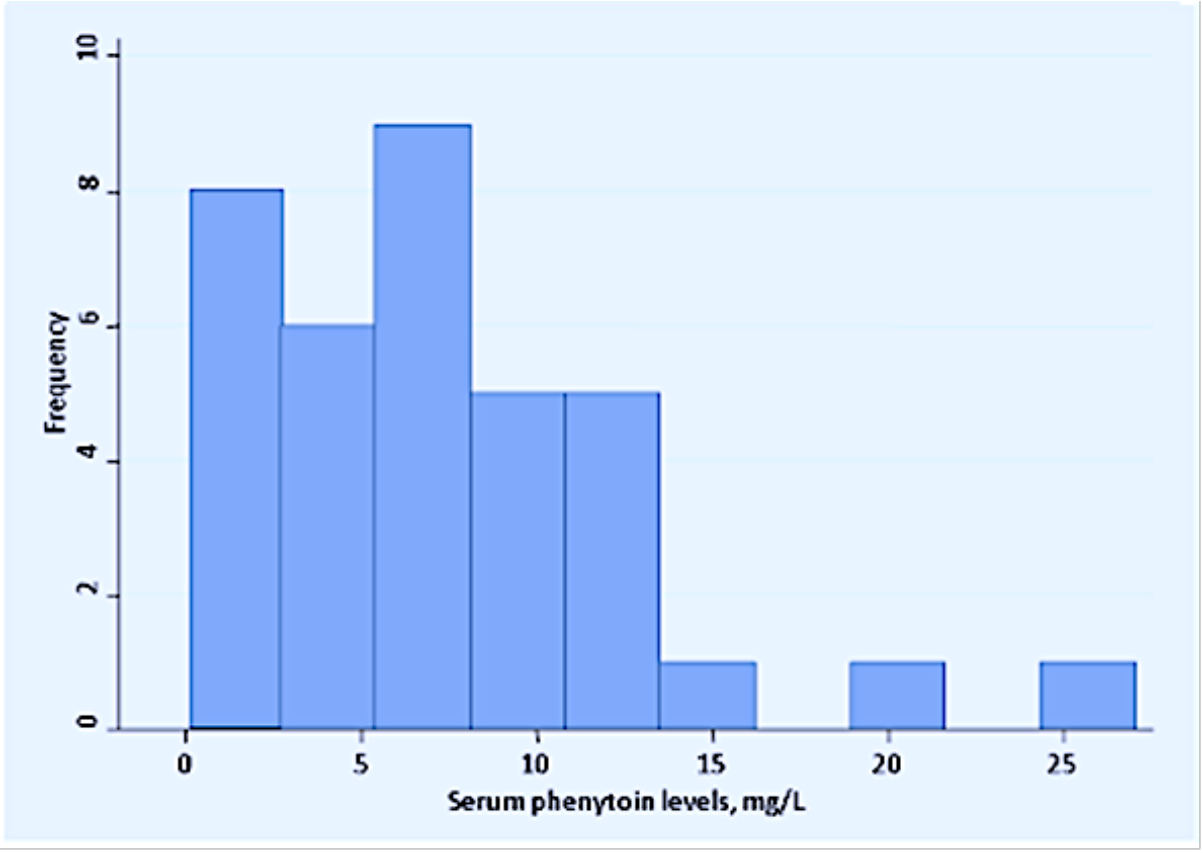

* The first bar contains one patient with a level of 1 mg/L and seven with 0mg/L

** 6 patients in the active group had missing serum phenytoin levels at one month (3 were lost to follow up and 3 results were missing)

Treatment effects on the primary outcome measure of the per protocol comparison echoed those of the intention to treat analysis and the adjusted active–placebo difference in the

mean 6 month affected eye RNFL thickness of 7.4 µm (p=0.03)(Table 6-4). Sectoral RNFL analysis demonstrated similar significant treatment effects on the superior RNFL quadrant thickness (p= 0.007) in the phenytoin adherent group. There were also near significant treatment effects on nasal quadrant RNFL thickness (p=0.07) but no significant effects on temporal or inferior quadrant RNFL thickness (p=0.36 and 0.26 respectively) (Table 6-4).

Similarly, treatment affects on mean total macular volume in the per protocol comparison mirrored the ITT analysis with an adjusted active-placebo 6-month macular volume was 0.2 mm^3 higher in the phenytoin group compared to placebo (p=0.01) (Table 6-4)

Table 6-4: Per protocol comparison of the primary endpoints at 6 months

	Phenytoin Adherent (n=29)	**Placebo (n=41)**	**Adjusted active-placebo difference¶ (95% CI)**	**p value**
RNFL thickness (*µm*)	82.2 (14.6)	74.3 (15.1)	7.4 (0.8, 14.0)	0.03
Temporal sector thickness (*µm*)	51.2 (14.1)	47.8 (14.0)	2.9 (-3.6,9.3)	0.37
Nasal sector thickness (*µm)*	61.9 (13.0)	57.5 (15.5)	5.45 (-0.5, 11.4)	0.07
Superior sector thickness (*µm)*	106.8 (21.6)	93.2 (20.8)	12.8 (3.6, 22.0)	0.007
Inferior sector thickness (*µm)*	108.4 (21.23)	100.8 (21.22)	5.3 (-4.0, 14.5)	0.26
Macular volume (mm^3)	8.3 (0.4)	8.1 (0.4)	0.2 (0.1, 0.4)	0.01

Data are mean (SD)

¶ Pre-specified adjustment for baseline unaffected value, centre, days between onset and baseline, days between steroid and baseline

There was no significant correlation between time to initiation of treatment and mean six-month RNFL thickness in the phenytoin adherent patients(r=0.07, p=0.73).

Figure 6-7: Scatter plot of mean RNFL atrophy at 6 months in the affected eye against 1-month serum phenytoin

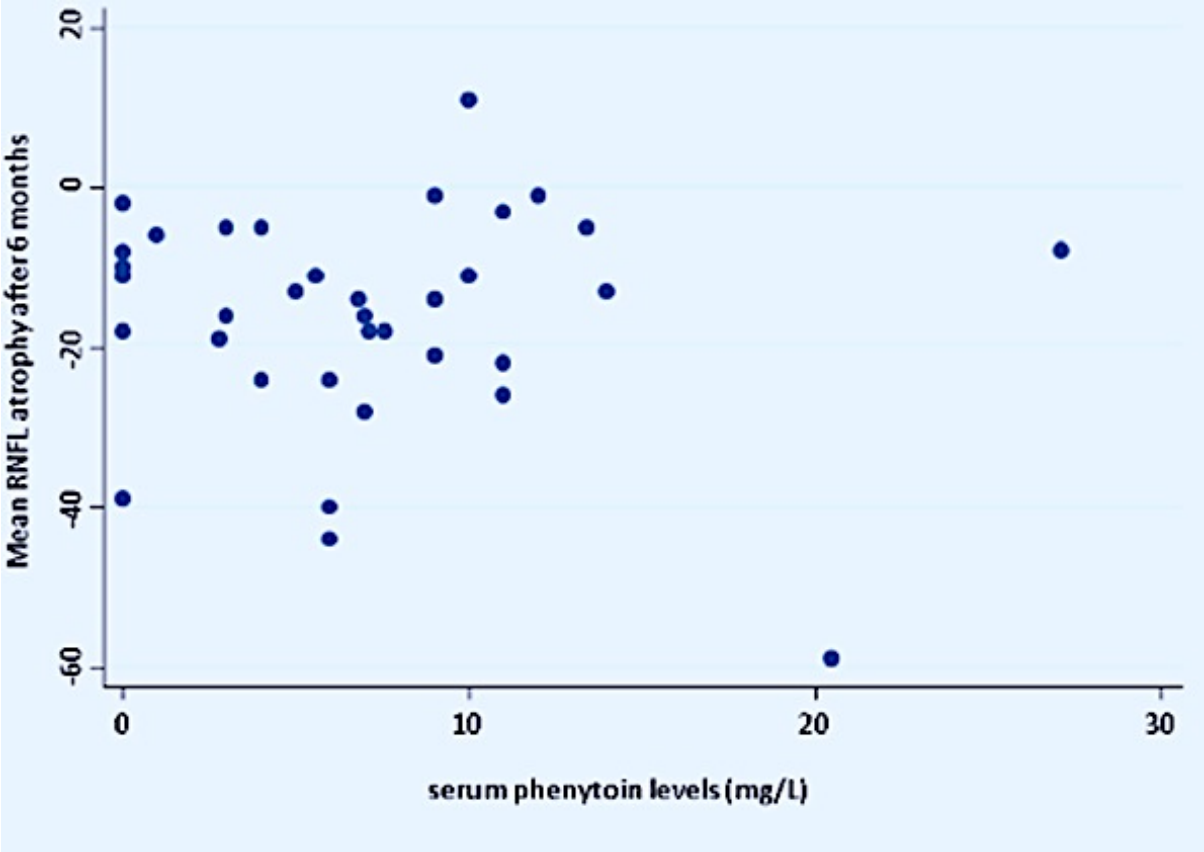

6.5 Relapses

In the per protocol comparison 5 patients in the phenytoin group (17%) and 9 in the placebo group (21%) suffered a further demyelinating relapse. Again this difference was not statistically significant (p=0.7). The per protocol log rank test for time to relapse was p=0.58

6.6 Adverse Events

Treatment with phenytoin was generally well tolerated and was not associated with abnormalities in the blood count or liver function. We did not note any acute deterioration of vision or other neurological function that might be attributed to conduction block from inhibition of sodium currents, or any rebound deterioration upon withdrawal of

treatment—effects that had previously been thought to potentially limit the use of drugs acting on this target in demyelinating disorders. Only one participant had a severe adverse reaction—a skin rash—attributable to phenytoin, but a further nine participants developed minor, self-limiting skin rashes and were withdrawn from treatment by the investigators as stipulated by the trial protocol. Similar proportions of patients in the phenytoin and placebo groups had adverse events, and serious adverse events were not attributable to phenytoin with the exception of a severe rash in one patient. (Table 6-5,Table 6-6) A higher, but not significant proportion of patients discontinued the study medication due to an adverse event in the active group (due to skin rash in all cases).

Table 6-5: Adverse events

Adverse Events	Phenytoin	Placebo
At least one adverse event	34 (81)	40 (91)
At least one adverse event leading to discontinuation of study medication	10 (24)	3 (7)
Any serious adverse event	5 (12)	2 (5)
Any event leading to death	0	0
Mean number (range) of all adverse events per patient	3.17 (0,10)	3.64 (0,14)

Data are number (%), except for last row

Table 6-6: Serious adverse events

	Phenytoin	Placebo
Breast Malignancy	1	0
Dilated superior ophthalmic vein seen on MRI (requiring catheter angiogram)	1	0
Appendicitis	2	0
Cellulitis	0	1
Severe rash	1	0
Congenital malformation	0	1

Data are number of serious adverse events

6.7 Discussion

The main finding in this phase 2 clinical trial is that treatment with phenytoin protects the RNFL and macula from degeneration after acute optic neuritis. The characteristics of the placebo and phenytoin groups at baseline were comparable and were typical of acute optic neuritis. Measures of visual function at baseline, in particular low contrast letter scores, were worse in the phenytoin group and baseline RNFL swelling was greater than in the placebo group. This could be interpreted in several ways 1) Firstly, given that lower baseline low contrast acuity is predictive of lower RNFL thickness at 6 months (Henderson et al 2010) our results could actually be conservative and therefore all the more consistent with a neuroprotective treatment effect of phenytoin 2) Secondly, that higher levels of inflammation at baseline (as reflected by greater RNFL swelling) in the phenytoin group lead to greater levels of astrogliosis at 6 months which was reflected in a 'falsely' higher 6 month RNFL thickness in the phenytoin group. Nevertheless, if this had occurred one would expect baseline RNFL thickness in the affected eye to be correlated with 6 month affected eye RNFL thickness and this was not the case ($r=0.13$ $p= 0.25$) 3) Thirdly that phenytoin exerted an

anti-inflammatory effect that reduced inflammatory axonal transaction and thus conferred secondary protection of axons. However, in this case one would also expect corticosteroids to be neuroprotective in optic neuritis and results of previous studies have suggested they are not (Naismith et al., 2009a; Hickman et al., 2003).

The loss of thickness of the RNFL in the placebo group after 6 months was consistent with previous natural history studies (Henderson et al., 2010; Costello et al., 2008). Treatment with phenytoin reduced this loss by 30%, and there was a 34% treatment effect on the loss of macular volume. These results suggest that phenytoin protects the compartment comprising the retinal ganglion cells (which make up 34% of macular volume (Sakai et al., 2011) and their axons in the RNFL. It should be noted that OCT measures of RNFL thickness do not allow us to directly visualize the surviving axons therefore we can only infer that increased RNFL thickness in the phenytoin group was due to a neuroprotective effect on axonal loss. An alternative explanation could be that the increased mean RNFL thickness at 6 months in the phenytoin group was due to higher levels of astrogliosis given that the phenytoin group had worse visual function and more RNFL swelling at baseline. However as discussed above if we were to assume that higher levels RNFL inflammation at baseline led to increased astrogliosis at 6 months then there should be a positive correlation between the baseline and 6 month affected eye RNFL thickness which was not the case (see above). In the future it may be possible to use techniques such as detection of apoptosing retinal cells (DARC) to directly visualise the amount of retinal ganglion cell loss. This could give us pathological insights into the timing of RGC loss after optic neuritis as well as allowing greater pathological specificity when testing neuroprotective treatments (Normando et al., 2015).

These results are consistent with the neuroprotective effect of sodium channel blockade in experimental models of optic neuritis and EAE (Garthwaite et al., 2002; Lo et al., 2003) and support the 'sodium hypothesis' of neuroaxonal loss within the context of acute relapses in vivo. Based on these results it is not possible to elucidate whether treatment with phenytoin had an additional anti-inflammatory effect by blocking $Na_v1.6$ channels on macrophages and microglia as well as along retinal ganglion cell axons but could have conceivably done both.

Although there were significant treatment effects on superior (p=0.005) and nasal sector RNFL thickness (p=0.058), the temporal (p=0.37) and inferior sector thicknesses (p=0.26) were not significantly preserved. Costello et al found that the rate of RNFL thinning varies between different sectors with significant thinning in the temporal sector occurring as early as 2 months after optic neuritis (Costello et al., 2008). Reductions in superior RNFL thickness occurred after longer periods of three months or more. The temporal sector of the RNFL receives small diameter nerve fibres from the fovea via the papillomacular bundle and may be more susceptible to early damage possibly due to the selective early loss of small axons. In support of this Evangelou et al 2001 found selective atrophy of smaller neurons in the parvocellular layer in the lateral geniculate nucleus in a post mortem study of eight patients with multiple sclerosis. They postulated that smaller axons may be preferentially susceptible to injury in multiple sclerosis (Evangelou et al., 2001).

The lack of treatment effect on temporal sector RNFL thickness could suggest that either 1) an even earlier time window of recruitment is required to prevent degeneration of smaller axons in the parvocellular pathway or 2) that the neuroprotective effect of sodium channel blockade did not manifest during the initial hyper acute inflammatory period after optic neuritis but rather during the subacute or even post-inflammatory period. This could explain the lack of correlation between RNFL thickness and time to initiation of treatment. Alternatively, because all patients were recruited within a very narrow time window, this may not have allowed for correlations with time to be seen.

There was one significant outlier in the phenytoin group who developed severe RNFL thinning despite high phenytoin levels and it may be that some patients have a particularly intense and destructive inflammatory period that is difficult to treat with neuroprotective therapy even if instituted early.

It is also important to note that this particular patient did have some atypical features with severe baseline visual loss (no perception of light) and virtually no visual recovery with a normal MRI brain. Despite being investigated extensively no other cause for the optic neuritis was found. Although, aquaporin 4 antibodies were negative it cannot be completed

excluded that this patient had a different pathological process causing the optic neuritis not amenable to neuroprotection with sodium channel blockade.

The fact that there was no significant difference in the occurrence of a second demyelinating relapse between the groups would suggest that phenytoin did not exert immunomodulatory effects in our cohort of patients. However, the relatively small number of relapses and short follow up period of 6 months means that it is difficult to draw definitive conclusions - this would need to be investigated further in larger phase three trials with longer follow up periods.

The conclusions in the present study may be affected by a relatively high, 31% rate of loss to follow up, withdrawal from treatment and non-adherence in the phenytoin group. This was largely due to an unusually high incidence of rashes in our cohort of patients. While this figure may affect the statistical power of the study, the robustness of the results is supported by the agreement between the intention to treat and per protocol analyses, and the consistency of treatment effects in the macula, RNFL and optic nerve. Mean serum phenytoin levels were 7mg/L in the phenytoin group which may be 'sub therapeutic' and are lower than the levels that were neuroprotective in experimental models (Lo et al., 2003) as well as the levels regarded as therapeutic in epilepsy (10-20 mgL/L). However, it should be stated that the 'therapeutic' level of phenytoin in optic neuritis has not yet been clearly defined. It is possible that a greater treatment effect may have been observed if not for the aforementioned problems.

It is also important to consider the relatively high percentage of patients who received corticosteroids at presentation, in case this treatment affected the baseline OCT measurements or the final outcome. Against this possibility are the facts that measurements of the RNFL and of macular volume remained stable in the unaffected eye in both the phenytoin and placebo groups, and that in previous reports corticosteroids did not affect atrophy of the RNFL (Naismith et al., 2009b) or optic nerve (Hickman et al., 2003), nor visual recovery after optic neuritis (Beck et al., 1992a). Care was also taken to adjust the calculation of outcome for the use and timing of corticosteroids.

Another potential confounding factor is the slightly higher proportion of patients with a pre-existing diagnosis of MS in the placebo group. This could theoretically increase the likelihood of a previous episode of subclinical optic neuritis and preexisting RNFL thinning in the affected eye. However, the absolute numbers of patients were small (3 in the placebo group), all of whom had early relapsing remitting MS with no evidence of subclinical optic neuritis in the fellow eye so the likelihood of this would seem low. Again care was taken to adjust for preexisting diagnosis of MS in the statistical analysis.

Chapter 7 Trial results- Secondary Endpoints

7.1 Intention to treat comparison

7.1.1 MRI

Lesional Optic nerve cross-sectional area

Consistent with previous longitudinal MRI studies there was initial swelling at baseline followed by subsequent atrophy at 6 months in the affected eye (Table 7.1). There was no significant change in the mean cross-sectional area of unaffected eye in either the phenytoin (p=0.30) or placebo group (p=0.27). In the placebo group the mean affected eye cross-sectional area fell by 0.84 mm^2 compared with the baseline unaffected eye. Mean cross-sectional area in the unaffected eye was consistent with recent publications on MRI measurements of the optic nerve (Yiannakas et al., 2013).

There was a borderline significant treatment effect on optic nerve cross-sectional area, with an adjusted active-placebo difference of 0.4 mm^2 (p=0.061) (Table 7-2) a 38% treatment effect.

Figure 7-1: Baseline unaffected eye and 6 month affected eye cross-sectional area by trial group

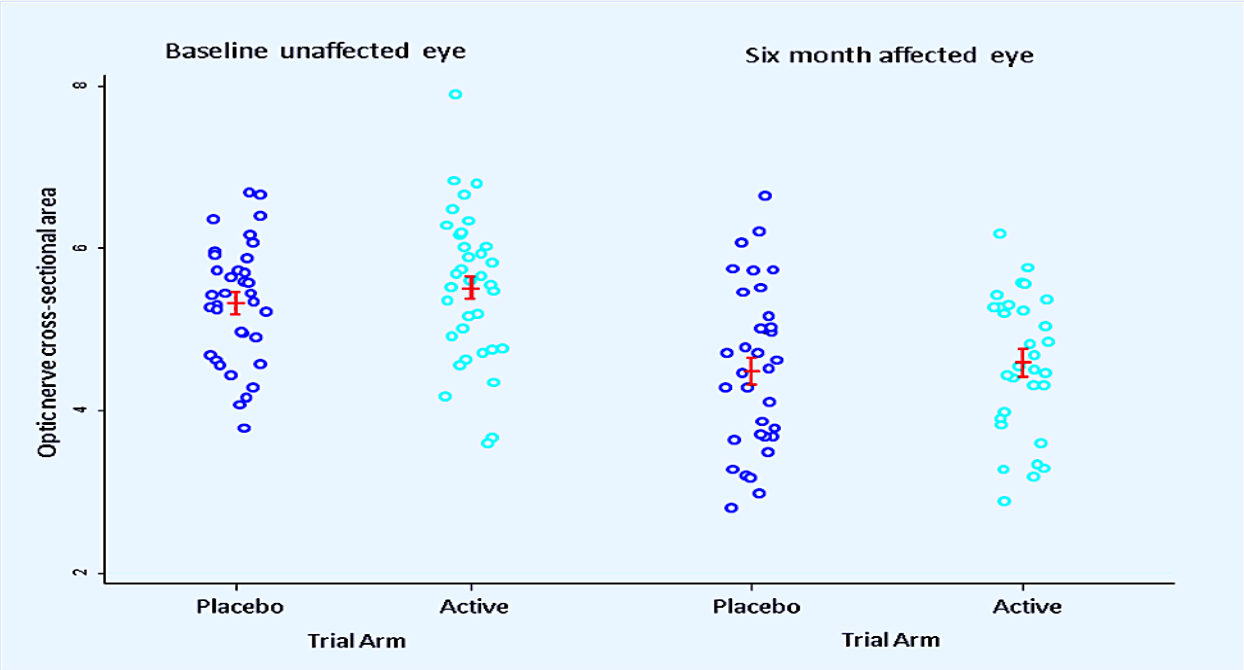

Bars are standard errors around unadjusted group means

A number of scans was excluded due to significant motion artifact that precluded accurate cross-sectional area measurements These were very plausibly missing at random and unlikely to cause bias The outcome analysis included only patients with recordable measurements in both the baseline unaffected eye and the six month affected eye.

	Phenytoin		Placebo	
	Baseline	**6 months**	**Baseline**	**6 months**
Affected eye optic nerve cross-sectional area (mm^2)	7.60 (1.55) (n=34)	4.58 (0.88) (n=31)	7.48 (1.43) (n=39)	4.48 (1.01) (n=34)
Unaffected eye cross-sectional area (mm^2)	5.51 (0.9) (n=35)	5.15 (0.82) (n=30)	5.32 (0.73) (n=35)	5.41 (0.72) (n=29)

Data are mean (SD) (n=number of scans)

Optic nerve lesion length

The optic nerve lesion was identified at baseline in 96% of the patients who had an MRI scan using a combination of the two T2 sequences. In the three patients in whom the baseline optic nerve lesion was not visualized (1 placebo and 2 phenytoin) clinical and VEP measurements were consistent with acute demyelinating optic neuritis and in 2 of these the lesion was subsequently seen at 6 months. Mean lesion length was 17.23 (SD 8.11) mm in the phenytoin group and 18.00 (SD 7.11) in the placebo group at baseline (Table 7-1).

Intention to treat comparison showed no significant difference in lesion length between the groups at 6 months (mean adjusted active-placebo difference -2.45 mm, p=0.29) (**Table 7-1**). This analysis did not adjust for the baseline lesion length in the affected eye due to concerns about comparing treatment effects on an active lesion in progress but was adjusted for the other minimization variables.

In a secondary analysis baseline lesion length was included as an additional covariate and the adjusted active – placebo difference was -2.12 (p =0.32, 95% CI -6.36 to 2.12)

Table 7-1: Intention to treat comparison of the secondary outcome measures at 6 months

	Active	Placebo	Adjusted active-placebo difference¶ (95% CI)	p value
Lesion length (mm)	15.15 (7.62) n=34	17.17 (10.11) n=36	-2.45 (-6.97-2.08)	0.29
Lesional optic nerve cross-sectional area (mm^2)	4.58 (0.88) n=31	4.48 (1.01) n=34	0.4 (-0.02-0.83)	0.06
Lesional MTR (pcu)	31.90 (3.33) n=29	31.89 (6.73) n=34	0.43 (-2.51 -3.36)	0.77
LogMar visual acuity	0.15 (0.41) n=39	0.10 (0.21) n=42	0.02 (-0.11-0.16)	0.73
1.25% low contrast letter score	13.38 (12.14) n=39	12.33 (12.13) n=42	1.19 (-4.16-6.53)	0.66
2.5% low contrast letter score	19.69 (13.80) n=39	17.55 (14.19) n=42	2.07 (-4.10-8.25)	0.51
FM Hue 100 total error score	181.28 (223.79) n=39	195.24 (212.61) n=42	-18.46 (-116.44-79.51)	0.71
VEP latency[a] (small check, ms)	133.0 (24.8) n=35	127.4 (19.3) n=40	5.7 (-4.56-15.99)	0.27
VEP amplitude[a] (small check, *u*V)	7.1 (4.6) n=35	7.3 (4.6) n=40	-0.18 (-1.83-1.46)	0.83

Data are mean (SD)

¶ Pre-specified adjustment for baseline unaffected value, centre, days between onset and baseline, days between steroid and baseline; centre was dropped for optic nerve area, and centre and baseline unaffected value were dropped for lesion length

[a] Comparison includes three active patients with affected eye vision too poor to give VEP values, for which amplitude 0μV and latency 200ms was used. (baseline affected eye measurements were not used in the primary comparison)

Lesional Magnetisation Transfer Ratio (MTR)

At baseline mean lesional MTR was lower by a mean of 5.92 pcu in the phenytoin and 6.78 pcu in the placebo group when compared to the unaffected eye. By 6 months mean lesional MTR had increased slightly by 1.75 pcu in the active group and 1.90 pcu in the placebo group but was still significantly lower than the baseline unaffected eye (Figure 7-2)

Figure 7-2: Graph illustrating mean baseline and 6 month affected eye MTR values compared to the baseline unaffected eye

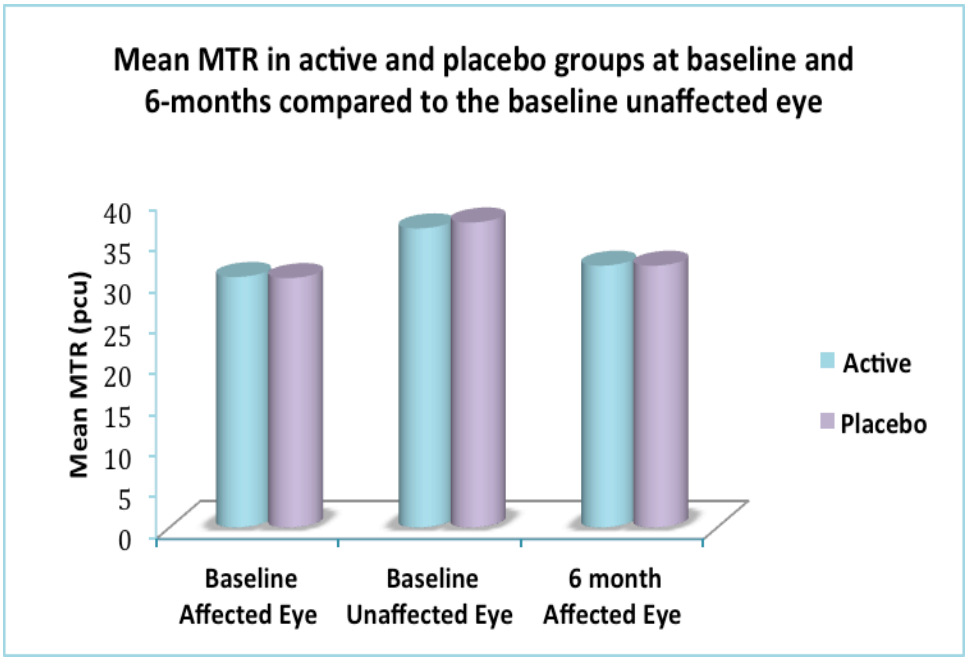

There was no significant active-placebo difference in mean adjusted lesional magnetization ratio (p= 0.43) at 6 months (Table 7-2).

7.1.2 Functional measurements

LogMAR visual acuity

Visual loss in the affected eye at baseline was slightly (but not significantly) worse in the phenytoin group (mean logMAR acuity = 1.11) compared to placebo (mean LogMAR acuity = 1.07). In general vision recovered well in both groups and the mean best-corrected log MAR visual acuity in the affected eye at 6 months was 0.09 (SD 0.4) in the active group and 0.04 (SD 0.18) in the placebo group**.** There was no significant difference in mean adjusted active-placebo in best corrected Log MAR visual acuity at 6 months (p=0.728) (Table 7-1).

Figure 7-3: LogMAR visual acuity in the baseline unaffected eye and 6 month affected eye in the phenytoin and placebo groups

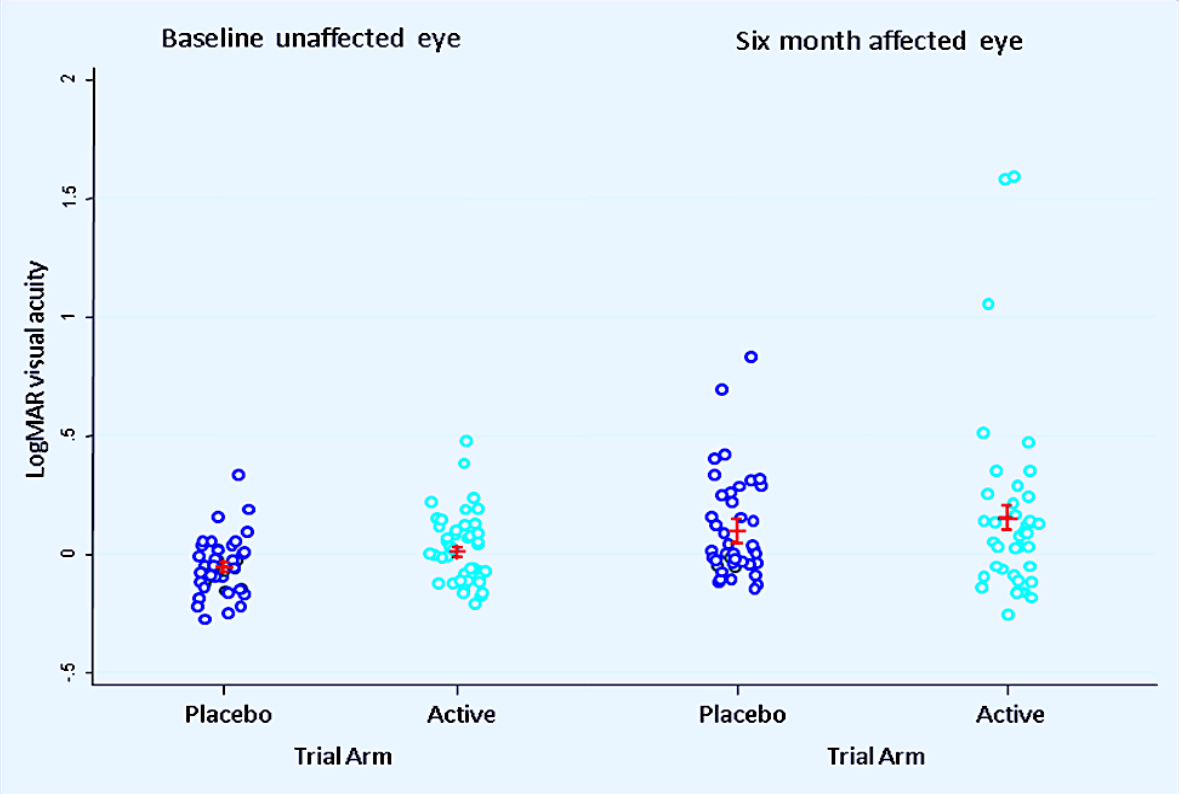

Bars are standard errors around the unadjusted group means

At one month and three months visual acuity was measured using the Snellen chart but for the purpose of statistical analysis this data was converted to the LogMAR scale by taking $-\log_{10}$ of the snellen fraction. The graph below demonstrates the trajectory of visual recovery in the phenytoin and placebo groups in the ITT comparison (Figure 7-4).

Figure 7-4: Trajectory of visual recovery in the ITT comparison

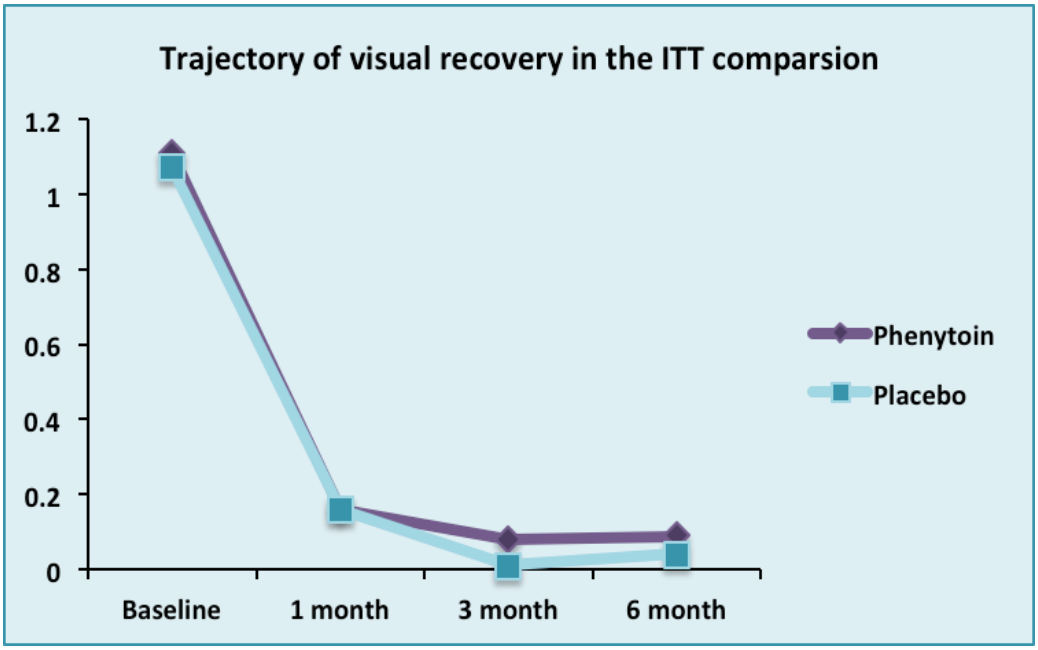

There were no significant differences in mean adjusted active-placebo logMAR visual acuity at one month (p=0.95) or three months (p=0.50).

Low contrast letter score

Due to the severity of visual loss in the affected eye there were floor effects in the measurements of low contrast letter scores at both 1.25% and 2.5% contrast levels at baseline.

As would be expected low contrast letter acuity at both contrast levels recovered less well than high contrast acuity in both the phenytoin and placebo groups at 6 months.

There was no significant treatment effect at either 1.25% or 2.5% contrast levels at 6 months (p= 0.66 and p=0.51 respectively) (Table 7-2).

Figure 7-5: Scatter plot of 2.5% low contrast letter scores in the baseline unaffected and 6 month affected eye by trial arm

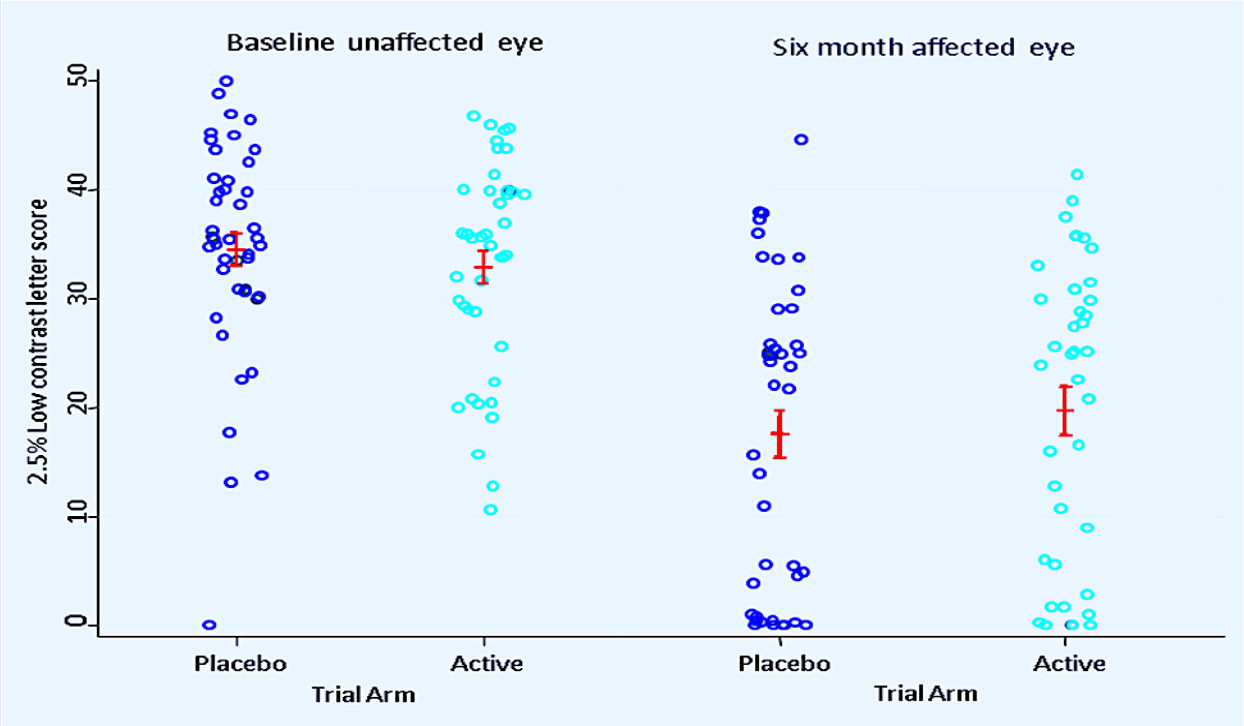

Bars are standard errors around unadjusted group means

Farnsworth Munsell-100 Hue test

At baseline 38% in the active group and 43% in the placebo group were unable to perform the test as their visual acuity was too poor.

Colour vision recovered less well than high contrast acuity in both the active and placebo groups (Table 7-1).

There was no significant difference in mean adjusted FM-100 Hue between the groups at 6 months (p= 0.71) (Table 7-1).

Visual evoked potential measures

46.15% of patients in the phenytoin group and 40.45% of patients in the placebo group had large check VEPs that were unrecordable at baseline. This increased to 51.28% (phenytoin)

46.51% (placebo) for small check VEPs. At 6 months no patients in the placebo group and 8.54% in the phenytoin group had unrecordable small and large check VEPs.

For those with recordable VEPS, as would be expected, VEP latencies for both check sizes were prolonged and VEP amplitudes reduced at baseline compared to the unaffected eye in both groups. Consistent with previous studies, there was shortening of VEP latency at 6 months in the affected eye in both groups (Brusa et al., 2001). However latency was still prolonged by an average of 28.99 ms in the phenytoin group and 22.67 ms in the placebo group compared to the baseline unaffected eye (small check). At 6 months VEP amplitudes in the affected eye had returned to within normal limits in both groups.

There was no significant difference in either small (p=0.27) or large (0.14) check VEP latency between the two groups at 6 months. Similarly adjusted active-placebo difference was not significant for either small (p=0.83) or large check (p=0.52) amplitude (Table 7-2).

7.2 Per Protocol Analysis (Table 7-3)

The per protocol analysis was consistent with intention to treat analysis for all the secondary outcome measures.

7.2.1 MRI

Optic nerve lesion length

The adjusted active-placebo difference in 6 month lesion length was -3.06 mm (See Table 7-3) and there was no significant treatment effect (p=0.24) NB: as in ITT analysis baseline lesion length was not adjusted for, however, when baseline lesion length was included as a covariate the active –placebo difference reduced further to -1.93 mm.

There was no evidence of a relationship between 1-month phenytoin levels in the active group and 6 month lesion length (r=0.09, p=0.65).

Lesional Optic nerve cross-sectional area

The adjusted difference in mean cross-sectional area was 0.37 mm^2 (p=0.11) (Table 7-3).

There was no evidence of a relationship between 1-month phenytoin levels in and 6-month optic nerve cross-sectional area in the active group (r=0.26, p=0.18).

Lesional Magnetisation transfer ratio

Adjusted active-placebo difference in mean lesional MTR was 0.39 pcu with no evidence of a significant treatment effect (p=0.82) (Table 7-3). There was no evidence of an association between 6-month lesional MTR and 1 month phenytoin levels in the active group.

7.2.2 Functional measurements

LogMAR visual acuity

At 6 months there was no significant difference in mean adjusted active –placebo best corrected visual (p= 0.91) (Table 7-3).

There was no significant association between 1-month phenytoin levels and 6 month LogMAR visual acuity (r= 0.105, p= 0.55)(Figure 7-6).

Figure 7-6: A Scatter graph of 1 month phenytoin levels against 6 month LogMAR visual

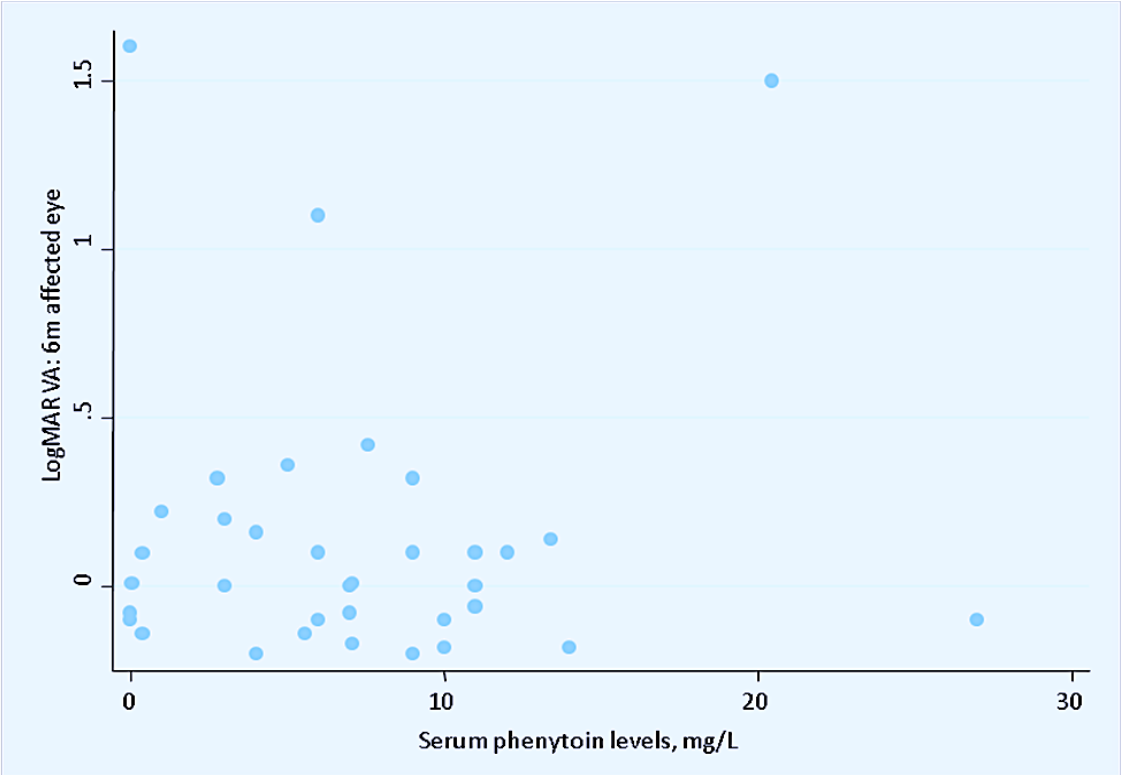

Snellen visual acuities taken at 1 and three months were converted as explained above. There was no significant active-placebo difference in LogMAR visual acuity at either 1 month (p=0.87) or 3 months (p=0.57) (See Figure 7-7 for trajectory of visual recovery in the phenytoin adherent and placebo groups).

At one month and three months there was no significant association between logMAR visual acuity and 1-month phenytoin levels (r=0.009, p=0.75 and r=0.006, p=0.8 respectively).

There was no evidence of an association between time to initiation of treatment and mean LogMAR visual acuity at 1 month (r= -0.15, p=0.43), 3 months (r= -0.13, p= 0.50) or 6 months in the phenytoin adherent patients (r=-0.20, p=0.30).

Figure 7-7: Trajectory of visual recovery in the per protocol

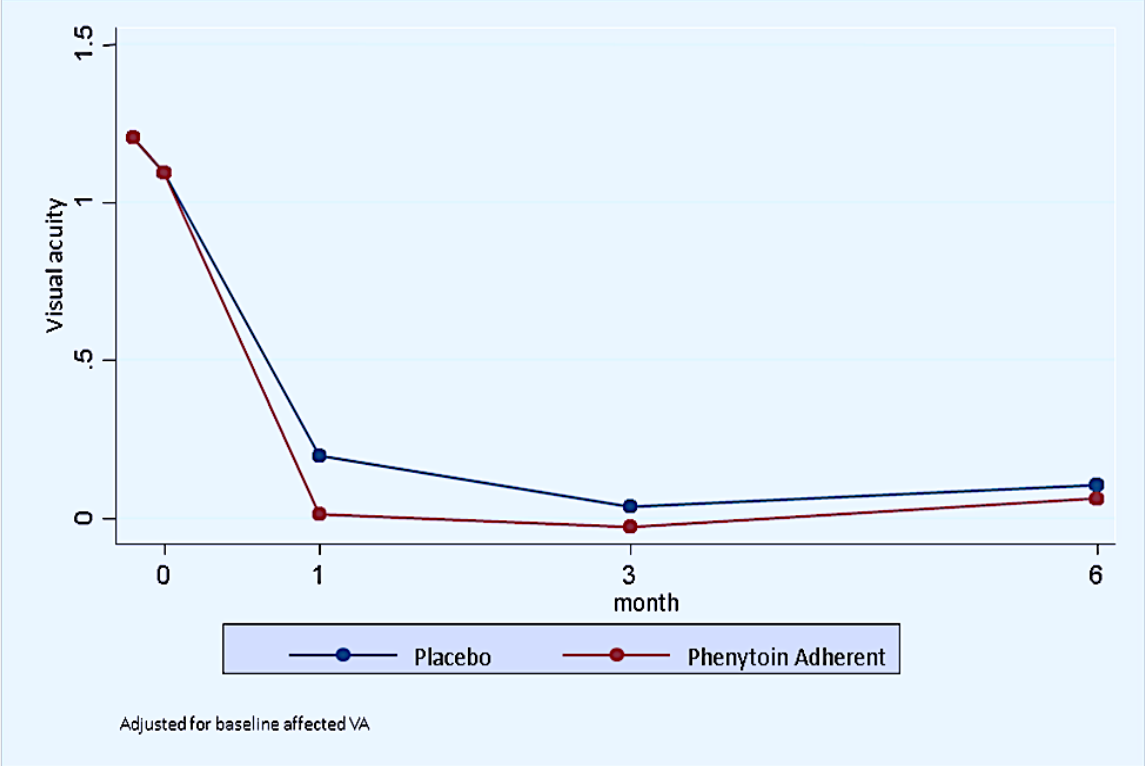

Low contrast letter score

There was no significant difference between the groups in low contrast letter scores at either 1.25% and 2.5% contrast levels at 6 months (p= 0.67 and p=0.48 respectively)(Table 7-3).

Equally there was no association between 6-month low contrast letter score at either contrast level and 1-month phenytoin levels.

In the phenytoin adherent group there was no evidence of an association between time to initiation of treatment and 6-month low contrast letter.

Farnsworth Munsell 100 Hue total error score

There was no significant difference in adjusted active-placebo FM 100 Hue total error score at 6 months (p= 0.57) (Table 7-3).

Visual evoked potentials

There were no significant between group differences in mean small or large check VEP latencies at 6 months (p=0.39 and p= 0.21). Likewise treatment with phenytoin had no significant effect on small or large check VEP amplitudes at 6 months (p=0.79 and p=0.58 respectively) (Table7-3).

Again there was no association between phenytoin levels at 1 month or time to initiation of treatment and any of the VEP metrics at 6 months.

Table 7-2: Per protocol comparison of the secondary endpoints at 6 months

	Phenytoin adherent (n=)	Placebo (n=)	Adjusted active-placebo difference¶	p value (95% CI)
Lesion length (mm)	14.72 (7.80) n= 25	17.17 (10.10) n=36	-3.06 (-8.17, 2.05)	0.24
Optic nerve cross-sectional area (mm^2)	4.66 (0.77) (n=24)	4.48 (1.01) (n= 34)	0.37 (-0.09, 0.84)	0.11
Lesional MTR	31.57 (2.83) (n=21)	31.89 (6.73) (n=34)	0.39 (-2.99, 3.77)	0.82
LogMAR visual acuity	0.12 (0.37) (n=29)	0.10 (0.21) (n=42)	-0.01 (-0.15, 0.14)	0.91
Low contrast letter score (1.25 %)	13.66 (12.29) (n=29)	12.33 (12.13) (n=42)	1.26 (-4.67, 7.19)	0.67
Low contrast letter score (2.5%)	20.17 (13.84) (n=29)	17.55 (14.19) (n=42)	2.44 (-4.44, 9.31)	0.48
FM Hue 100 Total error score	168.28 (206.13) (n=29)	195.24 (212.61) (n=42)	-29.84 (-134.90, 75.22)	0.57
VEP latency (small check, ms)	131.1 (n=27)	127.4 (n= 40)	4.48 (-5.92, 14.90)	0.39
VEP amplitude (small check *uV*)	6.8 (n=27)	7.3 (n=40)	-0.25 (-2.04, 1.5)	0.79

¶ Pre-specified adjustment for baseline unaffected value, centre, days between onset and baseline, days between steroid and baseline; centre was dropped for optic nerve area, and centre and baseline unaffected value were dropped for lesion length

7.3 Discussion

Consistent with the significant treatment effects on RNFL thickness and macular volume there was also a near significant treatment 38% treatment effect on the loss of optic nerve cross-sectional area (p=0.06). This follows, as protecting axons in the optic nerve should result in preservation of axons and their cell bodies in the retina.

Despite the observed neuroprotective effect on the structural OCT and MRI measures we did not demonstrate a corresponding significant treatment effect on any of the functional outcomes.

In general, high contrast visual acuity recovered well in the both the phenytoin and placebo groups with possible ceiling effects making any potential benefits of treatment difficult to demonstrate. It is important to note that this proof of concept, phase II trial was not powered to demonstrate significant treatment effects on visual function. Lack of power meant that we did not dwell on the results of colour vision and low contrast acuity (LCVA), which were actually better (albeit non-significantly) in the group treated with phenytoin. To establish significance, we calculated that the effect size on LCVA we found in our study (0.15 for 2.5% LCVA vs 0.45 for the RNFL) would require a trial involving 630 participants.

Furthermore, there is a degree of redundancy of axons in the anterior visual system that complicates the relationship between structural and functional outcomes. A threshold of axonal loss may be required to produce clinically significant high contrast visual loss. This is supported by a clinico pathological study by Frisen et al who obtained nerve fibre counts from the temporal quadrant of optic nerves from 14 eyes with known optic atrophy (of any cause). They found that normal visual acuity was possible despite a 40% loss of neural substrate(Frisen and Quigley, 1984). More recently, Costello et al demonstrated a threshold RNFL thickness of 75µms below which RNFL measurements predicted persistent visual dysfunction (Costello et al., 2006). Therefore, it may be that the level of axonal loss required for a clinically significant reduction in high contrast visual acuity was not reached in either group after a single episode of optic neuritis.

Reduced neuroaxonal loss may only translate into clinical benefit further down the line

either after repeated 'inflammatory hits' to the optic nerve or with the more insidious axonal loss known to occur over time in MS. In support of this, in eyes affected by two or more episode of optic neuritis retinal nerve fibre layer atrophy is more severe and the corresponding impact on visual outcome much more evident. For example, in one study eyes affected by recurrent optic neuritis (mean number of ON events 2.2) had a mean affected eye RNFL thickness of 64.2 µms and a median logMAR visual acuity of 0.32 compared to those with a single episode of optic neuritis who had a mean RNFL thickness of 86.3 µms and a median logMAR acuity of 0.23 (Costello et al., 2010).

However, it should be noted that the concept of functional reserve is controversial. It has been argued that the impression of functional reserve is only given by the logarithmic nature of measures of visual function such as logMAR visual acuity and visual field mean deviation and that the relationship is actually linear (as opposed to curvilinear) if the anti-log of the measurement is used. Additionally due to the higher variability and wider confidence intervals of functional tests statistically significant structural damage is identified before functional loss adding to the impression of functional reserve (Garway-Heath et al., 2002; Hood and Kardon, 2007).

Thirdly, neuroplasticity in higher cortical areas may also be an important determinant of visual outcome after optic neuritis. Jenkins et al found that greater baseline fMRI responses in the lateral occipital cortex were predictive of better visual outcome. This effect was independent of measures of neuroxonal loss (RNFL thickness and optic nerve cross-sectional area) and demyelination (VEP latency) (Jenkins et al., 2010). Thus, this could also contribute to the lack of any significant difference in visual outcome between the two groups, as neuroprotection would not be expected to have an effect on cortical adaptation.

Whereas both groups recovered well in terms of high contrast visual acuity, recovery of low contrast acuity and colour vision was not as good. There was a > 7 letter reduction in low contrast letter scores (at 1.25 % and 2.5%) in both groups when compared to the baseline unaffected eye, which has been demonstrated to be clinically meaningful (as this exceeds the amount of change that would be expected from repeated testing when there is no 'real' change and has been associated with significant reductions in vision related quality of life scores (Talman et al., 2010). Given the greater sensitivity of low contrast letter scores to

optic neuritis related visual loss it is surprising that we did not see a significant treatment effect. This could have several interpretations: 1) that although phenytoin protected ganglion cells and their axons they remained non-functioning and therefore the observed improvement in structural outcomes was not translated into functional gains 2) that the significantly higher RNFL thickness and macular volume in the phenytoin group was not due to preserved ganglion cells and their axons but rather due to increased astrogliosis and therefore we did not see any functional gains (although perhaps in this case one would have expected the phenytoin group to have worse low contrast letter scores at 6 months than the placebo group) 3) that due to the variability and greater subjectivity of low contrast letter scores they are not as sensitive to treatment effects as the structural outcomes and therefore may require either more potent neuroprotective agents with greater effect sizes or larger number of patients to demonstrate significant treatment effects in the future.

There was also no significant treatment effect on colour vision. This may be due to the greater susceptibility of smaller axons in the parvocellular pathway to inflammatory demyelination. Smaller axons have a larger surface area that may make them more susceptible to toxic diffusible substances such as nitric oxide and may also have less mitochondria rendering them more vulnerable to energy failure. In keeping with this, despite significant treatment effects on mean superior ($p=0.005$) and nasal sector RNFL thickness ($p=0.058$) phenytoin had no significant effect on temporal sector RNFL thickness ($p=0.39$). The temporal sector of the RNFL receives small diameter nerve fibres from the fovea via the papillomacular bundle, responsible for colour and central vision. There was a large amount of variability in the FM-hue 100 error scores and this test can be quite arduous for patients requiring a high level of attention and concentration. It is important to note that measures of visual function are subjective and are affected by factors such as temperature, stress and fatigue as well as being on reliant on patient attention and cooperation and so may not be as reliable as structural measures such as RNFL thickness.

Visual fields were not assessed as part of the trial protocol largely due to time constraints Assessment of visual fields could have potentially demonstrated better topographical correlations with the different RNFL quadrants and perhaps demonstrated treatment effects

on regions of the field corresponding to the superior and nasal sectors of the RNFL that were significantly higher in the phenytoin group.

There was no significant difference in either VEP latency or amplitude between the two groups. Delayed VEP latency is considered to be a measure of demyelination in the optic nerve. Although demyelination is a likely an important harbinger of axonal loss in MS it does not necessarily follow that reducing axonal loss promotes remyelination. Different mechanisms unrelated to axonal survival such as the availability of oligodendrocyte progenitor cells are likely to be required for the latter.

Previous studies have not demonstrated an association between RNFL thickness and VEP latency after optic neuritis (Trip et al., 2005), (Henderson et al., 2010) and this may explain why although phenytoin had a neuroprotective effect on axonal loss it did not appear to improve remyelination.

Also although the time course of axonal loss in the retina and optic nerve has been well studied the exact time course of remyelination is unclear. Brusa et al demonstrated that VEP latencies - and by inference remyelination - can continue to decrease up to 2 years after optic neuritis (Brusa et al., 2001). As our patients were only followed up for 6 months a longer period of follow up may be necessary to demonstrate any beneficial effects on remyelination.

In keeping with the lack of treatment effect on VEP latency there was no significant between group differences in mean lesional MTR at 6 mths. MTR is a measure of the degree of proton exchange between free water and macromolecules and is said to be an indirect measure of myelin. At baseline there was a reduction in mean lesional MTR in both groups compared to the unaffected eye. This is consistent with what occurs in acute brain lesions and likely represents demyelination and oedema in the optic nerve (Chen et al., 2008). There was a subsequent slight increase in lesional MTR by 6 months in both groups that may be indicative of remyelination. The fact that there was no significant treatment effect on lesional MTR supports the above conclusion that preservation of axons with sodium channel blockade does not improve remyelination.

Our baseline MTR results are not in concordance with the findings of Hickman et al. who found there was no change in optic nerve MTR at baseline (median time of 13 days from onset of optic neuritis) and on subsequent follow up imaging optic nerve MTR was reduced until it reached a nadir at 8 months. By 1 year there had been a slight increase optic nerve MTR (Hickman et al., 2004a). This study was performed on a smaller cohort of patients (29- although they were scanned more frequently) on a 1.5 T scanner and both optic nerves were imaged at the same time. Also our patients were recruited earlier (mean 8.1 days after optic neuritis) and the evolution of MTR in the present trial cohort of patients was more consistent with that which occurs in acute MS brain lesions (Chen et al., 2008).

The lack of neuroprotective effect on VEP amplitude is perhaps more surprising given this is thought to be a measure of axonal integrity. However conventional VEPs are dominated by central vision and the VEP signal is mainly derived from the macular region. It has been estimated that 65% of the total VEP response represents the central two degrees of visual field (Graham and Klistorner, 1998) and therefore conventional VEPs are unable to accurately record peripheral damage. Given that there was no significant treatment effect on temporal RNFL thickness it is not surprising that there was significant effect on VEP amplitude given that these fibres subserve macular function. VEP amplitude may also be confounded by demyelination because of temporal dispersion.

On the other hand multifocal VEPs assess the VEP signal not as a single global response but obtain simultaneous responses over multiple regions of the visual field at greater eccentricities providing topographic measurement of optic nerve function. The mean RNFL thickness samples the nerve fibre layer from the whole retina. Multifocal VEPs are likely to have been a more accurate way of picking up focal deficits in the visual field as well as being more comparable to RNFL thickness in terms of their coverage of the retina (Klistorner et al., 2008).

The use of multifocal VEPs may also have allowed a greater proportion of recordable VEPs at baseline, as they are capable of extracting responses from more peripheral locations.

For future trials, it is likely that better neuroprotection will be required to demonstrate treatment effects on clinical outcomes in reasonably sized trials. For this, trials might

consider: 1) more potent and specific inhibitors of sodium channels; 2) higher drug concentrations (phenytoin concentrations in this trial were possibly sub therapeutic); and 3) an even earlier window of treatment in the evolution of relapse, although in practice this may be difficult. The last two suggestions are consistent with the lack of correlation between structural outcomes and the concentration of phenytoin and time to initiation of treatment in the present study. A longer follow up period could also improve the trial design as although 6 months is an adequate time lag to demonstrate treatment effects on RNFL thinning, longer time periods may be required for other outcome measures.

Conversely, the results of the trial do not place a lower limit on the duration for which treatment is required for successful neuroprotection. Patients were treated for 3 months, i.e. well beyond the interval when gadolinium enhancement indicates inflammation in the optic nerve (Youl et al., 1991b), yet an exploratory analysis favored improved OCT outcomes in those who received treatment for only a mean of 18.4 days before it was withdrawn due to a skin rash.

The results support the utility of OCT for measuring outcome in future trials of neuroprotection in optic neuritis. In comparison, the specificity of MRI for estimating axonal loss in the optic nerve with MRI may be limited by the confounding effects of myelin and other supporting tissue, and there are inherent difficulties of imaging such a small and mobile structure. OCT also has obvious advantages of ease of use and lower cost, and has previously been used in three small trials of neuroprotection in optic neuritis. Memantine reduced the loss of the RNFL (Esfahani et al., 2012), while erythropoietin was effective in one trial (Suhs et al., 2012) but not in another (Shayegannejad et al., 2015). The present trial addressed limitations of these studies by correcting measurements in the affected eye for baseline measurements in the unaffected eye, and reporting MV data as well as more detailed MRI data.

At the average concentration achieved in this trial, phenytoin is an almost pure activity-dependent inhibitor of voltage-gated sodium channels (McLean and Macdonald, 1983). By analogy, other sodium channel inhibitors should also be neuroprotective in acute optic neuritis and, given its similarities to other relapses of multiple sclerosis, in those relapses as

well. In turn, the present trial design should enable proof of concept of neuroprotection after relapse for treatments with other modes of action.

Implications for treating progressive MS are harder to define because of possible differences in pathophysiology: microglial activation is likely to remain important in progressive disease (Mahad et al., 2015), whereas sodium channel expression may change (Black et al., 2007).

A previous trial of neuroprotection with sodium channel inhibition used lamotrigine in secondary progressive multiple sclerosis (Kapoor et al., 2010). Treatment had no effect on the rate of cerebral atrophy, but interpretation was hampered by a high rate of non-adherence, and in retrospect there were a number of positive signals in the study, including a significant positive treatment effects on the rate of deterioration of the timed walk and on serum neurofilament concentrations in the adherent group of patients (Gnanapavan et al., 2013).

In conclusion, the results of this clinical trial support the concept of neuroprotection using phenytoin to inhibit voltage-gated sodium channels in acute optic neuritis. These results should encourage larger, phase 3 trials of sodium channel inhibitors in optic neuritis and other relapses of multiple sclerosis. Future studies should also establish more precisely the optimal therapeutic window for neuroprotection in relapse.

Chapter 8 Conclusion

In conclusion, the results of this phase II clinical trial suggest that partial sodium channel blockade with phenytoin (given that in the doses used in the trial, phenytoin is a selective sodium channel blocker (Yaari et al., 1986)) protects the RNFL and macula from neurodegeneration after acute optic neuritis. However it should be noted that OCT measurements only allow us to measure the thickness of retinal layers and do not give any information about the cytological make up of these layers nor allow us to directly visualise the retinal ganglion cells and their axons. Therefore, an alternative explanation for the results would be that higher astrogliosis in the phenytoin group (due to more RNFL swelling at baseline) led to "falsely' higher RNFL thickness measures at 6 months. However, as discussed in section 6.7 if this were true one would have expected to see positive correlations between the baseline and 6 month affected eye RNFL measurements and also that increased levels of astrogliosis would have lead to worse visual function at 6 months in the phenytoin group. This was not reflected in the results. Novel techniques such as DARC may allow us to directly visualise retinal ganglion cell loss when testing neuroprotective agents in the future and allow greater certainty about the efficacy of these treatments (Normando et al., 2015).

Otherwise, at baseline the characteristics of the phenytoin and placebo groups were generally comparable and typical of acute optic neuritis. Only three of the 86 patients recruited had a pre-existing diagnosis of multiple sclerosis. Thus the cohort of patients studied consisted almost entirely of patients with clinically isolated optic neuritis, although nearly three quarters had at least one hyperintense T2 lesion on MRI brain (and are at high risk of developing clinically definite MS in the future, indeed 30% already satisfied McDonald's 2010 criteria for MS).

At baseline the best independent predictor of visual loss measured using logMAR visual acuity was conduction block on VEPs. The significant positive association between conduction block on VEPs and RNFL swelling as well as conduction block and lesion length would support the findings of Youl el al 1991 that inflammation and inflammatory mediators contribute to conduction block and loss of visual function initially (Youl et al., 1991a).

The characteristics of the lesion on MRI were important determinants of RNFL swelling at baseline with more anterior and longer lesions being associated with significantly more RNFL swelling. Lesion length (rather than location) was the best independent predictor of RNFL swelling perhaps suggesting that swelling in the retina is more often secondary to axoplasmic stasis proximal to the lesion in the optic nerve (rather than to direct extension of inflammation from an anteriorly located optic nerve lesion).

The lack of significant baseline associations between any of the MRI, OCT or VEP measures and low contrast letter scores may be due to a floor effect. This could limit the usefulness of low contrast letter scores during the acute phase of optic neuritis when vision is most impaired.

The loss of RNFL thickness in the placebo group after 6 months was consistent with previous natural history studies. Treatment with phenytoin reduced RNFL loss by 30%, and MV loss by 34%. Together with a near significant 38% decrease in loss of optic nerve cross-sectional area, these results suggest that phenytoin protects the compartment comprising retinal ganglion cells (which make up 34% of macular volume (Sakai et al., 2011) and their axons in the RNFL and optic nerve. These results are consistent with the neuroprotective effect of sodium channel blockade in experimental models of optic neuritis and EAE (Garthwaite et al., 2002; Lo et al., 2003) and support the 'sodium hypothesis' of neuroaxonal loss within the context of acute relapses in vivo.

In contrast, we observed no significant treatment effects on visual outcomes or on the VEP. High contrast visual acuity and VEP amplitude recovered well in both phenytoin and placebo groups and this ceiling effect may have limited their ability to demonstrate any benefits of treatment. Perhaps more surprisingly low contrast acuity and color vision were not significantly improved with phenytoin despite significant effects on structural outcomes. This could be interpreted in several ways including 1) that treatment with phenytoin resulted in the preservation of structurally intact but non-functioning axons, 2) that the relative imprecision of visual outcomes measures makes them less sensitive to treatment effects than structural outcomes or 3) that improved structural outcomes did not reflect

preservation of axons but rather increased levels of astrogliosis and therefore there was no improvement in visual function.

Additionally, It may be that the small fibres of the parvocellular pathway are selectively affected early on during the course of optic neuritis explaining the lack of treatment effect on colour vision as well as on the temporal sector of the RNFL (Evangelou et al., 2001) and may require even earlier intervention with neuroprotective therapies.

It should be noted that in our cohort of patients there was a highly significant but moderate negative association between RNFL thickness and logMAR visual acuity at 6 months ($p=<0.0001$, $r=-0.57$) and similar moderate correlations with low contrast letter acuity at 6 months perhaps suggesting that factors other than axonal loss contribute to visual outcome. This could explain some of the discrepancy in the treatment effects on structural and functional outcomes. In future, it may be important to gain a better understanding of the mechanism of functional recovery after optic neuritis and their relationship with structural outcomes in order to adequately power trials to demonstrate treatment effects on functional outcomes. For example the visual cortex and LGN contain 3-400 fold more neurons than the retina and this may contribute to neuroplasticity in higher visual areas which influences functional prognosis (Jenkins et al., 2010).

The concept of 'structural reserve' and 'redundancy' of axons in the anterior visual system needs to be explored further to establish if there is a threshold of axonal loss below which clinically significant visual dysfunction manifests. If this is the case, then the clinical benefits of neuroprotection may only become apparent later on after repeated 'inflammatory hits' on the optic nerve have a cumulative effect on axonal loss.

In future trials it will also be important to include patient reported outcomes such as the NEI-VFQ-25 quality of life score and to determine more precisely what are clinically relevant improvements in visual outcome, particularly in trials such as ours with a short duration of follow up. A composite visual score, comparable to the multiple sclerosis composite score (Rudick et al., 2002) for physical disability, comprising measurements of several components of visual function may be a better, more comprehensive functional outcome measure. This

would require consensus from the MS community and need validation before being used in clinical trials.

The lack of any significant reduction in VEP latency with phenytoin would suggest that the greater preservation of axons in the retina and optic nerve was not due to enhanced remyelination and that different biological processes are involved. However, clearly axon preservation is a requirement to allow remyelination to occur and the time frame for remyelination to occur may have exceeded the length of follow up in the trial.

The success of this trial would support the use of the anterior visual system as a model for testing potential neuroprotective treatments in MS. Using a sentinel lesion approach, the anterior visual system can be studied in detail thanks to the availability of validated, highly sensitive clinical, imaging and electrophysiological techniques. The anterior visual system is a structurally eloquent area of the CNS with biological traits that makes it ideal for modeling the processes of neurodegeneration and repair. In particular, the retinal nerve fibre layer is a relatively pure compartment of unmyelinated axons whose thickness can be measured sensitively and non-invasively using optical coherence tomography making it an attractive biomarker of axonal loss. In addition to this the natural history of optic neuritis has been well defined and the duration to outcome is relatively short meaning putative neuroprotective treatments can be tested quickly and efficiently.

The effect sizes demonstrated in this trial support the use of OCT measures as primary end points in future proof of concept optic neuritis trials. Our results would suggest that OCT is superior to MRI of the optic nerve in demonstrating treatment effects. This may be due to the confounding effects of myelin in the optic nerve. In addition to this, the inherent difficulties in imaging such a small and mobile structure means that optic nerve imaging with MRI involves longer scanning times and is very reliant on patient compliance during the scan to reduce motion artifact. Moreover, as opposed to the quick, automated RNFL measurements obtained with OCT, optic nerve cross-sectional area measurements are more labour intensive and currently not automated making them less reproducible. As a biomarker, it may not add much value to the structural measurements of the retinal nerve fibre layer.

There may nevertheless be benefits in performing optic nerve imaging with MRI in acute optic neuritis trials. Identification of the lesion in the optic nerve that can help with diagnostic certainty, in particular when patients need to be recruited quickly within a narrow time window. Additionally, measures such as lesion length and lesional MTR may prove useful in future trial especially when the therapeutic focus is on repair.

The advantages of our trial design are 1) we recruited a well-defined cohort of patients with early MS/ CIS patients in whom sodium channel blockade with phenytoin was generally well tolerated. 2) Patients were recruited and loaded with phenytoin early, within two weeks of symptom onset, and the read out time delayed until three months after cessation of treatment to incorporate the lag in RNFL atrophy. 3) There was a clear treatment target with good experimental evidence for its rationale. 4) The trial was properly powered using longitudinal natural history data to inform sample sizes.

Despite these advantages, this was a small proof of concept trial, and definitive confirmation of the findings would require a larger phase 3 trial; such a trial would also be needed to determine whether there is a more subtle benefit to vision that could only be detected in a large cohort.

Ten of the 39 active patients available at follow-up were non-adherent. While this may affect the power of the ITT analysis, the robustness of the results is supported by the agreement between the ITT and PP analyses as well as the consistency of treatment effects in the macula, RNFL and optic nerve. Patients in the active group who discontinued treatment (mainly due to a rash) remained on treatment for a mean of 18.4 days and an exploratory analysis demonstrated improved OCT outcomes compared to the placebo group even after this short length of time.

Regarding potential sources of bias care was taken to exclude patients with atypical acute optic neuritis, and none of the participants developed features of disorders such as neuromyelitis optica (for which antibodies were also tested at presentation) or chronic relapsing inflammatory optic neuropathy. Since the study started, further immunological subtypes of optic neuritis have been suggested (e.g. those with antibodies to myelin

oligodendrocyte glycoprotein) and appropriate testing of these subtypes for any differences in their response to neuroprotective therapies will be important to include in future studies.

It is unlikely that concomitant corticosteroid treatment would have influenced the neuroprotective findings because care was taken to adjust the analysis for the use and timing of corticosteroids. Also, measurements of the RNFL and of MV remained stable in the fellow eye in both the phenytoin and placebo groups, and previous studies showed that corticosteroids did not prevent atrophy of the RNFL (Naismith et al., 2009a) or optic nerve (Hickman et al., 2003), or visual recovery after optic neuritis (Beck et al., 1992b).

Although the read out time for our trial was timed to detect treatment effects on RNFL atrophy it is unclear whether a six-month follow period is long enough to detect beneficial effects on other outcome measures. For example, the time course of remyelination is unclear, with one study reporting a reduction in VEP latency up to 2 years post optic neuritis (Brusa et al., 2001). Also, the visual system may compensate well in the short term but may fail over longer periods with poorer functional outcome usually occurring after recurrent episodes of optic neuritis. Therefore longer follow up periods may be required to evaluate whether the increased structural reserve afforded by neuroprotection translates into functional gain further down the line.

Finally, a proportion of the patients recruited had a normal baseline brain MRI and it could be argued that they should not have been included in the study given the relatively low risk of them having an MS associated optic neuritis. However there was no statistical difference in the treatment effect (on the primary analysis) between participants with normal and abnormal brain MRI scans at baseline ($p=0.629$) and the pathological process may be similar in idiopathic optic neuritis.

Treatment with phenytoin was generally well tolerated and was not associated with abnormalities in the blood count or liver function. We did not note any acute deterioration of vision that might be attributed to conduction block from inhibition of sodium currents, or any rebound deterioration upon withdrawal of treatment—effects that had previously been thought to potentially limit the use of drugs acting on this target in demyelinating disorders.

Only one participant had a severe adverse reaction—a skin rash—attributable to phenytoin, but a further nine participants developed minor, self-limiting skin rashes and were withdrawn from treatment by the investigators according to protocol. Masking of participants to treatment allocation failed in some cases as a result of skin rashes. Although this unmasking might have had an effect on patient-based clinical assessment, it should not have affected the primary outcome

Future trials should consider the use of more potent and specific sodium channel inhibitors with better side effect profiles, even earlier treatment windows (although in practice this may be very difficult to achieve) and higher drug concentrations. Using data from this trial and other longitudinal studies of acute optic neuritis it may be possible to identify and select patients at baseline with a poorer prognosis who have the most to gain from neuroprotective treatments. Future studies should also establish more precisely the optimal therapeutic window for neuroprotection in relapses.

Some studies have suggested that the GC/IPL layer thickness in the macula may be a better biomarker of axonal loss after optic neuritis as, unlike the RNFL, its measurement is not affected by swelling acutely and GC/IPL layer thinning may occur earlier perhaps within days of symptom onset (Gabilondo et al., 2015). Also, compared to RNFL thickness measures there is less inter-patient variability in GC/IPL measures and so it may be a better primary outcome measure for future trials.

Also, new technology such as ultra high-resolution OCT imaging may enable better and more detailed and accurate measurements of the retinal layers in the macula (Zawadzki et al., 2005; Choi et al., 2008)

Furthermore, in addition to the structural measurements obtained with OCT, techniques such a ramen spectroscopy may allow us to obtain biochemical information on the molecular processes of neurodegeneration in the retina in MS. Also, it may be possible to make use of techniques such as detection of apoptosing retinal cells (DARC) that employs fluorescently labeled annexing 5 and confocal laser scanning ophthalmoscopy0 to directly visualise the amount of retinal ganglion cell loss. This could give us pathological insights into

the timing of RGC loss after optic neuritis as well as allowing greater pathological specificity when testing neurprotective treatment (Normando et al., 2015). Advances in functional MRI and electrophysiological techniques such as multifocal VEPs may also allow us to better elucidate the pathophysiological mechanisms of functional recovery and its failure.

As the pathophysiology of optic neuritis resembles that of other relapses in MS sodium channel blockade should be effective in these relapses as well. In turn, the present trial design should enable proof of concept of neuroprotection after relapse for treatments with other modes of action. However, whilst the mechanisms of neuroprotection with sodium channel blockade would seem more applicable within the context of other acute inflammatory lesions in relapsing MS, the implications for treating the more “slow burning” neurodegeneration of progressive MS are harder to define because of possible differences in pathophysiology. Microglial activation is likely to remain important in progressive disease, whereas sodium channel expression might change (Black et al., 2007).

In summary, the results of this clinical trial support the concept of neuroprotection using phenytoin to inhibit voltage-gated sodium channels in acute optic neuritis. These results should encourage larger, phase 3 trials of sodium channel inhibitors in optic neuritis and other relapses of MS. The present trial design should also enable proof of concept of neuroprotection after relapse for treatments with other modes of action.

References

Abegg, M., Dysli, M., Wolf, S., Kowal, J., Dufour, P. & Zinkernagel, M. 2014. Microcystic macular edema: retrograde maculopathy caused by optic neuropathy. *Ophthalmology,* 121(1)**,** pp 142-9.

Al-Izki, S., Pryce, G., Hankey, D. J., Lidster, K., von Kutzleben, S. M., Browne, L., Clutterbuck, L., Posada, C., Edith Chan, A. W., Amor, S., Perkins, V., Gerritsen, W. H., Ummenthum, K., Peferoen-Baert, R., van der Valk, P., Montoya, A., Joel, S. P., Garthwaite, J., Giovannoni, G., Selwood, D. L. & Baker, D. 2014. Lesional-targeting of neuroprotection to the inflammatory penumbra in experimental multiple sclerosis. *Brain,* 137(Pt 1)**,** pp 92-108.

Alamouti, B. & Funk, J. 2003. Retinal thickness decreases with age: an OCT study. *Br J Ophthalmol,* 87(7)**,** pp 899-901.

Albrecht, P., Ringelstein, M., Muller, A. K., Keser, N., Dietlein, T., Lappas, A., Foerster, A., Hartung, H. P., Aktas, O. & Methner, A. 2012. Degeneration of retinal layers in multiple sclerosis subtypes quantified by optical coherence tomography. *Mult Scler,* 18(10)**,** pp 1422-9.

Amesbury, E. C. & Schallhorn, S. C. 2003. Contrast sensitivity and limits of vision. *Int Ophthalmol Clin,* 43(2)**,** pp 31-42.

Andersen, O., Lygner, P. E., Bergström, T., Andersson, M. & Vahlne, A. 1993. Viral infections trigger multiple sclerosis relapses: a prospective seroepidemiological study. *J Neurol,* 240(7)**,** pp 417-22.

Baier, M. L., Cutter, G. R., Rudick, R. A., Miller, D., Cohen, J. A., Weinstock-Guttman, B., Mass, M. & Balcer, L. J. 2005. Low-contrast letter acuity testing captures visual dysfunction in patients with multiple sclerosis. *Neurology,* 64(6)**,** pp 992-5.

Balcer, L. J., Baier, M. L., Cohen, J. A., Kooijmans, M. F., Sandrock, A. W., Nano-Schiavi, M. L., Pfohl, D. C., Mills, M., Bowen, J., Ford, C., Heidenreich, F. R., Jacobs, D. A., Markowitz, C. E., Stuart, W. H., Ying, G. S., Galetta, S. L., Maguire, M. G. & Cutter, G. R. 2003. Contrast letter acuity as a visual component for the Multiple Sclerosis Functional Composite. *Neurology,* 61(10)**,** pp 1367-73.

Balcer, L. J., Baier, M. L., Pelak, V. S., Fox, R. J., Shuwairi, S., Galetta, S. L., Cutter, G. R. & Maguire, M. G. 2000. New low-contrast vision charts: reliability and test characteristics in patients with multiple sclerosis. *Mult Scler,* 6(3)**,** pp 163-71.

Balcer, L. J. & Frohman, E. M. 2010. Evaluating loss of visual function in multiple sclerosis as measured by low-contrast letter acuity. *Neurology,* 74 Suppl 3(S16-23).

Balcer, L. J., Galetta, S. L., Calabresi, P. A., Confavreux, C., Giovannoni, G., Havrdova, E., Hutchinson, M., Kappos, L., Lublin, F. D., Miller, D. H., O'Connor, P. W., Phillips, J. T., Polman, C. H., Radue, E. W., Rudick, R. A., Stuart, W. H., Wajgt, A., Weinstock-Guttman, B., Wynn, D. R., Lynn, F. & Panzara, M. A. 2007. Natalizumab reduces visual loss in patients with relapsing multiple sclerosis. *Neurology,* 68(16)**,** pp 1299-304.

Balcer, L. J., Galetta, S. L., Polman, C. H., Eggenberger, E., Calabresi, P. A., Zhang, A., Scanlon, J. V. & Hyde, R. 2012. Low-contrast acuity measures visual improvement in phase 3 trial of natalizumab in relapsing MS. *J Neurol Sci,* 318(1-2)**,** pp 119-24.

Balcer, L. J., Miller, D. H., Reingold, S. C. & Cohen, J. A. 2015. Vision and vision-related outcome measures in multiple sclerosis. *Brain,* 138(Pt 1)**,** pp 11-27.

Barnett, M. H. & Prineas, J. W. 2004. Relapsing and remitting multiple sclerosis: pathology of the newly forming lesion. *Ann Neurol,* 55(4)**,** pp 458-68.

Bechtold, D. A. & Smith, K. J. 2005. Sodium-mediated axonal degeneration in inflammatory demyelinating disease. *J Neurol Sci,* 233(1-2)**,** pp 27-35.

Beck, R. W., Cleary, P. A., Anderson, M. M., Jr., Keltner, J. L., Shults, W. T., Kaufman, D. I., Buckley, E. G., Corbett, J. J., Kupersmith, M. J., Miller, N. R. & et al. 1992a. A randomized, controlled trial of corticosteroids in the treatment of acute optic neuritis. The Optic Neuritis Study Group. *N Engl J Med,* 326(9)**,** pp 581-8.

Beck, R. W., Cleary, P. A., Anderson, M. M., Keltner, J. L., Shults, W. T., Kaufman, D. I., Buckley, E. G., Corbett, J. J., Kupersmith, M. J. & Miller, N. R. 1992b. A randomized, controlled trial of corticosteroids in the treatment of acute optic neuritis. The Optic Neuritis Study Group. *N Engl J Med,* 326(9)**,** pp 581-8.

Beck, R. W., Cleary, P. A., Trobe, J. D., Kaufman, D. I., Kupersmith, M. J., Paty, D. W. & Brown, C. H. 1993. The effect of corticosteroids for acute optic neuritis on the subsequent development of multiple sclerosis. The Optic Neuritis Study Group. *N Engl J Med,* 329(24)**,** pp 1764-9.

Beck, R. W., Gal, R. L., Bhatti, M. T., Brodsky, M. C., Buckley, E. G., Chrousos, G. A., Corbett, J., Eggenberger, E., Goodwin, J. A., Katz, B., Kaufman, D. I., Keltner, J. L., Kupersmith, M. J., Miller, N. R., Moke, P. S., Nazarian, S., Orengo-Nania, S., Savino, P. J., Shults, W. T., Smith, C. H., Trobe, J. D., Wall, M., Xing, D. & Group, O. N. S. 2004. Visual function more than 10 years

after optic neuritis: experience of the optic neuritis treatment trial. *Am J Ophthalmol,* 137(1)**,** pp 77-83.

Beck, R. W., Trobe, J. D., Moke, P. S., Gal, R. L., Xing, D., Bhatti, M. T., Brodsky, M. C., Buckley, E. G., Chrousos, G. A., Corbett, J., Eggenberger, E., Goodwin, J. A., Katz, B., Kaufman, D. I., Keltner, J. L., Kupersmith, M. J., Miller, N. R., Nazarian, S., Orengo-Nania, S., Savino, P. J., Shults, W. T., Smith, C. H., Wall, M. & Group, O. N. S. 2003. High- and low-risk profiles for the development of multiple sclerosis within 10 years after optic neuritis: experience of the optic neuritis treatment trial. *Arch Ophthalmol,* 121(7)**,** pp 944-9.

Bitsch, A., Schuchardt, J., Bunkowski, S., Kuhlmann, T. & Brück, W. 2000. Acute axonal injury in multiple sclerosis. Correlation with demyelination and inflammation. *Brain,* 123 (Pt 6)(1174-83.

Bjartmar, C., Kidd, G., Mörk, S., Rudick, R. & Trapp, B. D. 2000. Neurological disability correlates with spinal cord axonal loss and reduced N-acetyl aspartate in chronic multiple sclerosis patients. *Ann Neurol,* 48(6)**,** pp 893-901.

Black, J. A., Newcombe, J., Trapp, B. D. & Waxman, S. G. 2007. Sodium channel expression within chronic multiple sclerosis plaques. *J Neuropathol Exp Neurol,* 66(9)**,** pp 828-37.

Blumenthal, E. Z., Parikh, R. S., Pe'er, J., Naik, M., Kaliner, E., Cohen, M. J., Prabakaran, S., Kogan, M. & Thomas, R. 2009. Retinal nerve fibre layer imaging compared with histological measurements in a human eye. *Eye (Lond),* 23(1)**,** pp 171-5.

Bolaños, J. P., Almeida, A., Stewart, V., Peuchen, S., Land, J. M., Clark, J. B. & Heales, S. J. 1997. Nitric oxide-mediated mitochondrial damage in the brain: mechanisms and implications for neurodegenerative diseases. *J Neurochem,* 68(6)**,** pp 2227-40.

Boomer, J. A. & Siatkowski, R. M. 2003. Optic neuritis in adults and children. *Semin Ophthalmol,* 18(4)**,** pp 174-80.

Bostock, H. & Sears, T. A. 1978. The internodal axon membrane: electrical excitability and continuous conduction in segmental demyelination. *J Physiol,* 280(273-301.

Brecelj, J. 2014. Visual electrophysiology in the clinical evaluation of optic neuritis, chiasmal tumours, achiasmia, and ocular albinism: an overview. *Doc Ophthalmol,* 129(2)**,** pp 71-84.

Brex, P. A., Ciccarelli, O., O'Riordan, J. I., Sailer, M., Thompson, A. J. & Miller, D. H. 2002. A longitudinal study of abnormalities on MRI and disability from multiple sclerosis. *N Engl J Med,* 346(3)**,** pp 158-64.

Brex, P. A., O'Riordan, J. I., Miszkiel, K. A., Moseley, I. F., Thompson, A. J., Plant, G. T. & Miller, D. H. 1999. Multisequence MRI in clinically isolated syndromes and the early development of MS. *Neurology,* 53(6)**,** pp 1184-90.

Brusa, A., Jones, S. J. & Plant, G. T. 2001. Long-term remyelination after optic neuritis: A 2-year visual evoked potential and psychophysical serial study. *Brain,* 124(Pt 3)**,** pp 468-79.

Brusaferri, F. & Candelise, L. 2000. Steroids for multiple sclerosis and optic neuritis: a meta-analysis of randomized controlled clinical trials. *J Neurol,* 247(6)**,** pp 435-42.

Burkholder, B. M., Osborne, B., Loguidice, M. J., Bisker, E., Frohman, T. C., Conger, A., Ratchford, J. N., Warner, C., Markowitz, C. E., Jacobs, D. A., Galetta, S. L., Cutter, G. R., Maguire, M. G., Calabresi, P. A., Balcer, L. J. & Frohman, E. M. 2009. Macular volume

determined by optical coherence tomography as a measure of neuronal loss in multiple sclerosis. *Arch Neurol,* 66(11)**,** pp 1366-72.

Cettomai, D., Pulicken, M., Gordon-Lipkin, E., Salter, A., Frohman, T. C., Conger, A., Zhang, X., Cutter, G., Balcer, L. J., Frohman, E. M. & Calabresi, P. A. 2008. Reproducibility of optical coherence tomography in multiple sclerosis. *Arch Neurol,* 65(9)**,** pp 1218-22.

Chen, J. T., Collins, D. L., Atkins, H. L., Freedman, M. S., Arnold, D. L. & Canadian, M. S. B. M. T. S. G. 2008. Magnetization transfer ratio evolution with demyelination and remyelination in multiple sclerosis lesions. *Ann Neurol,* 63(2)**,** pp 254-62.

Choi, S. S., Zawadzki, R. J., Keltner, J. L. & Werner, J. S. 2008. Changes in cellular structures revealed by ultra-high resolution retinal imaging in optic neuropathies. *Invest Ophthalmol Vis Sci,* 49(5)**,** pp 2103-19.

Comi, G., Filippi, M., Barkhof, F., Durelli, L., Edan, G., Fernández, O., Hartung, H., Seeldrayers, P., Sørensen, P. S., Rovaris, M., Martinelli, V., Hommes, O. R. & Group, E. T. o. M. S. S. 2001. Effect of early interferon treatment on conversion to definite multiple sclerosis: a randomised study. *Lancet,* 357(9268)**,** pp 1576-82.

Comi, G., Martinelli, V., Rodegher, M., Moiola, L., Bajenaru, O., Carra, A., Elovaara, I., Fazekas, F., Hartung, H. P., Hillert, J., King, J., Komoly, S., Lubetzki, C., Montalban, X., Myhr, K. M., Ravnborg, M., Rieckmann, P., Wynn, D., Young, C., Filippi, M. & group, P. s. 2009. Effect of glatiramer acetate on conversion to clinically definite multiple sclerosis in patients with clinically isolated syndrome (PreCISe study): a randomised, double-blind, placebo-controlled trial. *Lancet,* 374(9700)**,** pp 1503-11.

Compston, A. 1978. HLA and neurologic disease. *Neurology,* 28(5)**,** pp 413-4.

Costello, F., Coupland, S., Hodge, W., Lorello, G. R., Koroluk, J., Pan, Y. I., Freedman, M. S., Zackon, D. H. & Kardon, R. H. 2006. Quantifying axonal loss after optic neuritis with optical coherence tomography. *Ann Neurol,* 59(6)**,** pp 963-9.

Costello, F., Hodge, W., Pan, Y. I., Eggenberger, E., Coupland, S. & Kardon, R. H. 2008. Tracking retinal nerve fiber layer loss after optic neuritis: a prospective study using optical coherence tomography. *Mult Scler,* 14(7)**,** pp 893-905.

Costello, F., Hodge, W., Pan, Y. I., Eggenberger, E. & Freedman, M. S. 2010. Using retinal architecture to help characterize multiple sclerosis patients. *Can J Ophthalmol,* 45(5)**,** pp 520-6.

Craner, M. J., Damarjian, T. G., Liu, S., Hains, B. C., Lo, A. C., Black, J. A., Newcombe, J., Cuzner, M. L. & Waxman, S. G. 2005. Sodium channels contribute to microglia/macrophage activation and function in EAE and MS. *Glia,* 49(2)**,** pp 220-9.

Craner, M. J., Newcombe, J., Black, J. A., Hartle, C., Cuzner, M. L. & Waxman, S. G. 2004. Molecular changes in neurons in multiple sclerosis: altered axonal expression of Nav1.2 and Nav1.6 sodium channels and Na+/Ca2+ exchanger. *Proc Natl Acad Sci U S A,* 101(21)**,** pp 8168-73.

Curcio, C. A., Sloan, K. R., Kalina, R. E. & Hendrickson, A. E. 1990. Human photoreceptor topography. *J Comp Neurol,* 292(4)**,** pp 497-523.

Dacey, D. M. & Lee, B. B. 1994. The 'blue-on' opponent pathway in primate retina originates from a distinct bistratified ganglion cell type. *Nature,* 367(6465)**,** pp 731-5.

Dalton, C. M., Brex, P. A., Miszkiel, K. A., Fernando, K., MacManus, D. G., Plant, G. T., Thompson, A. J. & Miller, D. H. 2003. Spinal cord MRI in clinically isolated optic neuritis. *J Neurol Neurosurg Psychiatry,* 74(11)**,** pp 1577-80.

Dalton, C. M., Brex, P. A., Miszkiel, K. A., Hickman, S. J., MacManus, D. G., Plant, G. T., Thompson, A. J. & Miller, D. H. 2002. Application of the new McDonald criteria to patients with clinically isolated syndromes suggestive of multiple sclerosis. *Ann Neurol,* 52(1)**,** pp 47-53.

de Seze, J., Arndt, C., Jeanjean, L., Zephir, H., Blanc, F., Labauge, P., Bouyon, M., Ballonzoli, L., Fleury, M., Vermersch, P. & Speeg, C. 2008. Relapsing inflammatory optic neuritis: is it neuromyelitis optica? *Neurology,* 70(22)**,** pp 2075-6.

DeLuca, G. C., Ebers, G. C. & Esiri, M. M. 2004. Axonal loss in multiple sclerosis: a pathological survey of the corticospinal and sensory tracts. *Brain,* 127(Pt 5)**,** pp 1009-18.

Dichtl, A., Jonas, J. B. & Naumann, G. O. 1999. Retinal nerve fiber layer thickness in human eyes. *Graefes Arch Clin Exp Ophthalmol,* 237(6)**,** pp 474-9.

Doyle, A. J. 1990. Optic chiasm position on MR images. *AJNR Am J Neuroradiol,* 11(3)**,** pp 553-5.

Esfahani, M. R., Harandi, Z. A., Movasat, M., Nikdel, M., Adelpour, M., Momeni, A., Merat, H. & Fard, M. A. 2012. Memantine for axonal loss of optic neuritis. *Graefes Arch Clin Exp Ophthalmol,* 250(6)**,** pp 863-9.

Evangelou, N., Konz, D., Esiri, M. M., Smith, S., Palace, J. & Matthews, P. M. 2001. Size-selective neuronal changes in the anterior optic pathways suggest a differential susceptibility to injury in multiple sclerosis. *Brain,* 124(Pt 9)**,** pp 1813-20.

Farnsworth, D. 1943. The Farnsworth-Munsell 100-hue and dichotomous tests for colour vision. J Opt Soc Am

Felts, P. A., Baker, T. A. & Smith, K. J. 1997. Conduction in segmentally demyelinated mammalian central axons. *J Neurosci,* 17(19)**,** pp 7267-77.

Ferguson, B., Matyszak, M. K., Esiri, M. M. & Perry, V. H. 1997. Axonal damage in acute multiple sclerosis lesions. *Brain,* 120 (Pt 3)(393-9.

Filippi, M., Rocca, M. A., Ciccarelli, O., De Stefano, N., Evangelou, N., Kappos, L., Rovira, A., Sastre-Garriga, J., Tintorè, M., Frederiksen, J. L., Gasperini, C., Palace, J., Reich, D. S., Banwell, B., Montalban, X., Barkhof, F. & Group, M. S. 2016. MRI criteria for the diagnosis of multiple sclerosis: MAGNIMS consensus guidelines. *Lancet Neurol,* 15(3)**,** pp 292-303.

Fisher, J. B., Jacobs, D. A., Markowitz, C. E., Galetta, S. L., Volpe, N. J., Nano-Schiavi, M. L., Baier, M. L., Frohman, E. M., Winslow, H., Frohman, T. C., Calabresi, P. A., Maguire, M. G., Cutter, G. R. & Balcer, L. J. 2006. Relation of visual function to retinal nerve fiber layer thickness in multiple sclerosis. *Ophthalmology,* 113(2)**,** pp 324-32.

Fitzgibbon, T. & Taylor, S. F. 1996. Retinotopy of the human retinal nerve fibre layer and optic nerve head. *J Comp Neurol,* 375(2)**,** pp 238-51.

Flanagan, P. & Markulev, C. 2005. Spatio-temporal selectivity of loss of colour and luminance contrast sensitivity with multiple sclerosis and optic neuritis. *Ophthalmic Physiol Opt,* 25(1)**,** pp 57-65.

Foster, R. E., Whalen, C. C. & Waxman, S. G. 1980. Reorganization of the axon membrane in demyelinated peripheral nerve fibers: morphological evidence. *Science,* 210(4470)**,** pp 661-3.

Fraser, C. L., Klistorner, A., Graham, S. L., Garrick, R., Billson, F. A. & Grigg, J. R. 2006. Multifocal visual evoked potential analysis of inflammatory or demyelinating optic neuritis. *Ophthalmology,* 113(2)**,** pp 323.e1-323.e2.

Frederiksen, J. L., Larsson, H. B., Henriksen, O. & Olesen, J. 1989. Magnetic resonance imaging of the brain in patients with acute monosymptomatic optic neuritis. *Acta Neurol Scand,* 80(6)**,** pp 512-7.

Frederiksen, J. L. & Petrera, J. 1999. Serial visual evoked potentials in 90 untreated patients with acute optic neuritis. *Surv Ophthalmol,* 44 Suppl 1(S54-62.

Frederiksen, J. L., Sørensen, T. L. & Sellebjerg, F. T. 1997. Residual symptoms and signs after untreated acute optic neuritis. A one-year follow-up. *Acta Ophthalmol Scand,* 75(5)**,** pp 544-7.

Frisen, L. & Quigley, H. A. 1984. Visual acuity in optic atrophy: a quantitative clinicopathological analysis. *Graefes Arch Clin Exp Ophthalmol,* 222(2)**,** pp 71-4.

Frohman, E. M., Fujimoto, J. G., Frohman, T. C., Calabresi, P. A., Cutter, G. & Balcer, L. J. 2008. Optical coherence tomography: a window into the mechanisms of multiple sclerosis. *Nat Clin Pract Neurol,* 4(12)**,** pp 664-75.

Frohman, E. M., Racke, M. K. & Raine, C. S. 2006. Multiple sclerosis--the plaque and its pathogenesis. *N Engl J Med,* 354(9)**,** pp 942-55.

Gabilondo, I., Martínez-Lapiscina, E. H., Fraga-Pumar, E., Ortiz-Perez, S., Torres-Torres, R., Andorra, M., Llufriu, S., Zubizarreta, I., Saiz, A., Sanchez-Dalmau, B. & Villoslada, P. 2015. Dynamics of retinal injury after acute optic neuritis. *Ann Neurol,* 77(3)**,** pp 517-28.

Ganter, P., Prince, C. & Esiri, M. M. 1999. Spinal cord axonal loss in multiple sclerosis: a post-mortem study. *Neuropathol Appl Neurobiol,* 25(6)**,** pp 459-67.

Garcia-Martin, E., Polo, V., Larrosa, J. M., Marques, M. L., Herrero, R., Martin, J., Ara, J. R., Fernandez, J. & Pablo, L. E. 2014. Retinal layer segmentation in patients with multiple sclerosis using spectral domain optical coherence tomography. *Ophthalmology,* 121(2)**,** pp 573-9.

Garthwaite, G., Goodwin, D. A., Batchelor, A. M., Leeming, K. & Garthwaite, J. 2002. Nitric oxide toxicity in CNS white matter: an in vitro study using rat optic nerve. *Neuroscience,* 109(1)**,** pp 145-55.

Gartner, S. 1953. Optic neuropathy in multiple sclerosis; optic neuritis. *AMA Arch Ophthalmol,* 50(6)**,** pp 718-26.

Garway-Heath, D. F., Holder, G. E., Fitzke, F. W. & Hitchings, R. A. 2002. Relationship between electrophysiological, psychophysical, and anatomical measurements in glaucoma. *Invest Ophthalmol Vis Sci,* 43(7)**,** pp 2213-20.

Garway-Heath, D. F., Poinoosawmy, D., Fitzke, F. W. & Hitchings, R. A. 2000. Mapping the visual field to the optic disc in normal tension glaucoma eyes. *Ophthalmology,* 107(10)**,** pp 1809-15.

Gass, A. & Moseley, I. F. 2000. The contribution of magnetic resonance imaging in the differential diagnosis of optic nerve damage. *J Neurol Sci,* 172 Suppl 1(S17-22.

Gass, A., Moseley, I. F., Barker, G. J., Jones, S., MacManus, D., McDonald, W. I. & Miller, D. H. 1996. Lesion discrimination in optic neuritis using high-resolution fat-suppressed fast spin-echo MRI. *Neuroradiology,* 38(4)**,** pp 317-21.

Gelfand, J. M., Cree, B. A., Nolan, R., Arnow, S. & Green, A. J. 2013. Microcystic inner nuclear layer abnormalities and neuromyelitis optica. *JAMA Neurol,* 70(5)**,** pp 629-33.

Gelfand, J. M., Nolan, R., Schwartz, D. M., Graves, J. & Green, A. J. 2012. Microcystic macular oedema in multiple sclerosis is associated with disease severity. *Brain,* 135(Pt 6)**,** pp 1786-93.

Glaser, J. & Sadun, A. 1990. *Neuro-opthalmology*, Philadeliphia, PA: Lippincott.

Gnanapavan, S., Grant, D., Morant, S., Furby, J., Hayton, T., Teunissen, C. E., Leoni, V., Marta, M., Brenner, R., Palace, J., Miller, D. H., Kapoor, R. & Giovannoni, G. 2013. Biomarker report from the phase II lamotrigine trial in secondary progressive MS - neurofilament as a surrogate of disease progression. *PLoS One,* 8(8)**,** pp e70019.

Gordon-Lipkin, E., Chodkowski, B., Reich, D. S., Smith, S. A., Pulicken, M., Balcer, L. J., Frohman, E. M., Cutter, G. & Calabresi, P. A. 2007. Retinal nerve fiber layer is associated with brain atrophy in multiple sclerosis. *Neurology,* 69(16)**,** pp 1603-9.

Graham, S. L. & Klistorner, A. 1998. Electrophysiology: a review of signal origins and applications to investigating glaucoma. *Aust N Z J Ophthalmol,* 26(1)**,** pp 71-85.

Green, A. J., McQuaid, S., Hauser, S. L., Allen, I. V. & Lyness, R. 2010. Ocular pathology in multiple sclerosis: retinal atrophy and inflammation irrespective of disease duration. *Brain,* 133(Pt 6)**,** pp 1591-601.

Group, O. N. S. 1991. The clinical profile of optic neuritis. Experience of the Optic Neuritis Treatment Trial. Optic Neuritis Study Group. *Arch Ophthalmol,* 109(12)**,** pp 1673-8.

Group, O. N. S. 1997. The 5-year risk of MS after optic neuritis. Experience of the optic neuritis treatment trial. *Neurology,* 49(5)**,** pp 1404-13.

Group, O. N. S. 2008. Visual function 15 years after optic neuritis: a final follow-up report from the Optic Neuritis Treatment Trial. *Ophthalmology,* 115(6)**,** pp 1079-1082.e5.

Gundogan, F. C., Tas, A., Altun, S., Oz, O., Erdem, U. & Sobaci, G. 2013. Color vision versus pattern visual evoked potentials in the assessment of subclinical optic pathway involvement in multiple sclerosis. *Indian J Ophthalmol,* 61(3)**,** pp 100-3.

Guy, J., Fitzsimmons, J., Ellis, E. A., Beck, B. & Mancuso, A. 1992. Intraorbital optic nerve and experimental optic neuritis. Correlation of fat suppression magnetic resonance imaging and electron microscopy. *Ophthalmology,* 99(5)**,** pp 720-5.

Halliday, A. M., McDonald, W. I. & Mushin, J. 1972. Delayed visual evoked response in optic neuritis. *Lancet,* 1(7758)**,** pp 982-5.

Halliday, A. M., McDonald, W. I. & Mushin, J. 1973. Delayed pattern-evoked responses in optic neuritis in relation to visual acuity. *Trans Ophthalmol Soc U K,* 93(0)**,** pp 315-24.

Hauser, S. L., Oksenberg, J. R., Lincoln, R., Garovoy, J., Beck, R. W., Cole, S. R., Moke, P. S., Kip, K. E., Gal, R. L. & Long, D. T. 2000. Interaction between HLA-DR2 and abnormal brain MRI in optic neuritis and early MS. Optic Neuritis Study Group. *Neurology,* 54(9)**,** pp 1859-61.

Hayreh, S. 2011. *Ischaemic Optic Neuropathies*, 1: Springer Berlin Heidelberg.

Hayreh, S. S., Massanari, R. M., Yamada, T. & Hayreh, S. M. 1981. Experimental allergic encephalomyelitis. I. Optic nerve and central nervous system manifestations. *Invest Ophthalmol Vis Sci,* 21(2)**,** pp 256-69.

Hely, M. A., McManis, P. G., Doran, T. J., Walsh, J. C. & McLeod, J. G. 1986. Acute optic neuritis: a prospective study of risk factors for multiple sclerosis. *J Neurol Neurosurg Psychiatry,* 49(10)**,** pp 1125-30.

Henderson, A. P., Altmann, D. R., Trip, A. S., Kallis, C., Jones, S. J., Schlottmann, P. G., Garway-Heath, D. F., Plant, G. T. & Miller, D. H. 2010. A serial study of retinal changes

following optic neuritis with sample size estimates for acute neuroprotection trials. *Brain,* 133(9)**,** pp 2592-602.

Henderson, A. P., Altmann, D. R., Trip, S. A., Miszkiel, K. A., Schlottmann, P. G., Jones, S. J., Garway-Heath, D. F., Plant, G. T. & Miller, D. H. 2011. Early factors associated with axonal loss after optic neuritis. *Ann Neurol,* 70(6)**,** pp 955-63.

Hendry, S. H. & Yoshioka, T. 1994. A neurochemically distinct third channel in the macaque dorsal lateral geniculate nucleus. *Science,* 264(5158)**,** pp 575-7.

Hickman, S. J., Brex, P. A., Brierley, C. M., Silver, N. C., Barker, G. J., Scolding, N. J., Compston, D. A., Moseley, I. F., Plant, G. T. & Miller, D. H. 2001. Detection of optic nerve atrophy following a single episode of unilateral optic neuritis by MRI using a fat-saturated short-echo fast FLAIR sequence. *Neuroradiology,* 43(2)**,** pp 123-8.

Hickman, S. J., Brierley, C. M., Brex, P. A., MacManus, D. G., Scolding, N. J., Compston, D. A. & Miller, D. H. 2002a. Continuing optic nerve atrophy following optic neuritis: a serial MRI study. *Mult Scler,* 8(4)**,** pp 339-42.

Hickman, S. J., Dalton, C. M., Miller, D. H. & Plant, G. T. 2002b. Management of acute optic neuritis. *Lancet,* 360(9349)**,** pp 1953-62.

Hickman, S. J., Kapoor, R., Jones, S. J., Altmann, D. R., Plant, G. T. & Miller, D. H. 2003. Corticosteroids do not prevent optic nerve atrophy following optic neuritis. *J Neurol Neurosurg Psychiatry,* 74(8)**,** pp 1139-41.

Hickman, S. J., Miszkiel, K. A., Plant, G. T. & Miller, D. H. 2005. The optic nerve sheath on MRI in acute optic neuritis. *Neuroradiology,* 47(1)**,** pp 51-5.

Hickman, S. J., Toosy, A. T., Jones, S. J., Altmann, D. R., Miszkiel, K. A., MacManus, D. G., Barker, G. J., Plant, G. T., Thompson, A. J. & Miller, D. H. 2004a. Serial magnetization transfer imaging in acute optic neuritis. *Brain,* 127(Pt 3)**,** pp 692-700.

Hickman, S. J., Toosy, A. T., Miszkiel, K. A., Jones, S. J., Altmann, D. R., MacManus, D. G., Plant, G. T., Thompson, A. J. & Miller, D. H. 2004b. Visual recovery following acute optic neuritis--a clinical, electrophysiological and magnetic resonance imaging study. *J Neurol,* 251(8)**,** pp 996-1005.

Holder, G. E. 2001. Pattern electroretinography (PERG) and an integrated approach to visual pathway diagnosis. *Prog Retin Eye Res,* 20(4)**,** pp 531-61.

Holder, G. E., Celesia, G. G., Miyake, Y., Tobimatsu, S., Weleber, R. G. & Neurophysiology, I. F. o. C. 2010. International Federation of Clinical Neurophysiology: recommendations for visual system testing. *Clin Neurophysiol,* 121(9)**,** pp 1393-409.

Hood, D. C. & Kardon, R. H. 2007. A framework for comparing structural and functional measures of glaucomatous damage. *Prog Retin Eye Res,* 26(6)**,** pp 688-710.

Huang, D., Swanson, E. A., Lin, C. P., Schuman, J. S., Stinson, W. G., Chang, W., Hee, M. R., Flotte, T., Gregory, K., Puliafito, C. A. & et al. 1991. Optical coherence tomography. *Science,* 254(5035)**,** pp 1178-81.

Inglese, M., Ghezzi, A., Bianchi, S., Gerevini, S., Sormani, M. P., Martinelli, V., Comi, G. & Filippi, M. 2002. Irreversible disability and tissue loss in multiple sclerosis: a conventional and magnetization transfer magnetic resonance imaging study of the optic nerves. *Arch Neurol,* 59(2)**,** pp 250-5.

Jacobs, L. D., Beck, R. W., Simon, J. H., Kinkel, R. P., Brownscheidle, C. M., Murray, T. J., Simonian, N. A., Slasor, P. J. & Sandrock, A. W. 2000. Intramuscular interferon beta-1a therapy initiated during a first demyelinating event in multiple sclerosis. CHAMPS Study Group. *N Engl J Med,* 343(13)**,** pp 898-904.

Jenkins, T. M., Toosy, A. T., Ciccarelli, O., Miszkiel, K. A., Wheeler-Kingshott, C. A., Henderson, A. P., Kallis, C., Mancini, L., Plant, G. T., Miller, D. H. & Thompson, A. J. 2010. Neuroplasticity predicts outcome of optic neuritis independent of tissue damage. *Ann Neurol,* 67(1)**,** pp 99-113.

Jin, Y. P., de Pedro-Cuesta, J., Söderström, M. & Link, H. 1999. Incidence of optic neuritis in Stockholm, Sweden, 1990-1995: II. Time and space patterns. *Arch Neurol,* 56(8)**,** pp 975-80.

Jin, Y. P., de Pedro-Cuesta, J., Söderström, M., Stawiarz, L. & Link, H. 1998. Incidence of optic neuritis in Stockholm, Sweden 1990-1995: I. Age, sex, birth and ethnic-group related patterns. *J Neurol Sci,* 159(1)**,** pp 107-14.

Jonas, J. B. & Dichtl, A. 1996. Evaluation of the retinal nerve fiber layer. *Surv Ophthalmol,* 40(5)**,** pp 369-78.

Jonas, J. B. & Schiro, D. 1994. Localised wedge shaped defects of the retinal nerve fibre layer in glaucoma. *Br J Ophthalmol,* 78(4)**,** pp 285-90.

Kapoor, R., Davies, M., Blaker, P. A., Hall, S. M. & Smith, K. J. 2003. Blockers of sodium and calcium entry protect axons from nitric oxide-mediated degeneration. *Ann Neurol,* 53(2)**,** pp 174-80.

Kapoor, R., Furby, J., Hayton, T., Smith, K. J., Altmann, D. R., Brenner, R., Chataway, J., Hughes, R. A. & Miller, D. H. 2010. Lamotrigine for neuroprotection in secondary progressive multiple sclerosis: a randomised, double-blind, placebo-controlled, parallel-group trial. *Lancet Neurol,* 9(7)**,** pp 681-8.

Kapoor, R., Miller, D. H., Jones, S. J., Plant, G. T., Brusa, A., Gass, A., Hawkins, C. P., Page, R., Wood, N. W., Compston, D. A., Moseley, I. F. & McDonald, W. I. 1998. Effects of intravenous methylprednisolone on outcome in MRI-based prognostic subgroups in acute optic neuritis. *Neurology,* 50(1)**,** pp 230-7.

Kappos, L., Polman, C. H., Freedman, M. S., Edan, G., Hartung, H. P., Miller, D. H., Montalban, X., Barkhof, F., Bauer, L., Jakobs, P., Pohl, C. & Sandbrink, R. 2006. Treatment with interferon beta-1b delays conversion to clinically definite and McDonald MS in patients with clinically isolated syndromes. *Neurology,* 67(7)**,** pp 1242-9.

Katz, B. 1995. The dyschromatopsia of optic neuritis: a descriptive analysis of data from the optic neuritis treatment trial. *Trans Am Ophthalmol Soc,* 93(685-708.

Kaufhold, F., Zimmermann, H., Schneider, E., Ruprecht, K., Paul, F., Oberwahrenbrock, T. & Brandt, A. U. 2013. Optic neuritis is associated with inner nuclear layer thickening and microcystic macular edema independently of multiple sclerosis. *PLoS One,* 8(8)**,** pp e71145.

Kaufman, D. I., Trobe, J. D., Eggenberger, E. R. & Whitaker, J. N. 2000. Practice parameter: the role of corticosteroids in the management of acute monosymptomatic optic neuritis. Report of the Quality Standards Subcommittee of the American Academy of Neurology. *Neurology,* 54(11)**,** pp 2039-44.

Kawasaki, A., Moore, P. & Kardon, R. H. 1996. Long-term fluctuation of relative afferent pupillary defect in subjects with normal visual function. *Am J Ophthalmol,* 122(6)**,** pp 875-82.

Keltner, J. L., Johnson, C. A., Spurr, J. O. & Beck, R. W. 1994. Visual field profile of optic neuritis. One-year follow-up in the Optic Neuritis Treatment Trial. *Arch Ophthalmol,* 112(7)**,** pp 946-53.

Kerrison, J. B., Flynn, T. & Green, W. R. 1994. Retinal pathologic changes in multiple sclerosis. *Retina,* 14(5)**,** pp 445-51.

Khanna, S., Sharma, A., Huecker, J., Gordon, M., Naismith, R. T. & Van Stavern, G. P. 2012. Magnetic resonance imaging of optic neuritis in patients with neuromyelitis optica versus multiple sclerosis. *J Neuroophthalmol,* 32(3)**,** pp 216-20.

Kincaid, M. & Green, W. 1999. *Anatomy of the vitreous, retina and choroid*, New York: Thieme.

Klistorner, A., Arvind, H., Nguyen, T., Garrick, R., Paine, M., Graham, S., O'Day, J., Grigg, J., Billson, F. & Yiannikas, C. 2008. Axonal loss and myelin in early ON loss in postacute optic neuritis. *Ann Neurol,* 64(3)**,** pp 325-31.

Klistorner, A., Arvind, H., Nguyen, T., Garrick, R., Paine, M., Graham, S., O'Day, J. & Yiannikas, C. 2009. Multifocal VEP and OCT in optic neuritis: a topographical study of the structure-function relationship. *Doc Ophthalmol,* 118(2)**,** pp 129-37.

Klistorner, A., Graham, S., Fraser, C., Garrick, R., Nguyen, T., Paine, M., O'Day, J., Grigg, J., Arvind, H. & Billson, F. A. 2007. Electrophysiological evidence for heterogeneity of lesions in optic neuritis. *Invest Ophthalmol Vis Sci,* 48(10)**,** pp 4549-56.

Kolappan, M., Henderson, A. P., Jenkins, T. M., Wheeler-Kingshott, C. A., Plant, G. T., Thompson, A. J. & Miller, D. H. 2009. Assessing structure and function of the afferent visual pathway in multiple sclerosis and associated optic neuritis. *J Neurol,* 256(3)**,** pp 305-19.

Kolb, H., Fernandez, E. & Nelson, R. 1995. *The Organization of the Retina and Visual System*, Salt Lake City, UT:National Library of Medicine: National Institutes of Health.

Kolb, H. & Marshak, D. 2003. The midget pathways of the primate retina. *Doc Ophthalmol,* 106(1)**,** pp 67-81.

Kupersmith, M. J., Alban, T., Zeiffer, B. & Lefton, D. 2002. Contrast-enhanced MRI in acute optic neuritis: relationship to visual performance. *Brain,* 125(Pt 4)**,** pp 812-22.

Laron, M., Cheng, H., Zhang, B., Schiffman, J. S., Tang, R. A. & Frishman, L. J. 2010. Comparison of multifocal visual evoked potential, standard automated perimetry and optical coherence tomography in assessing visual pathway in multiple sclerosis patients. *Mult Scler,* 16(4)**,** pp 412-26.

Lassmann, H. 1998. Neuropathology in multiple sclerosis: new concepts. *Mult Scler,* 4(3)**,** pp 93-8.

Leist, T. P., Comi, G., Cree, B. A., Coyle, P. K., Freedman, M. S., Hartung, H. P., Vermersch, P., Casset-Semanaz, F., Scaramozza, M. & Group, o. c. f. e. M. O. M. S. 2014. Effect of oral cladribine on time to conversion to clinically definite multiple sclerosis in patients with a first demyelinating event (ORACLE MS): a phase 3 randomised trial. *Lancet Neurol,* 13(3)**,** pp 257-67.

Lightman, S., McDonald, W. I., Bird, A. C., Francis, D. A., Hoskins, A., Batchelor, J. R. & Halliday, A. M. 1987. Retinal venous sheathing in optic neuritis. Its significance for the pathogenesis of multiple sclerosis. *Brain,* 110 (Pt 2)(405-14.

Livingstone, M. & Hubel, D. 1988. Segregation of form, color, movement, and depth: anatomy, physiology, and perception. *Science,* 240(4853)**,** pp 740-9.

Lo, A. C., Saab, C. Y., Black, J. A. & Waxman, S. G. 2003. Phenytoin protects spinal cord axons and preserves axonal conduction and neurological function in a model of neuroinflammation in vivo. *J Neurophysiol,* 90(5)**,** pp 3566-71.

Lovas, G., Szilágyi, N., Majtényi, K., Palkovits, M. & Komoly, S. 2000. Axonal changes in chronic demyelinated cervical spinal cord plaques. *Brain,* 123 (Pt 2)(308-17.

Lucas, R. M., Ponsonby, A. L., Dear, K., Valery, P., Pender, M. P., Burrows, J. M., Burrows, S. R., Chapman, C., Coulthard, A., Dwyer, D. E., Dwyer, T., Kilpatrick, T., Lay, M. L., McMichael, A. J., Taylor, B. V., van der Mei, I. A. & Williams, D. 2011. Current and past Epstein-Barr virus infection in risk of initial CNS demyelination. *Neurology,* 77(4)**,** pp 371-9.

Lucchinetti, C., Brück, W., Parisi, J., Scheithauer, B., Rodriguez, M. & Lassmann, H. 2000. Heterogeneity of multiple sclerosis lesions: implications for the pathogenesis of demyelination. *Ann Neurol,* 47(6)**,** pp 707-17.

Lui, G., Volpe, N., Steven, L. & Galetta, M. 2010. *Neuro-Opthalmology: Diagnosis and Management*, 2nd: Saunders.

Lumsden, C. 1970. *Handbook of Clinical Neurology*, Amsterdam, The Netherlands.

Ma, S. L., Shea, J. A., Galetta, S. L., Jacobs, D. A., Markowitz, C. E., Maguire, M. G. & Balcer, L. J. 2002. Self-reported visual dysfunction in multiple sclerosis: new data from the VFQ-25 and development of an MS-specific vision questionnaire. *Am J Ophthalmol,* 133(5)**,** pp 686-92.

Mahad, D. H., Trapp, B. D. & Lassmann, H. 2015. Pathological mechanisms in progressive multiple sclerosis. *Lancet Neurol,* 14(2)**,** pp 183-93.

Martinelli, V., Dalla Costa, G., Colombo, B., Dalla Libera, D., Rubinacci, A., Filippi, M., Furlan, R. & Comi, G. 2014. Vitamin D levels and risk of multiple sclerosis in patients with clinically isolated syndromes. *Mult Scler,* 20(2)**,** pp 147-55.

Martínez-Lapiscina, E. H., Ortiz-Pérez, S., Fraga-Pumar, E., Martínez-Heras, E., Gabilondo, I., Llufriu, S., Bullich, S., Figueras, M., Saiz, A., Sánchez-Dalmau, B. & Villoslada, P. 2014. Colour vision impairment is associated with disease severity in multiple sclerosis. *Mult Scler*.

McLean, M. J. & Macdonald, R. L. 1983. Multiple actions of phenytoin on mouse spinal cord neurons in cell culture. *J Pharmacol Exp Ther,* 227(3)**,** pp 779-89.

Miller, A. E., Wolinsky, J. S., Kappos, L., Comi, G., Freedman, M. S., Olsson, T. P., Bauer, D., Benamor, M., Truffinet, P., O'Connor, P. W. & Group, T. S. 2014. Oral teriflunomide for patients with a first clinical episode suggestive of multiple sclerosis (TOPIC): a randomised, double-blind, placebo-controlled, phase 3 trial. *Lancet Neurol,* 13(10)**,** pp 977-86.

Miller, D., Barkhof, F., Montalban, X., Thompson, A. & Filippi, M. 2005. Clinically isolated syndromes suggestive of multiple sclerosis, part I: natural history, pathogenesis, diagnosis, and prognosis. *Lancet Neurol,* 4(5)**,** pp 281-8.

Miller, D. H., Barkhof, F., Frank, J. A., Parker, G. J. & Thompson, A. J. 2002. Measurement of atrophy in multiple sclerosis: pathological basis, methodological aspects and clinical relevance. *Brain,* 125(Pt 8)**,** pp 1676-95.

Miller, D. H., Newton, M. R., van der Poel, J. C., du Boulay, E. P., Halliday, A. M., Kendall, B. E., Johnson, G., MacManus, D. G., Moseley, I. F. & McDonald, W. I. 1988a. Magnetic resonance imaging of the optic nerve in optic neuritis. *Neurology,* 38(2)**,** pp 175-9.

Miller, D. H., Ormerod, I. E., McDonald, W. I., MacManus, D. G., Kendall, B. E., Kingsley, D. P. & Moseley, I. F. 1988b. The early risk of multiple sclerosis after optic neuritis. *J Neurol Neurosurg Psychiatry,* 51(12)**,** pp 1569-71.

Mowry, E. M., Loguidice, M. J., Daniels, A. B., Jacobs, D. A., Markowitz, C. E., Galetta, S. L., Nano-Schiavi, M. L., Cutter, G. R., Maguire, M. G. & Balcer, L. J. 2009. Vision related quality of life in multiple sclerosis: correlation with new measures of low and high contrast letter acuity. *J Neurol Neurosurg Psychiatry,* 80(7)**,** pp 767-72.

Naismith, R. T., Tutlam, N. T., Xu, J., Klawiter, E. C., Shepherd, J., Trinkaus, K., Song, S. K. & Cross, A. H. 2009a. Optical coherence tomography differs in neuromyelitis optica compared with multiple sclerosis. *Neurology,* 72(12)**,** pp 1077-82.

Naismith, R. T., Tutlam, N. T., Xu, J., Shepherd, J. B., Klawiter, E. C., Song, S. K. & Cross, A. H. 2009b. Optical coherence tomography is less sensitive than visual evoked potentials in optic neuritis. *Neurology,* 73(1)**,** pp 46-52.

Nilsson, P., Larsson, E. M., Maly-Sundgren, P., Perfekt, R. & Sandberg-Wollheim, M. 2005. Predicting the outcome of optic neuritis: evaluation of risk factors after 30 years of follow-up. *J Neurol,* 252(4)**,** pp 396-402.

Normando, E. M., Dehabadi, M. H., Guo, L., Turner, L. A., Pollorsi, G. & Cordeiro, M. F. 2015. Real-time imaging of retinal cell apoptosis by confocal scanning laser ophthalmoscopy. *Methods Mol Biol,* 1254(227-37.

Noseworthy, J. H., O'Brien, P. C., Petterson, T. M., Weis, J., Stevens, L., Peterson, W. K., Sneve, D., Cross, S. A., Leavitt, J. A., Auger, R. G., Weinshenker, B. G., Dodick, D. W., Wingerchuk, D. M. & Rodriguez, M. 2001. A randomized trial of intravenous immunoglobulin in inflammatory demyelinating optic neuritis. *Neurology,* 56(11)**,** pp 1514-22.

Noval, S., Contreras, I., Munoz, S., Oreja-Guevara, C., Manzano, B. & Rebolleda, G. 2011. Optical coherence tomography in multiple sclerosis and neuromyelitis optica: an update. *Mult Scler Int,* 2011(472790.

Ogden, T. E. 1983. Nerve fiber layer of the primate retina: thickness and glial content. *Vision Res,* 23(6)**,** pp 581-7.

Oksenberg, J. R., Baranzini, S. E., Sawcer, S. & Hauser, S. L. 2008. The genetics of multiple sclerosis: SNPs to pathways to pathogenesis. *Nat Rev Genet,* 9(7)**,** pp 516-26.

Ormerod, I. E., McDonald, W. I., du Boulay, G. H., Kendall, B. E., Moseley, I. F., Halliday, A. M., Kakigi, R., Kriss, A. & Peringer, E. 1986. Disseminated lesions at presentation in patients with optic neuritis. *J Neurol Neurosurg Psychiatry,* 49(2)**,** pp 124-7.

Oyster, C. 1999. *The Human Eye-Structure and Function*, Sunderland, Massachusetts: Sinauer Associates.

Parisi, V., Manni, G., Spadaro, M., Colacino, G., Restuccia, R., Marchi, S., Bucci, M. G. & Pierelli, F. 1999. Correlation between morphological and functional retinal impairment in multiple sclerosis patients. *Invest Ophthalmol Vis Sci,* 40(11)**,** pp 2520-7.

Perkin, G. D. & Rose, F. C. 1976. Uhthoff's syndrome. *Br J Ophthalmol,* 60(1)**,** pp 60-3.

Petzold, A. 2014. Optical Coherence Tomography to Assess Neurodegeneration in Multiple Sclerosis. *Methods Mol Biol*.

Petzold, A., de Boer, J. F., Schippling, S., Vermersch, P., Kardon, R., Green, A., Calabresi, P. A. & Polman, C. 2010. Optical coherence tomography in multiple sclerosis: a systematic review and meta-analysis. *Lancet Neurol,* 9(9)**,** pp 921-32.

Polman, C. H., Reingold, S. C., Banwell, B., Clanet, M., Cohen, J. A., Filippi, M., Fujihara, K., Havrdova, E., Hutchinson, M., Kappos, L., Lublin, F. D., Montalban, X., O'Connor, P., Sandberg-Wollheim, M., Thompson, A. J., Waubant, E., Weinshenker, B. & Wolinsky, J. S. 2011. Diagnostic criteria for multiple sclerosis: 2010 revisions to the McDonald criteria. *Ann Neurol,* 69(2)**,** pp 292-302.

Polyak, S. 1941. *The retina*, 1st, Chicago: University of Chicago press.

Prasad, S. & Galetta, S. L. 2011. Anatomy and physiology of the afferent visual system. *Handb Clin Neurol,* 102(3-19.

Pulicken, M., Gordon-Lipkin, E., Balcer, L. J., Frohman, E., Cutter, G. & Calabresi, P. A. 2007. Optical coherence tomography and disease subtype in multiple sclerosis. *Neurology,* 69(22)**,** pp 2085-92.

Raftopoulos, R. E. & Kapoor, R. 2013. Neuroprotection for acute optic neuritis-Can it work? *Mult Scler Relat Disord,* 2(4)**,** pp 307-11.

Ramsaransing, G., Maurits, N., Zwanikken, C. & De Keyser, J. 2001. Early prediction of a benign course of multiple sclerosis on clinical grounds: a systematic review. *Mult Scler,* 7(5)**,** pp 345-7.

Raphael, B. A., Galetta, K. M., Jacobs, D. A., Markowitz, C. E., Liu, G. T., Nano-Schiavi, M. L., Galetta, S. L., Maguire, M. G., Mangione, C. M., Globe, D. R. & Balcer, L. J. 2006. Validation and test characteristics of a 10-item neuro-ophthalmic supplement to the NEI-VFQ-25. *Am J Ophthalmol,* 142(6)**,** pp 1026-35.

Redford, E. J., Kapoor, R. & Smith, K. J. 1997. Nitric oxide donors reversibly block axonal conduction: demyelinated axons are especially susceptible. *Brain,* 120 (Pt 12)(2149-57.

Richman, J., Spaeth, G. L. & Wirostko, B. 2013. Contrast sensitivity basics and a critique of currently available tests. *J Cataract Refract Surg,* 39(7)**,** pp 1100-6.

Rizzo, J. 1994. *Walsh and Hoyt's Clinical Neuro-opthalmology*, 6th, Philadelphia, PA: Lippincott and Wilkins.

Rizzo, J. F. & Lessell, S. 1988. Risk of developing multiple sclerosis after uncomplicated optic neuritis: a long-term prospective study. *Neurology,* 38(2)**,** pp 185-90.

Rocca, M. A., Hickman, S. J., Bö, L., Agosta, F., Miller, D. H., Comi, G. & Filippi, M. 2005. Imaging the optic nerve in multiple sclerosis. *Mult Scler,* 11(5)**,** pp 537-41.

Rodriguez, M., Siva, A., Cross, S. A., O'Brien, P. C. & Kurland, L. T. 1995. Optic neuritis: a population-based study in Olmsted County, Minnesota. *Neurology,* 45(2)**,** pp 244-50.

Roed, H. G., Langkilde, A., Sellebjerg, F., Lauritzen, M., Bang, P., Mørup, A. & Frederiksen, J. L. 2005. A double-blind, randomized trial of IV immunoglobulin treatment in acute optic neuritis. *Neurology,* 64(5)**,** pp 804-10.

Roesner, S., Appel, R., Gbadamosi, J., Martin, R. & Heesen, C. 2012. Treatment of steroid-unresponsive optic neuritis with plasma exchange. *Acta Neurol Scand,* 126(2)**,** pp 103-8.

Rolak, L. A., Beck, R. W., Paty, D. W., Tourtellotte, W. W., Whitaker, J. N. & Rudick, R. A. 1996. Cerebrospinal fluid in acute optic neuritis: experience of the optic neuritis treatment trial. *Neurology,* 46(2)**,** pp 368-72.

Rudick, R. A., Cutter, G. & Reingold, S. 2002. The multiple sclerosis functional composite: a new clinical outcome measure for multiple sderosis trials. *Mult Scler,* 8(5)**,** pp 359-65.

Saidha, S., Sotirchos, E. S., Ibrahim, M. A., Crainiceanu, C. M., Gelfand, J. M., Sepah, Y. J., Ratchford, J. N., Oh, J., Seigo, M. A., Newsome, S. D., Balcer, L. J., Frohman, E. M., Green, A. J., Nguyen, Q. D. & Calabresi, P. A. 2012. Microcystic macular oedema, thickness of the inner nuclear layer of the retina, and disease characteristics in multiple sclerosis: a retrospective study. *Lancet Neurol,* 11(11)**,** pp 963-72.

Saidha, S., Sotirchos, E. S., Oh, J., Syc, S. B., Seigo, M. A., Shiee, N., Eckstein, C., Durbin, M. K., Oakley, J. D., Meyer, S. A., Frohman, T. C., Newsome, S., Ratchford, J. N., Balcer, L. J., Pham, D. L., Crainiceanu, C. M., Frohman, E. M., Reich, D. S. & Calabresi, P. A. 2013. Relationships between retinal axonal and neuronal measures and global central nervous system pathology in multiple sclerosis. *JAMA Neurol,* 70(1)**,** pp 34-43.

Saidha, S., Syc, S. B., Durbin, M. K., Eckstein, C., Oakley, J. D., Meyer, S. A., Conger, A., Frohman, T. C., Newsome, S., Ratchford, J. N., Frohman, E. M. & Calabresi, P. A. 2011a. Visual dysfunction in multiple sclerosis correlates better with optical coherence tomography derived estimates of macular ganglion cell layer thickness than peripapillary retinal nerve fiber layer thickness. *Mult Scler,* 17(12)**,** pp 1449-63.

Saidha, S., Syc, S. B., Ibrahim, M. A., Eckstein, C., Warner, C. V., Farrell, S. K., Oakley, J. D., Durbin, M. K., Meyer, S. A., Balcer, L. J., Frohman, E. M., Rosenzweig, J. M., Newsome, S. D., Ratchford, J. N., Nguyen, Q. D. & Calabresi, P. A. 2011b. Primary retinal pathology in multiple sclerosis as detected by optical coherence tomography. *Brain,* 134(Pt 2)**,** pp 518-33.

Sakai, R. E., Feller, D. J., Galetta, K. M., Galetta, S. L. & Balcer, L. J. 2011. Vision in multiple sclerosis: the story, structure-function correlations, and models for neuroprotection. *J Neuroophthalmol,* 31(4)**,** pp 362-73.

Schippling, S., Balk, L. J., Costello, F., Albrecht, P., Balcer, L., Calabresi, P. A., Frederiksen, J. L., Frohman, E., Green, A. J., Klistorner, A., Outteryck, O., Paul, F., Plant, G. T., Traber, G., Vermersch, P., Villoslada, P., Wolf, S. & Petzold, A. 2015. Quality control for retinal OCT in multiple sclerosis: validation of the OSCAR-IB criteria. *Mult Scler,* 21(2)**,** pp 163-70.

Selhorst, J., Saul, R. & Waybright, E. 1982. Optic nerve conduction: Opposing effects of exercise and hyperventilation. *Trans Am Neurol Assoc,* 106(1-4.

Sepulcre, J., Murie-Fernandez, M., Salinas-Alaman, A., Garcia-Layana, A., Bejarano, B. & Villoslada, P. 2007. Diagnostic accuracy of retinal abnormalities in predicting disease activity in MS. *Neurology,* 68(18)**,** pp 1488-94.

Shams, P. N. & Plant, G. T. 2009. Optic neuritis: a review. *Int MS J,* 16(3)**,** pp 82-9.

Shayegannejad, V., Shahzamani, S., Dehghani, A., Dast Borhan, Z., Rahimi, M. & Mirmohammadsadeghi, A. 2015. A double-blind, placebo-controlled trial of adding erythropoietin to intravenous methylprednisolone for the treatment of unilateral acute optic neuritis of unknown or demyelinative origin. *Graefes Arch Clin Exp Ophthalmol*.

Sibley, W. A., Bamford, C. R. & Clark, K. 1985. Clinical viral infections and multiple sclerosis. *Lancet,* 1(8441)**,** pp 1313-5.

Smith, K. J., Kapoor, R., Hall, S. M. & Davies, M. 2001. Electrically active axons degenerate when exposed to nitric oxide. *Ann Neurol,* 49(4)**,** pp 470-6.

Smith, K. J. & Lassmann, H. 2002. The role of nitric oxide in multiple sclerosis. *Lancet Neurol,* 1(4)**,** pp 232-41.

Smith, K. J. & McDonald, W. I. 1999. The pathophysiology of multiple sclerosis: the mechanisms underlying the production of symptoms and the natural history of the disease. *Philos Trans R Soc Lond B Biol Sci,* 354(1390)**,** pp 1649-73.

Spoor, T. C. & Rockwell, D. L. 1988. Treatment of optic neuritis with intravenous megadose corticosteroids. A consecutive series. *Ophthalmology,* 95(1)**,** pp 131-4.

Sriram, P., Wang, C., Yiannikas, C., Garrick, R., Barnett, M., Parratt, J., Graham, S. L., Arvind, H. & Klistorner, A. 2014. Relationship between optical coherence tomography and electrophysiology of the visual pathway in non-optic neuritis eyes of multiple sclerosis patients. *PLoS One,* 9(8)**,** pp e102546.

Stys, P. K., Waxman, S. G. & Ransom, B. R. 1992. Ionic mechanisms of anoxic injury in mammalian CNS white matter: role of Na+ channels and Na(+)-Ca2+ exchanger. *J Neurosci,* 12(2)**,** pp 430-9.

Suhs, K. W., Hein, K., Sattler, M. B., Gorlitz, A., Ciupka, C., Scholz, K., Kasmann-Kellner, B., Papanagiotou, P., Schaffler, N., Restemeyer, C., Bittersohl, D., Hassenstein, A., Seitz, B., Reith, W., Fassbender, K., Hilgers, R., Heesen, C., Bahr, M. & Diem, R. 2012. A randomized, double-blind, phase 2 study of erythropoietin in optic neuritis. *Ann Neurol,* 72(2)**,** pp 199-210.

Swanton, J. K., Fernando, K. T., Dalton, C. M., Miszkiel, K. A., Altmann, D. R., Plant, G. T., Thompson, A. J. & Miller, D. H. 2009. Early MRI in optic neuritis: the risk for disability. *Neurology,* 72(6)**,** pp 542-50.

Swanton, J. K., Fernando, K. T., Dalton, C. M., Miszkiel, K. A., Altmann, D. R., Plant, G. T., Thompson, A. J. & Miller, D. H. 2010. Early MRI in optic neuritis: the risk for clinically definite multiple sclerosis. *Mult Scler,* 16(2)**,** pp 156-65.

Syc, S. B., Saidha, S., Newsome, S. D., Ratchford, J. N., Levy, M., Ford, E., Crainiceanu, C. M., Durbin, M. K., Oakley, J. D., Meyer, S. A., Frohman, E. M. & Calabresi, P. A. 2012. Optical coherence tomography segmentation reveals ganglion cell layer pathology after optic neuritis. *Brain,* 135(Pt 2)**,** pp 521-33.

Syc, S. B., Warner, C. V., Hiremath, G. S., Farrell, S. K., Ratchford, J. N., Conger, A., Frohman, T., Cutter, G., Balcer, L. J., Frohman, E. M. & Calabresi, P. A. 2010. Reproducibility of high-resolution optical coherence tomography in multiple sclerosis. *Mult Scler,* 16(7)**,** pp 829-39.

Talman, L. S., Bisker, E. R., Sackel, D. J., Long, D. A., Galetta, K. M., Ratchford, J. N., Lile, D. J., Farrell, S. K., Loguidice, M. J., Remington, G., Conger, A., Frohman, T. C., Jacobs, D. A., Markowitz, C. E., Cutter, G. R., Ying, G. S., Dai, Y., Maguire, M. G., Galetta, S. L., Frohman, E. M., Calabresi, P. A. & Balcer, L. J. 2010. Longitudinal study of vision and retinal nerve fiber layer thickness in multiple sclerosis. *Ann Neurol,* 67(6)**,** pp 749-60.

Tatrai, E., Simo, M., Iljicsov, A., Nemeth, J., Debuc, D. C. & Somfai, G. M. 2012. In vivo evaluation of retinal neurodegeneration in patients with multiple sclerosis. *PLoS One,* 7(1)**,** pp e30922.

Thorpe, J. W., Barker, G. J., Jones, S. J., Moseley, I., Losseff, N., MacManus, D. G., Webb, S., Mortimer, C., Plummer, D. L. & Tofts, P. S. 1995. Magnetisation transfer ratios and transverse magnetisation decay curves in optic neuritis: correlation with clinical findings and electrophysiology. *J Neurol Neurosurg Psychiatry,* 59(5)**,** pp 487-92.

Toosy, A. T., Hickman, S. J., Miszkiel, K. A., Jones, S. J., Plant, G. T., Altmann, D. R., Barker, G. J., Miller, D. H. & Thompson, A. J. 2005. Adaptive cortical plasticity in higher visual areas after acute optic neuritis. *Ann Neurol,* 57(5)**,** pp 622-33.

Trapp, B. D., Peterson, J., Ransohoff, R. M., Rudick, R., Mörk, S. & Bö, L. 1998. Axonal transection in the lesions of multiple sclerosis. *N Engl J Med,* 338(5)**,** pp 278-85.

Trip, S. A., Schlottmann, P. G., Jones, S. J., Altmann, D. R., Garway-Heath, D. F., Thompson, A. J., Plant, G. T. & Miller, D. H. 2005. Retinal nerve fiber layer axonal loss and visual dysfunction in optic neuritis. *Ann Neurol,* 58(3)**,** pp 383-91.

Trip, S. A., Schlottmann, P. G., Jones, S. J., Li, W. Y., Garway-Heath, D. F., Thompson, A. J., Plant, G. T. & Miller, D. H. 2006. Optic nerve atrophy and retinal nerve fibre layer thinning

following optic neuritis: evidence that axonal loss is a substrate of MRI-detected atrophy. *Neuroimage,* 31(1)**,** pp 286-93.

Tsakiri, A., Kallenbach, K., Fuglø, D., Wanscher, B., Larsson, H. & Frederiksen, J. 2012. Simvastatin improves final visual outcome in acute optic neuritis: a randomized study. *Mult Scler,* 18(1)**,** pp 72-81.

van Waesberghe, J. H., Kamphorst, W., De Groot, C. J., van Walderveen, M. A., Castelijns, J. A., Ravid, R., Lycklama à Nijeholt, G. J., van der Valk, P., Polman, C. H., Thompson, A. J. & Barkhof, F. 1999. Axonal loss in multiple sclerosis lesions: magnetic resonance imaging insights into substrates of disability. *Ann Neurol,* 46(5)**,** pp 747-54.

Villoslada, P., Cuneo, A., Gelfand, J., Hauser, S. L. & Green, A. 2012. Color vision is strongly associated with retinal thinning in multiple sclerosis. *Mult Scler,* 18(7)**,** pp 991-9.

Wakakura, M., Ishikawa, S., Oono, S., Tabuchi, A., Kani, K., Tazawa, Y., Nakao, Y., Kiyosawa, M., Kawai, K. & Oohira, A. 1995. [Incidence of acute idiopathic optic neuritis and its therapy in Japan. Optic Neuritis Treatment Trial Multicenter Cooperative Research Group (ONMRG)]. *Nippon Ganka Gakkai Zasshi,* 99(1)**,** pp 93-7.

Walter, S. D., Ishikawa, H., Galetta, K. M., Sakai, R. E., Feller, D. J., Henderson, S. B., Wilson, J. A., Maguire, M. G., Galetta, S. L., Frohman, E., Calabresi, P. A., Schuman, J. S. & Balcer, L. J. 2012. Ganglion cell loss in relation to visual disability in multiple sclerosis. *Ophthalmology,* 119(6)**,** pp 1250-7.

Wang, Y., van der Walt, A., Paine, M., Klistorner, A., Butzkueven, H., Egan, G. F., Kilpatrick, T. J. & Kolbe, S. C. 2012. Optic nerve magnetisation transfer ratio after acute optic neuritis predicts axonal and visual outcomes. *PLoS One,* 7(12)**,** pp e52291.

Waxman, S. G. 1998. Demyelinating diseases--new pathological insights, new therapeutic targets. *N Engl J Med,* 338(5)**,** pp 323-5.

Werring, D. J., Bullmore, E. T., Toosy, A. T., Miller, D. H., Barker, G. J., MacManus, D. G., Brammer, M. J., Giampietro, V. P., Brusa, A., Brex, P. A., Moseley, I. F., Plant, G. T., McDonald, W. I. & Thompson, A. J. 2000. Recovery from optic neuritis is associated with a change in the distribution of cerebral response to visual stimulation: a functional magnetic resonance imaging study. *J Neurol Neurosurg Psychiatry,* 68(4)**,** pp 441-9.

Wisniewski, H., Oppenheimer, D. & McDonald, W. 1976. Relation between myelination and function in MS and EAE. *J Neuropath Exp Neurol* 35(327.

Wu, G. F., Schwartz, E. D., Lei, T., Souza, A., Mishra, S., Jacobs, D. A., Markowitz, C. E., Galetta, S. L., Nano-Schiavi, M. L., Desiderio, L. M., Cutter, G. R., Calabresi, P. A., Udupa, J. K. & Balcer, L. J. 2007. Relation of vision to global and regional brain MRI in multiple sclerosis. *Neurology,* 69(23)**,** pp 2128-35.

Yaari, Y., Selzer, M. E. & Pincus, J. H. 1986. Phenytoin: mechanisms of its anticonvulsant action. *Ann Neurol,* 20(2)**,** pp 171-84.

Yiannakas, M. C., Toosy, A. T., Raftopoulos, R. E., Kapoor, R., Miller, D. H. & Wheeler-Kingshott, C. A. 2013. MRI acquisition and analysis protocol for in vivo intraorbital optic nerve segmentation at 3T. *Invest Ophthalmol Vis Sci,* 54(6)**,** pp 4235-40.

Youl, B. D., Turano, G., Miller, D. H., Towell, A. D., MacManus, D. G., Moore, S. G., Jones, S. J., Barrett, G., Kendall, B. E. & Moseley, I. F. 1991a. The pathophysiology of acute optic

neuritis. An association of gadolinium leakage with clinical and electrophysiological deficits. *Brain,* 114 (Pt 6)(2437-50.

Youl, B. D., Turano, G., Miller, D. H., Towell, A. D., MacManus, D. G., Moore, S. G., Jones, S. J., Barrett, G., Kendall, B. E., Moseley, I. F. & et al. 1991b. The pathophysiology of acute optic neuritis. An association of gadolinium leakage with clinical and electrophysiological deficits. *Brain,* 114 (Pt 6)(2437-50.

Zawadzki, R. J., Jones, S. M., Olivier, S. S., Zhao, M., Bower, B. A., Izatt, J. A., Choi, S., Laut, S. & Werner, J. S. 2005. Adaptive-optics optical coherence tomography for high-resolution and high-speed 3D retinal in vivo imaging. *Opt Express,* 13(21)**,** pp 8532-8546.

Zimmermann, H., Freing, A., Kaufhold, F., Gaede, G., Bohn, E., Bock, M., Oberwahrenbrock, T., Young, K. L., Dörr, J., Wuerfel, J. T., Schippling, S., Paul, F. & Brandt, A. U. 2013. Optic neuritis interferes with optical coherence tomography and magnetic resonance imaging correlations. *Mult Scler,* 19(4)**,** pp 443-50.